

RWD 5854-EN-01

2

DTIC FILE COPY

AD

AD-A213 277

FLOOD INUNDATION MODELLING
USING MILHY

Interim
Final Technical Report

by

L.Baird and M.G.Anderson

Volume 1

June 1989

European Research Office
U.S. Corps of Engineers
London England

DTIC
ELECTE
OCT 10 1989
S E D

CONTRACT NUMBER DAJA 45-87-C-0053

Dr.M.G.Anderson

Approved for Public Release : Distribution Unlimited

89 10 10151

PREFACE

This report details work undertaken under contract DAJA-45-87-C-0053 to July 1989. We report the further development of the ungauged forecasting model MILHY. Specifically, new routines are introduced to allow discrete routing in channel and floodplain zones, and allowance is made for turbulent exchange between channel and floodplain. The program (MILHY3) is applied to the Fulda watershed in West Germany.

In addition, a 2-dimensional finite element scheme (RMA2) is applied to a 30 km reach of the River Fulda. We conclude that it should be perfectly feasible to couple MILHY3 to RMA2: MILHY3 generating the inflow hydrograph and RMA2 predicting the detail of inundation downstream as well as predicting stage at the final outflow. This latter component of the study has been undertaken at the Hydrologic Engineering Center at Davis, California. With funds available at Bristol University we propose to continue this research and development work over the next 18 months to October 1989 under the aegis of the contract research area.

The code for MILHY3, as developed on a Sun 3/60 workstation by Laura Baird, is contained in an appendix to this report.

Approved for	
By	X
Date	
Use	
Just	
By	
Date	
As	
Dist	
A-1	

CONTENTS

<u>VOLUME I</u>	Page
<u>SECTION 1 : INTRODUCTION</u>	1
1.1 Background	1
1.2 Objectives	2
<u>SECTION 2 : RESEARCH DESIGN</u>	10
2.1 Introduction	10
2.2 Research design for the current investigation	10
<u>SECTION 3 : IDENTIFICATION OF KEY PARAMETERS AND PROCESSES FOR CONVEYANCE</u>	14
3.1 Difficulties of modelling two-stage channels	14
3.1.1 The complexity of physical processes	14
3.1.2 Modelling alternatives	18
3.1.3 MILHY : present frictional capability	20
3.2 Selection of a two-stage conveyance model	25
3.2.1 The Ervine and Ellis model	25
3.2.2 Quantifying the energy losses	28
3.3 Sensitivity analysis of the Ervine and Ellis model	33
3.3.1 Sensitivity analysis design	33
3.3.2 Results	34
3.3.3 Conclusions	42
3.4 Implications for the improvement of MILHY	43
3.4.1 Incorporation of the effects of turbulence into MILHY	43
3.4.2 Incorporation of multiple routing pathways	44
3.5 Logical development of a research scheme	44
3.5.1 Implementation of research scheme	45
3.5.2 Work identified for the next eighteen months	46
<u>SECTION 4 : INCORPORATION OF MOMENTUM TRANSFER BETWEEN FLOODPLAIN AND CHANNEL SEGMENTS</u>	47
4.1 Hydraulics of momentum transfer	47
4.2 Modelling of momentum transfer	51
4.2.1 A theoretical approach	51
4.2.2 Flume experiments investigating apparent shear stresses	52
4.2.3 Implications for discharge predictions	58

4.3	Incorporation of momentum transfer into MILHY	62
4.3.1	Selection of methods for incorporation into MILHY	62
4.3.2	Incorporation of the four methods into MILHY	63
4.4	Sensitivity of the rating curve to interface inclination	63
4.4.1	Application of the four interface inclination methods	66
4.4.2	Sensitivity of the rating curve to the computation stage increment	68
4.4.3	Results of the sensitivity analysis	70
4.4.4	Conclusions	81
4.5	Implications for the improvement of MILHY	82
	<u>SECTION 5 : INCORPORATION OF MULTIPLE ROUTING REACHES</u>	83
5.1	The behaviour of two-stage channel flow	83
5.1.1	Comparison of main channel and floodplain boundary roughness	83
5.1.2	Objective of investigating multiple routing reaches	84
5.2	Modelling alternatives	84
5.3	Incorporating multiple routing into MILHY	87
5.4	Application of multiple routing reaches	87
5.4.1	Application to the Bad Hersfeld to Rotenburg reach	89
5.4.2	Application to a hypothetical reach	96
5.4.3	Conclusions	98
	<u>SECTION 6 : VALIDATION OF MILHY3</u>	104
6.1	Selection of a field site	106
6.1.1	Prerequisites of a study catchment	106
6.1.2	The River Fulda Catchment	108
6.2	Establishment of the River Fulda Catchment	111
6.2.1	Establishment of the data set	117
6.2.2	Soils classification problems	121
6.3	Design of a sensitivity analysis	122
6.3.1	Alternative methods of undertakings, a sensitive analysis	127
6.3.2	The optimization approach	130
6.3.3	Application of the factor perturbation technique to the Fulda dataset	134
6.4	Sensitivity of the outflow hydrograph to model structure	135
6.4.1	Storm 1 : 1 in 10 year event	136
6.4.2	Storm 3 : 1 in 1.5 year event	145

6.4.3	Comparison of the two storms	153
6.4.4	Conclusions	158
6.5	Optimization results	158
6.5.1	Sensitivity to parameter variability	162
6.5.2	Sensitivity variations associated with the computation method	169
6.5.3	Conclusions	170
6.6	Conclusions	171
 <u>SECTION 7 : FLOODPLAIN MODELLING</u>		172
7.1	Introduction	172
7.2	Existing applications of finite element methods for river reach studies	172
7.3	Large scale floodplain modelling with finite element methods	173
7.4	Model selection	173
7.5	Research design	175
7.6	Study reach	176
7.7	System schematization	177
7.8	Computational aspects	179
7.9	Results	179
7.10	Discussion	186
 <u>SECTION 8 : CONCLUSIONS AND PROPOSALS FOR NEXT 12 MONTHS</u>		187
8.1	Conclusions	187
8.2	Proposals for next twelve months	187
 <u>SECTION 9 : REFERENCES</u>		189

VOLUME II

Page

Appendix 1 : MILHY3 : Programme details
Appendix 2 : MILHY3 : Dataset details
Appendix 3 : MILHY3 : Source code

196
237
243

Nomenclature

A	cross-sectional area
B	channel width
g	gravitational constant
h	bankfull depth
h_f	frictional head loss
n_f	Manning friction coefficient
Q	discharge rate
r	sinuosity of channel meander (curved channel length) (straight valley length)
R	hydraulic radius of channel
R_c	radius of curvature of meander bend
S_c	longitudinal bed slope
S_o	friction slope
V_o	streamwise velocity
W_m	width of meander belt
W^m	total floodway width
f^t	Darcy-Weisbach friction factor
m	meander wavelength angle of meandering channel to streamwise direction
K	boundary roughness dimension
R_e	Reynolds number
h_l	headloss due to transverse circulation in channel
h_e	headloss due to expansion
h^e	headloss due to contraction
C_c	contraction loss coefficient
C_L	

Subscripts

c	main channel
f	floodplain
f_1	floodplain area 1, within meander width belt
f_2	floodplain area 2

1. INTRODUCTION

1.1 Background

This study relates to the further development of an operational model for ungauged catchment forecasting. The model used as the starting basis for the project was MILHY2; a model delivered to Waterways Experiment Station in 1986 under contract DAJA-45-83-C-0029.

The history of MILHY development as an ungauged forecasting model and research scheme is as follows:

- MILHY: model for ungauged flow forecasting using Curve Number (CN) scheme to generate runoff, 1982
- MILHY1: adaptation of MILHY under contracts DAJA-37-82-C-0092 and DAJA-37-81-C-0221 by Dr M G Anderson to replace CN scheme by a physically based runoff generation method (finite difference) 1984
- MILHY2: development and validation of MILHY1 on small subcatchment scale (1 km²) watersheds, by Dr M G Anderson and Dr S Howes under contract DAJA-45-83-C-0029. Code delivered to WES in 1986.
- MILHY3: further development of MILHY2 and the subject of research in the current contract as specified in Figure 1.2 below.

Upon the initiation of the current contract MILHY2 represented a fully working scheme (figures 1.1 and 1.2). MILHY2 was subjected to limited validation as shown in table 1.1 and figures 1.3 and 1.4. The main conclusions of contract DAJA-45-83-C-0029 relating to the development of MILHY2 were that:

- (1) the correlation between predicted and measured peak discharge using MILHY2 was high ($r = 0.91$)

- (ii) the time to peak discharge estimation was good using MILHY2 ($r = 0.97$)
- (iii) a comparison of MILHY and MILHY2 for 32 experimental frames showed strong evidence of the overall improvement achieved by MILHY2.

There was, therefore, a strong basis for pursuing the further development of MILHY2, to explore the scope for improvement in the channel routing component.

1.2 Objectives and scope

The overall objective is the further development of MILHY2 in the following specific areas:

- (i) employment of alternative equations for flow conveyance in compound channels
- (ii) the improvement in the handling of out-of-bank roughness
- (iii) the validation of the revised MILHY scheme on the West German watersheds of the Fulda and Haune.

It has been possible within the scope of the project to augment the above objectives with that of evaluating the performance of a finite element model (RMA2) in estimating floodplain inundation. This work has been undertaken at the Hydrologic Engineering Center, Davis California, and will continue, with available funds at Bristol University, for a further eighteen months to October 1990.

The above objectives can be directly translated to research questions:

- (1) can MILHY3 accommodate improved channel routing procedures?
- (ii) can MILHY3, as presented schematically in figure 1.5 satisfy the restricted data needs for an ungauged model?

(iii) can MILHY3 be coupled to a finite element scheme (such as RMA2) to provide an enhanced inundation capability and, if so, what are the appropriate scales for such a model linkage?

(iv) can MILHY3 be adequately validated?

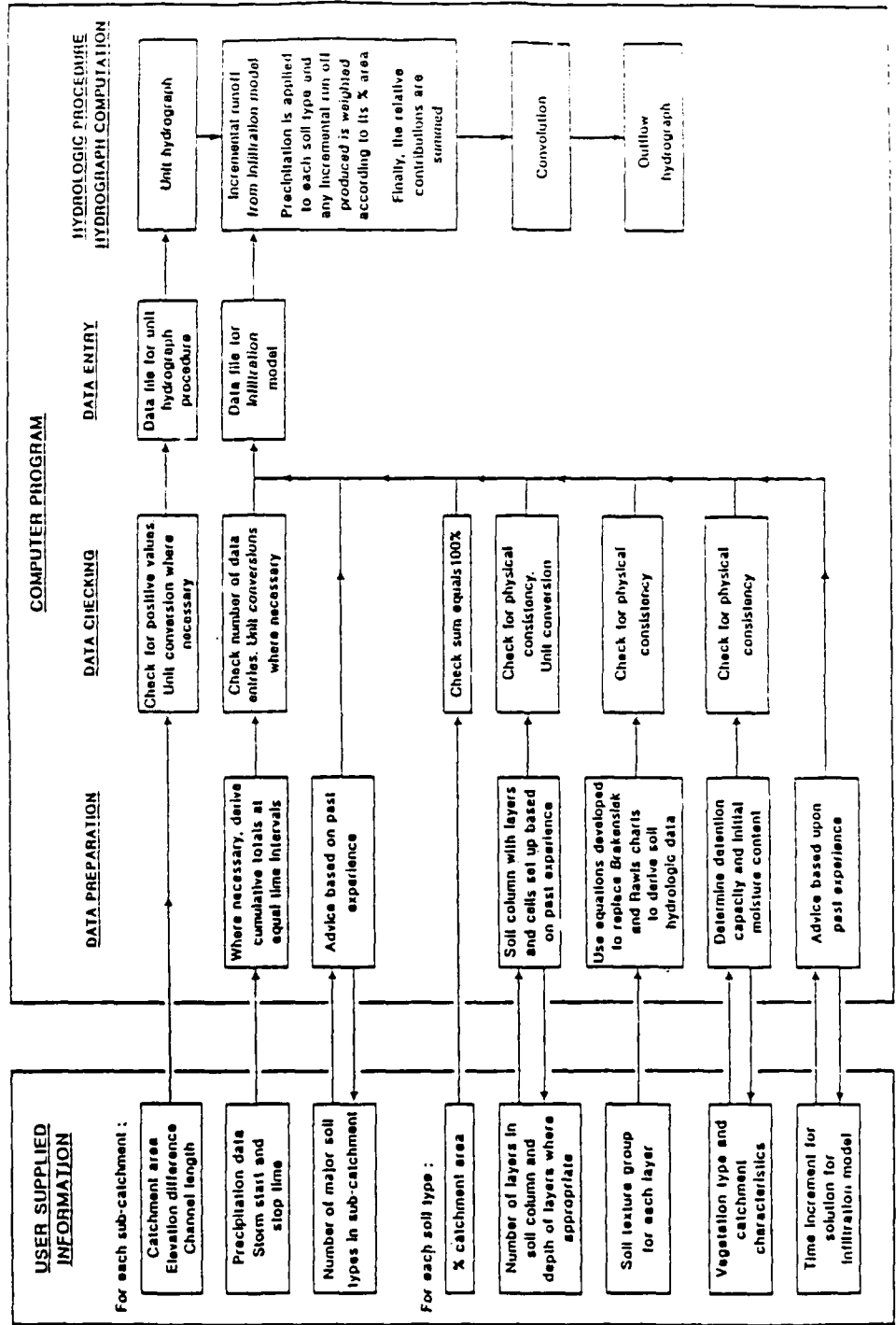


Figure 1.1 : MLBY2

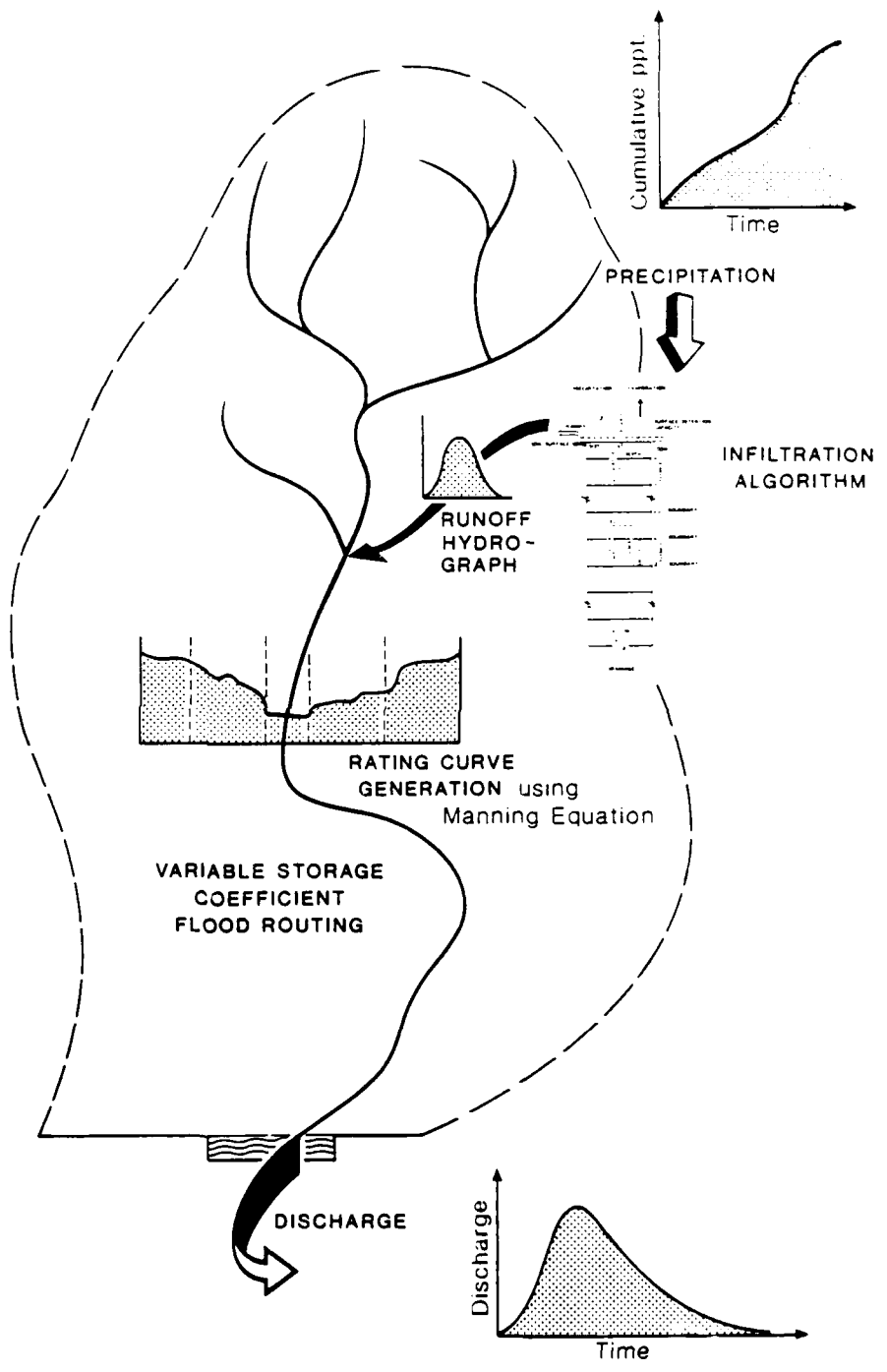


Figure 1.2. MILHY2
Conceptual Structure

Table 1.1: Comparison of catchment characteristics which are required by the unit hydrograph procedure

	Area (km ²)	Difference in elevation (m)	Length of Main channel (km)
W-2 North Danville Vermont	0.6	79.3	1.2
W-1 Treyvor, Iowa	0.3	27.4	1.1
W-2 Treyvor, Iowa	0.3	21.3	0.9
W-3 Treyvor, Iowa	0.4	27.4	0.9
W-4 Treyvor, Iowa	0.6	30.5	0.6

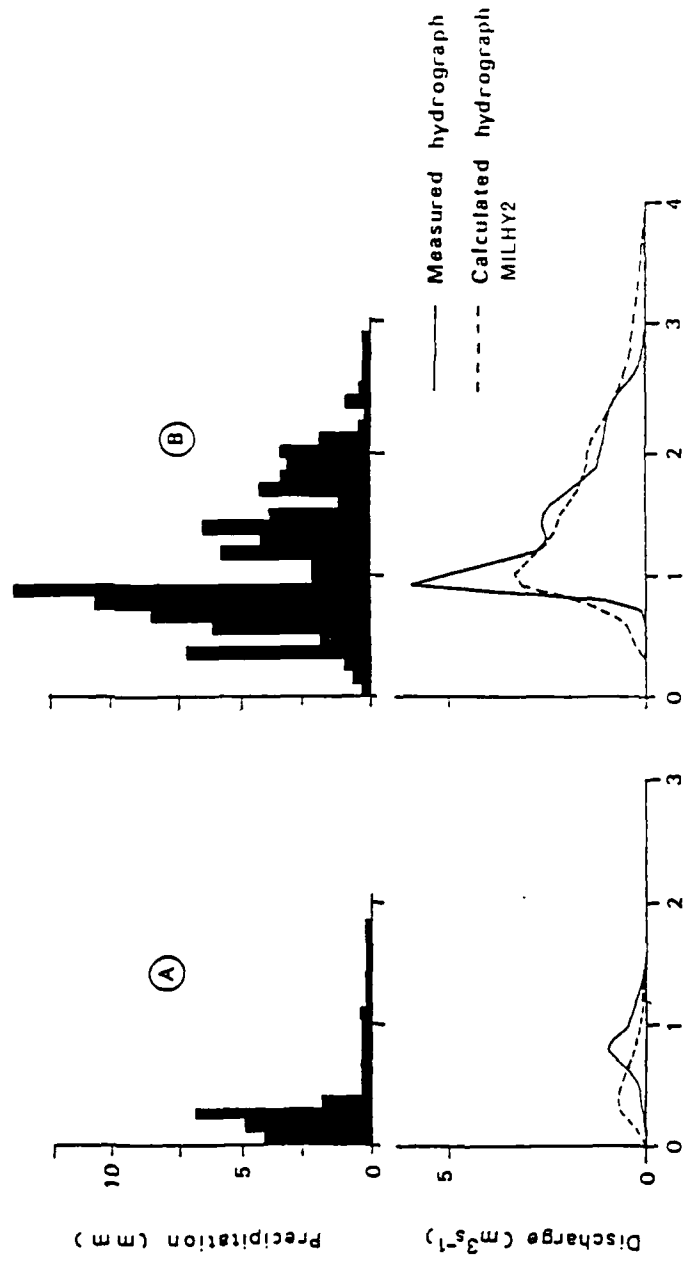


Figure 1.3 : Comparison of calculated and measured hydrographs for

W-3, Reynor, Iowa:

(A) Storm 4, 20 June 1987

(B) Storm 5, 7 Dec 1987

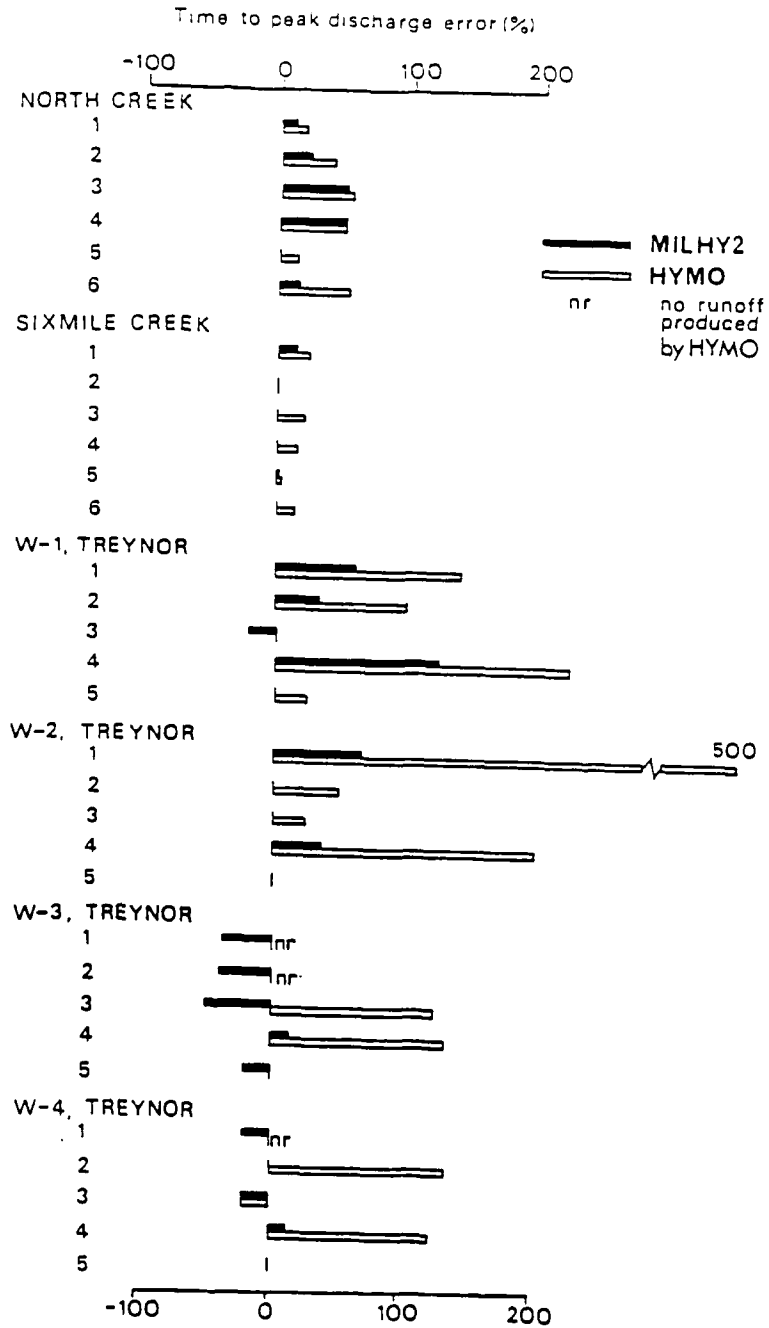


Figure 1.4 : Comparison of percentage time to peak discharge error of MILHY2 and HYMO, 32 experimental frames

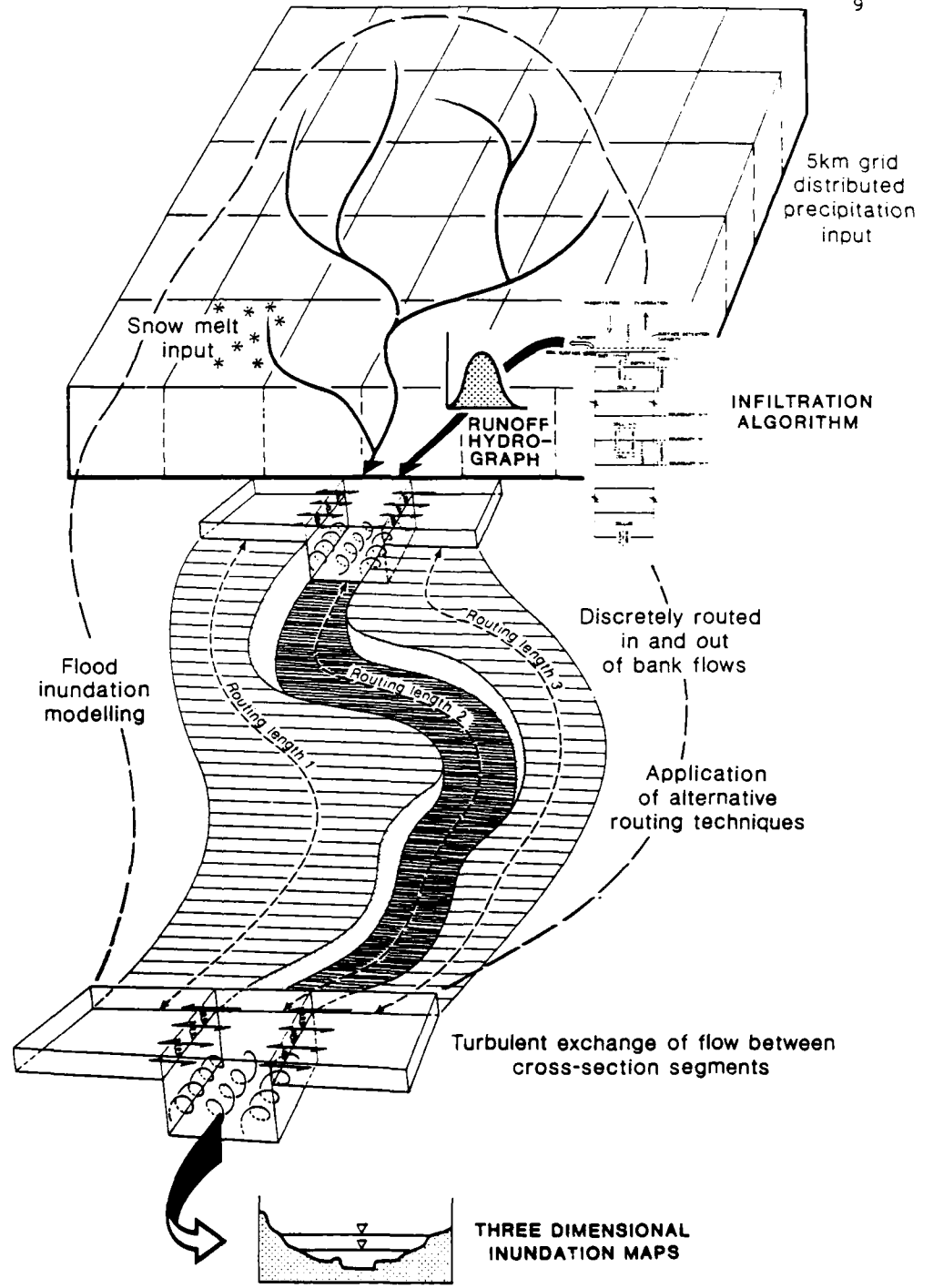


Figure 1.5 : MILHY3, Conceptual Structure

2. RESEARCH DESIGN

2.1 Introduction

The overall research design of the MILHY project as developed by Dr. Anderson's group at Bristol University over the last six years is shown in figure 2.1. The initial decision regarding MILHY1 related to utilisation of finite difference methods for runoff generation. Subsequent research identification suggested the need to examine alternatives for compound channel modelling and it is this development that is the major constituent of MILHY3. However, more general issues are raised here in the context of the interaction of hydraulic and hydrologic schemes, and their respective suitability for ungauged inundation modelling.

With the development of MILHY3 to larger watershed scales (1000 km²) the potential for hydraulic handling of this problem is deemed worthy of investigation. As we will discuss in Chapter 7 of this report, little work has been done on the application of 2-dimensional finite element models for river applications at this scale, let alone exploring the suggestion we make in our overall research strategy for examination of the possibility of coupling hydrological (MILHY3) and hydraulic schemes (RMA2) - see figure 2.1.

2.2 Research design for the current investigation

Any model design is essentially a two dimensional matrix of components. This is illustrated in general terms in figure 2.2. Decisions have to be made in the two principal areas: (1) submodel inclusion, and (2) resolution of the selected submodel. The area of submodel inclusion in general terms has been left unaltered from earlier versions of MILHY. It is the latter decision area that has proved the focus of the current research. In particular, we have sought to examine the effects of changes in the channel routing submodel, in the context of examining and implementing alternative models for compound channel flow conditions. In addition, a somewhat lesser effort has been expended in an examination of

the precipitation. Figure 2.2 shows the scope of the submodel resolution development. An important consideration here relates to achieving a submodel resolution that is considered, broadly at least, to be consistent between all submodels. This is an issue to which we will return; submodel resolution cannot of course be divorced from the resolution of the user supplied information (figure 1.1). Varying, perhaps unavoidable, resolution in the user supplied information may be considered, potentially at least, to have significant ramifications for submodel and model overall performance. Thus user supplied data resolution cannot, and should not, be divorced from model formulation, design and validation. Regrettably, in many cases, this association is not made. As we will discuss in later sections, this concept is central to the issue of design, implementation and validation of MILHY3.

1983	1984	1986	1989	1989----
<u>MILHY</u> Basic model	<u>MILHY1</u> CN replaced by physically based infil- tration scheme	<u>MILHY2</u> Validation at subcatchment scale and code enhancement	<u>MILHY3</u> Discrete rout- ing, turbulent exchange and large catch- ment validation	MILHY3 to be developed and utilised for cold region applicat- ions
		<u>Code of MILHY2</u> delivered to <u>WES</u>	<u>Code of MILHY3</u> delivered to <u>WES</u>	System implement- ation of MILHY3 and A.I. inclusion for user require- ments
				Coupling of MILHY3 and RMA2 for ungauged inundat- ion uses
				Application of <u>RMA2</u> to flood inundation at HEC

Figure 2.1 : Bristol University overall research design
for the MILHY project

Decision 1 : submodel inclusion

Precipitation	Land use	Infiltration	Subcatchment identification	Channel routing	Hydrograph
4. Higher resolution radar	3. Change model to include vegetation 2. K changes	4. 3-D modelling 3. 2-D finite difference	3. n ~ 40	4. 2-D Hydraulic finite element out-of-channel model	
MILHY3 - Model Resolution					
3. Radar 5 km grid	1. Organic matter-suction/	2. 1-dimensional infiltration	2. n ~ 8 subcatchments	3. Discrete routing methods. Turbulent exchange models	
2. 1 gauge per subcatchment		1. Green-Ampt style equation	1. Small computer: n ~ 3 sub-catchments	2. Hysteresis in stage-discharge	
1. Single gauge				1. Fixed Mannings n in channel - Simple reduction out of channel	

Decision 2 : Submodel resolution

See previous reports DAJA45-83-C-0029 and DAJA37-81-C-0221

Figure 2.2 : Component logic structure for MILHY3

3. IDENTIFICATION OF KEY PARAMETERS AND PROCESSES FOR CONVEYANCE

To achieve the main objective of improving the predictive capability of the conveyance section of MILHY, it was important firstly to identify the most important processes and parameters. An optimal method of identification would be to undertake a sensitivity analysis of an existing model of two-stage flow.

3.1 Difficulties of modelling two-stage channels

Two-stage channels consist of a main channel and adjoining floodplains which are subject to inundation. Water on the floodplains may be either stationary, where the floodplains act as stores of water, or flowing when the floodplains act as another channel.

3.1.1 The complexity of physical processes

Two-stage channels are a complex three-dimensional system. The inclusion of the floodplain system is not simply a matter of extending the cross-sectional area of the main channel. As Bhowmik and Demissie (1982) have shown, the carrying capacity of a two-stage channel is not directly proportional to cross-sectional area. Figure 3.1 illustrates the theoretical line of proportionality between area and discharge, and the relationship developed from field data collected from five rivers in the USA. From figure 3.1 it is possible to conclude that two-stage channels may not be considered as a single system.

Bhowmik and Demissie's data also confirmed flume studies by Rajaratnam and Ahmadi (1979), that there is interaction between the water on the floodplain and water in the main channel. Rajaratnam and Ahmadi (1979) found discontinuity in the velocity fields of the main channel and bed shear at the boundary between the channel and floodplain. Figure 3.2 shows the stage/velocity relationship in Salt Creek, USA, and illustrates the discontinuity of velocity in the main channel.

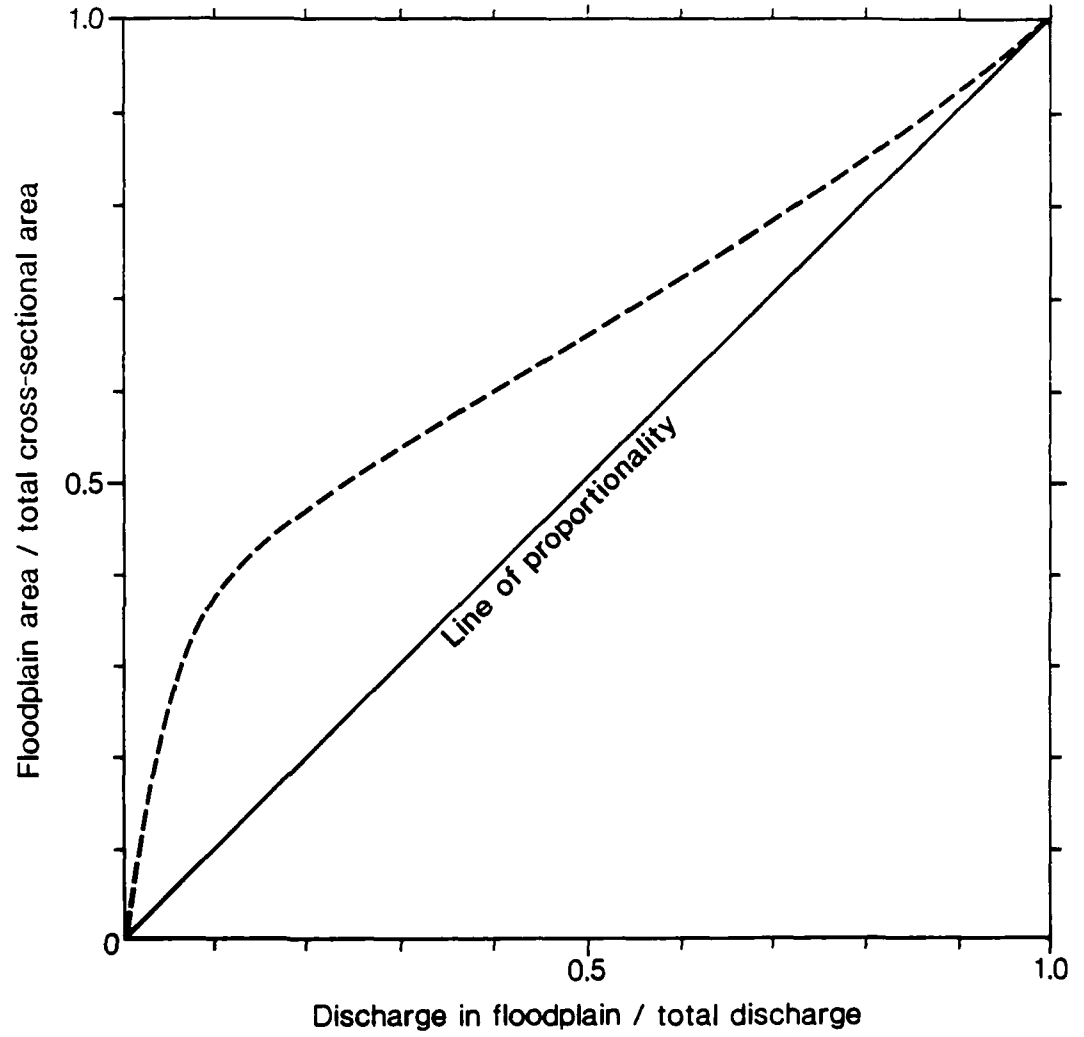


Figure 3.1 : Relationship between the carrying capacity and floodplain area (after Showmik and Demissie, 1982)

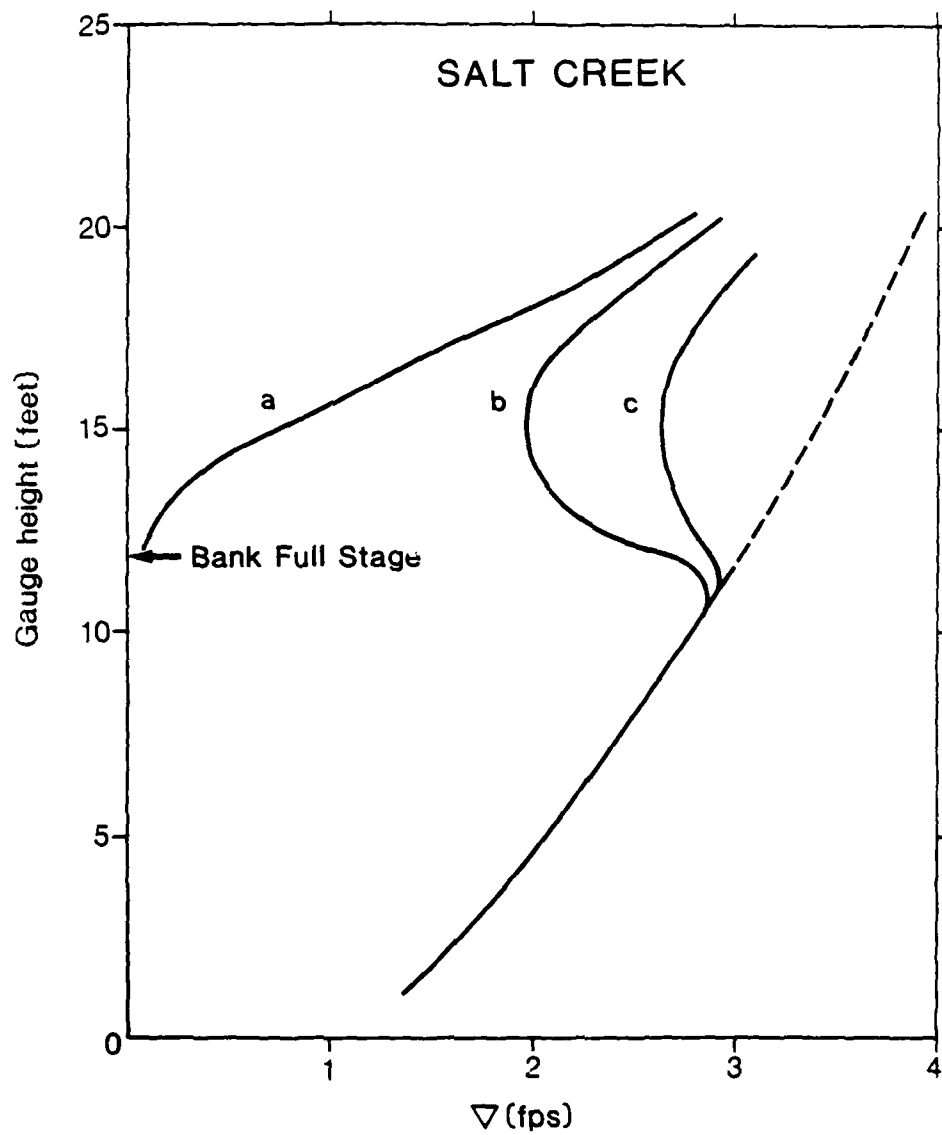


Figure 3.2 : Stage/velocity relationship in a two-stage channel (after Bhowmik and Demissie, 1982)
a - floodplain
b - combined
c - channel

The reduction in the velocity of flow in the main channel as overbank conditions are reached suggested that there was transverse mass transfer between the floodplain and the main channel, effectively retarding flows in the main channel and accelerating them in the floodplain. This momentum transfer may be envisaged to occur through the action of turbulent shear stresses, first recognised and photographed by Sellin (1964).

From figure 3.2, it can be seen that the minimum channel velocity occurs when the floodplain stage elevation is approximately 35% of the main channel stage, and that as floodplain stage increases the system converges to the composite value. Bhowmik and Demissie's results suggest, therefore, that the behaviour of the two-stage channel depends on the depth of inundation of the floodplain.

Plan geometry must also be included when attempting to expose the processes active in two-stage channels. Varying cross-sectional geometries associated with meandering main channels cause floodplain inundation at different points along a reach. Wolman and Leopold (1957) showed that the return period of floodplain inundation increased as the width/depth ratio of the main channel increased. The downstream and orthogonal floodplain slopes then determine if the floodplain water rejoins the main channel or, as Fread (1976) suggests, routes downstream along a different path to the main channel.

Toebes and Sooky (1967) in a series of flume experiments showed that the momentum transfer between floodplain and main channel flows are exacerbated where the floodplain flow is at an angle to the main channel flow, primarily in meandering flows. Chang (1983) showed that the increased energy expenditure in a mature meandering channel is due to:

- i) internal fluid friction caused by transverse circulation (secondary currents)

- ii) boundary resistance associated with transverse shear

With data from Poudre Supply Canal, Fort Collins, Colorado, Chang was able to conclude that where the depth/radius is high or the roughness is low, the transverse circulation energy losses may be greater than those associated with the primary or longitudinal flow.

3.1.2 Modelling alternatives

Research into modelling of two-stage channels has included both hydraulic and hydrologic approaches. Hydraulic engineers solve both the conservation of mass and a simplified form of the conservation of momentum (equations 3.1 and 3.2), whilst hydrologists use only the conservation of mass (equation 3.3) and a relationship between flow and storage.

Conservation of mass:

$$\frac{\partial(AV)}{\partial x} + \frac{\partial A}{\partial t} = 0 \quad 3.1$$

Conservation of momentum:

$$\frac{\partial V}{\partial t} + \frac{V\partial V}{\partial x} + g \left(\frac{\partial h}{\partial x} + S_o \right) = 0 \quad 3.2$$

Conservation of mass:

$$I - O = \Delta S / \Delta t \quad 3.3$$

A = area	S_o = friction slope
V = velocity	t = time
x = longitudinal axis	I = inflow
g = gravitational acceleration	O = outflow
h = stage	S = storage

Hydrologic approaches have been limited to one-dimension, whilst hydraulic models include both one and two dimensions and even a prototype three-dimensional turbulence model (Krisnappen and Lau, 1986).

One-dimensional approaches (solving the St. Venant equations of flow in hydraulic models) either:

- 1) treat the channel/floodplain cross-section as a single system and average boundary roughness and velocities
- 2) or treat the floodplain as an area for storing water only, for example, the Hydrologic Engineering Centre model (HEC-1, 1981)
- 3) or divide the cross-section into homogeneous segments of flow but do not consider momentum transfers between these segments, for example Tingsanchali and Ackermann (1976).

The two-dimensional process of momentum transfer between the main channel and floodplain segments can only be modelled using a two-dimensional hydraulic approach using the Reynolds equations. However, empirical relationships have been derived for the relationship between the boundary shear stresses, (apparent stresses produced by momentum transfer) and the cross-sectional geometry of the two-stage channel (Knight and Demetriou, 1983). Pasche and Rouve (1985) have developed a one-dimensional model incorporating these boundary shear stresses and a hydraulically-based velocity distribution. Incorporation of these boundary shear stresses is more fully investigated in section 4.

Modelling of the process of momentum transfer has been incorporated in two-dimensional hydraulically-based finite-difference and finite-element models. They usually employ one of the three methods below to quantify the effects of momentum transfer:

- 1) compute the force to provide equilibrium in each segment of flow (apparent boundary shear force)

- 2) compute effective friction factors for each segment
- 3) compute the iteration between a shear layer and the velocity profile (turbulence model)

An investigation of these models and the application of a finite-element model to a two-stage channel is reported in Section 7.

3.1.3 MILHY : present frictional capability

The handling of friction has remained unaltered in all versions of MILHY where it is handled as the Manning 'n' coefficient, utilized in the Manning equation (equation 3.4) to compute the stage/discharge capability:

$$v = \frac{R^{1/3} \cdot S^{1/2}}{n} \quad 3.4$$

The cross section is divided up by the user such that each segment of the section is frictionally homogeneous and hence one value of 'n' per segment is entered to compute the stage/discharge relationship. In selecting the most appropriate 'n' value for each segment, the user must consider the following factors:-

- 1) **surface roughness**
- 2) **vegetation**
- 3) **channel irregularity**
- 4) **channel alignment**
- 5) **silting and scouring**
- 6) **obstructions**
- 7) **size and shape of channel**
- 8) **stage and discharge**
- 9) **seasonal change**
- 10) **suspended material and bed load**

It is a difficult task to select one empirical 'n' value that successfully describes a particular channel. Manning's 'n' attempts to incorporate many of the physical processes active in the river channel system as well as the effects of boundary friction. The aim of the sensitivity analysis reported below is to identify which of the physical processes active in a two-stage channel are dominant. In later sections, alternative methods to the Manning's 'n' coefficient of handling these processes are investigated.

At present, the only additional complexity to the Manning's 'n' handling of friction incorporated in MILHY, is an algorithm (equation 3.5) to reduce the 'n' value with increasing stage.

$$n' = n - 0.0025R \quad 3.5$$

If the dominant process active in a channel is boundary roughness then this algorithm will improve the prediction of the carrying capacity of the cross-section. In the main channel as stage increases then the area of flow will increase faster than the wetted perimeter, thus reducing the retarding effects of friction along the wetted boundary (SCS, 1954). On the floodplains too, Manning's 'n' may decrease as the depth of inundation increases and the frictional effects of vegetation become less important. Table 3.1, taken from Chow (1959), illustrates this decline for pasture and meadows, typical in the floodplains of the River Fulda catchment in West Germany.

Petryk and Bosmajian (1975) showed, however, that this is an over-simplification of the frictional effects of vegetation. When the vegetation is submerged then 'n' will decrease with increasing stage, but below the top of the vegetation then there is a complex relationship between the vegetation density and Manning's 'n'. Petryk and Bosmajian (1975) used equation 3.6 to calculate the change in 'n' with depth.

$$n = n_b \sqrt{1 + \frac{C_d \sum A_v}{2gAL} \left(\frac{1}{n_b}\right)^2 R^{4/3}} \quad 3.6$$

Table 3.1
Mannings 'n' value for pasture and meadow floodplains
from Chow (1959)

Depth of Inundation (feet)	Mannings 'n' value	
	Pasture	Meadow
Less than 1	0.05	0.10
1-2	0.05	0.08
2-3	0.04	0.07
3-4	0.04	0.06
Over 4	0.04	0.05

where n_b = Manning 'n' value with vegetation effects
 C_d = vegetation drag coefficient dependent on vegetation type
 L = length of reach
 A_i = projected area of the i th plant
 A = cross-sectional area of flow

Petryk and Bosmajian (1975) scheme would not be suitable for the ungauged application, however it does show the inability of one Manning's 'n' value to represent the effects of all the conditions listed above. In two-stage channels this is even more of a problem as the dominant processes change as the floodwave overtops the main channel and floods out over the floodplains.

The n reduction algorithm, equation 3.5, assumes that boundary roughness is the dominant process; in the two-stage channel this is not the case. As stage increases enough so that the floodplain is inundated, not only is there a rapid increase in the wetted perimeter but turbulent eddies between the main channel and floodplains occur. The frictional effects of these eddies are much greater than the increase in boundary friction (Pasche and Rouve, 1985).

However, in application of MILHY2 to two-stage channels in the River Fulda catchment, a more immediate problem occurred. As floodplain inundation depths increased, the hydraulic radius increased such that n' in equation 3.5 became negative. An example of this problem is found in Table 3.2, illustrating a typical stage/discharge relationship produced by MILHY2 under out-of-bank conditions. For this reason the algorithm has been removed from MILHY3 and is not included in any of the simulations reported here.

The aim of the work reported here is therefore to retain the Manning 'n' coefficient to incorporate the boundary friction effects on the floodplain and all of the ten factors identified earlier for the in-bank channel. Incorporation of the additional frictional effects in the two-stage are investigated in section 4 and 5.

Table 3.2

Rating curve valley section		
Water surface Elev.	Flow area sq. ft.	Flow rate CFS ($\times 10^3$)
591.88	86.4	0
595.45	299.6	1
599.02	573.3	3
602.59	1030.0	7
606.16	4106.6	12
609.73	8436.7	63
613.30	12920.8	256
616.86	18078.9	35615
620.43	23984.5	-54
624.00	30582.6	-327

MILHY2 ROUGHNESS
REDUCTION FORMULA:
 $n' = n \sim 0.0025R$

3.2 Selection of a two-stage conveyance model

From section 3.1 it would seem that a successful conveyance model must incorporate:

- 1) plan and cross-sectional geometries
- 2) momentum transfer of flow between floodplain and main channel segments

An ideal solution therefore would be a two-dimensional hydraulic model. However, as Section 7 will show, such models have not been applied to the scale of the reach under investigation here (i.e. greater than 10 km in length). A one-dimensional approach was therefore accepted.

From the literature it seemed that most of the investigations into two-stage channel conveyance have concentrated on the transfer of momentum across the section and techniques for its inclusion are well established. It was seen as a priority, therefore, to select a one-dimensional model which would permit concentration of the sensitivity analysis on plan geometry processes and parameters. Hence, the model selected was a state-of-the-art model developed by Ervine and Ellis (1937), which considers the three-dimensional system using a series of analytical equations.

3.2.1 The Ervine and Ellis Model

Ervine and Ellis' model allows a meandering plan geometry to be modelled by dividing flow into three segments, shown on figures 3.3a and b, and defined as:

- 1) main channel flow
- 2) floodplain flow contained within the meander belt of the main channel
- 3) floodplain flow outside of the meander belt

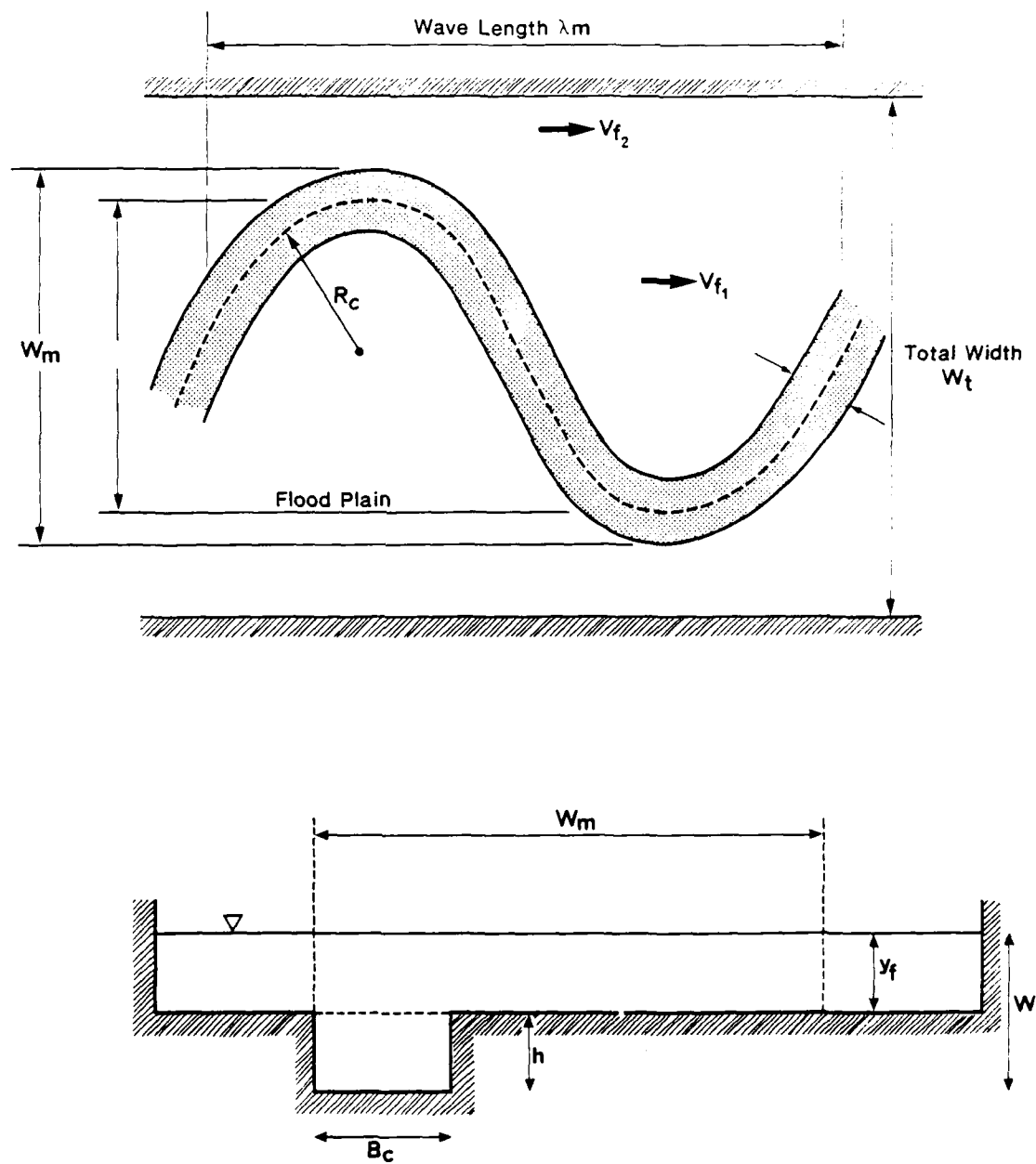


Figure 3.3 : Definition diagrams for Ervine and Ellis (1987) scheme

For each segment, the energy loss is computed and hence the mean velocity for each segment and discharge total are calculated. Ervine and Ellis firstly identified the main sources of energy loss of each segment of flow and then brought together a series of geometric and fictional relationships to explain them.

Main channel energy losses

Ervine and Ellis considered there to be four possible sources of energy loss:-

- a) frictional losses at the boundaries
- b) transverse currents (secondary currents) at meander bends
- c) turbulent shear stress (momentum transfer to floodplains)
- d) pool/riffle sequences causing head loss at low flows

Ervine and Ellis chose to omit the turbulent shear stresses and pool/riffle losses in their computation. Shear stresses were omitted because three-dimensional interpretations of established techniques (e.g. Knight and Demetriou (1983)) are still under investigation by Willetts (see Ervine and Ellis (1987)). Pool/riffle losses are considered less important in times of overbank flow, when bed form effects are usually flooded out.

Floodplain energy losses

Two sources of loss were identified:

- a) frictional losses at the boundaries
- b) expansion and contraction losses, shown in figure 3.4, where flow orthogonal to the main channel, suddenly expands as it drops into the channel, and contracts as it re-enters the floodplain region

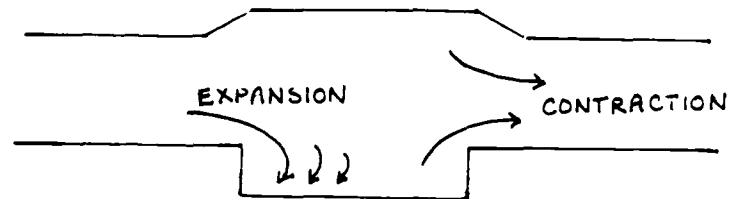


Fig. 3.4

3.2.2 Quantifying the energy losses

Main channel energy losses

a) Friction

Head losses due to friction are computed over a meander wavelength ($r\lambda_m$) as:

$$h_f = \left(\frac{f_c}{4}\right) \left(\frac{r\lambda_m}{R}\right) \frac{V_c^2}{2g} \quad 3.7$$

where f_c is the Colebrook-White friction factor, given by

$$\frac{1}{\sqrt{f_c}} = -2 \log \left(\frac{K}{14.8R} + \frac{2.51}{Re \sqrt{f_c}} \right) \quad 3.8$$

b) Transverse currents

Head losses due to secondary currents at meander bends are computed using a simplified method developed by Chang (1983). Chang used a mean transverse current (secondary current) velocity because over a meander amplitude, the velocity varies from a maximum at the apex to a theoretical zero at the cross-over thalweg. Chang ignored the effects of superlevation, where centrifugal forces cause the water level on the outside of the bend to be higher than those on the inside; (Yen, 1967, showed

that in two-stage flow, superelevation effects are suppressed by the head of water above the main channel).

Head loss due to transverse currents computed over a meander wavelength is given by:

$$h_L = \left[\frac{2.86\sqrt{f_c} + 2.07f_c}{0.565 + \sqrt{f_c}} \right] \left(\frac{R}{R_c} \right)^2 \left(\frac{r\lambda_m}{y_c} \right) \frac{V_c^2}{2g} \quad 3.9$$

Floodplain within the meander belt width

a) Friction

As in the main channel, the total frictional head loss along a meander wavelength is described by:

$$h_f = \left(\frac{f_{f1}}{4} \right) \left(\frac{1}{y_f} \right) \left(\frac{V_{f1}^2}{2g} \right) W_m \lambda_m - r \lambda_m B_c \quad 3.10$$

where the last term is the wetted area.

b) Expansion losses

Assuming; $y_c \approx y_f + h$ 3.11

the head loss due to expansion of floodplain flow into the main channel over a meander wavelength is given by:

$$h_e = r \lambda_m \left(1 - \frac{y_f}{y_c} \right)^2 \cdot \frac{V_{f1}^2}{2g} \cdot \sin^2 \bar{\theta} \quad 3.12$$

where $\bar{\theta}$ is the average mean angle of the floodplain flow to the main channel over a meander wavelength.

c) Contraction losses

The total head loss due to contraction if floodplain flow leaving the main channel (illustrated in fig. 3.4) is given by

$$h_c = C_L \cdot \frac{V_{f1}^2}{2g} \cdot \sin^2 \bar{\theta} \cdot (r \lambda m) \quad 3.13$$

where C_L is a loss coefficient, generated by Yen and Yen (1984), and is a function of:

- i) the density, specific weight and kinematic viscosity of the flow
- ii) meander wave length and amplitude, the mean angle of incidence of floodplain flow to the main channel, the valley width, valley slope, floodplain roughness, and the width and depth of the main channel
- iii) discharge and shape

Yen and Yen (1984) using data collected from flume experiments computed the total loss coefficient after flow had been subjected to expansion and contraction. Then assuming

$$C = C_E + C_L \quad \text{where } C = \text{total loss coefficient} \quad 3.14$$

$C_E = \text{loss coefficient due to expansion}$

$C_L = \text{loss coefficient due to contraction}$

$$\text{and } C_E = \left(1 - \frac{y_f}{y_c}\right)^2 \quad \text{as in 3.12} \quad 3.15$$

the contraction loss coefficients were computed, as shown in Table 3.3.

Yen and Yen consider that these coefficients should be treated as upper limits because the channel sidewalls in their flume experiments were vertical rather than a more realistic trapezoidal slope.

Floodplain flow outside the meander belt

a) Friction

In the floodplain outside the meander belt, flow is considered to be uniform, therefore the friction slope is given by

$$S_o = \left(\frac{f_{f2}}{4} \right) \left(\frac{1}{y_f} \right) \cdot \frac{V_{f2}^2}{2g} \quad 3.16$$

Combining all the head loss equations, Ervine and Ellis (1987) obtained:-

i) for the main channel

$$\left(\frac{f_c}{4} \right) \left(\frac{r \lambda_m}{R} \right) \frac{V_c^2}{2g} + \left[\frac{2.86 \sqrt{f_c} + 2.07 f_c}{0.565 + \sqrt{f_c}} \right] \quad 3.17$$

$$\left(\frac{R}{R_c} \right)^2 \cdot \frac{r \lambda_m}{R} \cdot \frac{V_c^2}{2g} = S_o \lambda_m$$

ii) for the floodplain inside the meander belt width

$$\left(\frac{f_{f1}}{4} \right) \left(\frac{1}{y_f} \right) \left(\frac{V_{f1}^2}{2g} \right) (W_m y_m - \lambda_m B_c r) + \quad 3.18$$

$$r \lambda_m \cdot \left(\frac{V_{f1}}{2g} \right) \sin^2 \bar{\theta} \left[\left(1 - \frac{y_f}{y_c} \right)^2 + C_L \right] = S_o \lambda_m W_m$$

Table 3.3 : Contraction Loss Coefficients
(after Yen and Yen, 1984)

y_F											
y_C	0.0	0.1	0.2	0.3	0.4	0.5	0.6	0.7	0.8	0.9	1.0
C_L	0.5	0.48	0.45	0.41	0.36	0.29	0.21	0.13	0.07	0.01	0

iii) for the floodplain outside the meander belt width

$$\left(\frac{f_{f_2}}{4}\right)\left(\frac{1}{y_f}\right)\frac{V_{f_2}^2}{2g} = S_o \quad 3.19$$

alongside with total discharge, using the continuity equation which is given by

$$Q = V_c (B_c h) + V_{f1} (y_f W_m) + V_{f2} y_f (W_t - W_m) \quad 3.20$$

3.3 Sensitivity Analysis of the Ervine and Ellis Model

The objective of undertaking a sensitivity analysis of Ervine and Ellis' model was to identify the physical processes controlling the velocity and discharge predictions. Once identified the most appropriate method of incorporating these processes into the MILHY scheme can be investigated.

3.3.1 Sensitivity analysis design

Analysis of equations 3.7 to 3.16 and 3.20 identified five groups of parameters which controlled the processes identified and modelled by Ervine and Ellis. These five groups are:-

- i) slope
- ii) plan geometry (channel width, floodplain, meander belt width and radius of curvature)
- iii) depth of flow (in channel and floodplain segments)
- iv) sinuosity (sinuosity and angle of incidence of floodplain flow to the main channel)
- v) friction (for consistency with later MILHY analysis the sensitivity of the model to Manning 'n' was used, utilizing the conversion equation 3.21, below):

$$f = \frac{8gn^2}{R^{1/3}} \quad 3.21$$

Each of these five groups were investigated individually by varying each group independently by a systematic 30% and 5% reduction and 5% and 30% increase in parameter values.

The model was applied to a hypothetical reach because the sinuosity variables only allow for a constant amplitude and wavelength values for the main channel throughout the reach length. However, all parameter values were taken from topographic information collected from the River Fulda, West Germany. The values applied are shown in Table 3.4 and the velocity predictions for each flow segments and discharge predictions by the model for these values are also shown. Observed stage/discharge relationships from the River Fulda confirm that these model predictions give realistic discharge values.

3.3.2 Results

The results from the sensitivity analysis are tabulated in Tables 3.5 to 3.9, and show the percentage deviation from the computed values tabulated in Table 3.4. Below is an analysis of the velocity predictions by considering each of the sources of head loss identified by Ervine and Ellis:

- i) Frictional losses are modelled in all three flow segments and Table 3.5 to 3.7 show that variation in the frictional parameter values cause the largest variation in the velocity predictions. However, in the main channel the Darcy-Weisbach friction factor is also linked to the modelling of the transverse (secondary) circulation. From the first term in equation 3.9, it can be seen that as the friction factor decreases, head losses from the transverse currents decrease, and when the friction factor increases head losses are increased. Therefore the velocity variations shown in Table 3.5 incorporate both friction head losses and transverse circulation losses.
- ii) The transverse circulation in the main channel can be attributed to friction (as noted above) and the ratio of hydraulic radius to radius of curvature. This ratio is included in the geometry variation reported on Table 3.5, which shows that the velocity predictions are

Table 3.4: Parameter specification for hypothetical reach

	<u>SI units</u>
Bed slope	0.0007
Sinuosity	1.3
Hydraulic radius	2.5
Radius of curvature	125.0
Width of meander belt	175.0
Total floodplain width	300.0
Channel width	30.0
Friction channel (f)	0.071
Friction floodplain 1	0.356
Friction floodplain 2	0.356
Depth channel	3.5
Depth flood plain	0.5
Angle of flood plain flow to channel (radians)	0.785
Contraction loss coefficient	0.47
 <u>Results</u>	
Main channel velocity	1.205
Floodplain, area 1 velocity	0.360
Floodplain, area 2 velocity	0.278
Discharge	157.2

Table 3.5: Channel Velocity Results
 (% deviation from origin velocity)

% Change in variable	Decrease 30%	Decrease 5%	Increase 5%	Increase 30%
Slope	-19	-2	+ 3	+13
Channel friction	+50	+5	- 4	-24
Geometry	- 5	-0.5	+ 1	+ 3
Sinuosity	+20	+3	-11	- 12

Table 3.6: Flood plain (area 1) velocity results
(% deviation from origin velocity)

% Change in variable	Decrease 30%	Decrease 5%	Increase 5%	Increase 30%
Slope	-19	- 2	+ 3	+13
Friction	+23	+ 5	- 4	-27
Geometry	- 4	- 0.5	+ 1	+ 2
Sinuosity	+ 1	0.0	0.0	- 1
Contraction coefficient	0.0	0.0	0.0	0.0

Table 3.7: Floodplain (area 2) velocity results
(% deviation from origin velocity)

% Change in variable	Decrease 30%	Decrease 5%	Increase 5%	Increase 30%
Slope	-19	- 2	+ 3	+13
Floodplain friction	+25	+ 5	- 5	-28

Table 3.8: Flow depth effects on velocity and discharge
(% deviation from origin)

Depth (metres)		Channel Velocity	Flood Plain Velocity		Discharge
Y_f	Y_c		Area 1	Area 2	
0.33	2.31	-12	-33	-23	-29
0.475	3.325	- 2	-20	-20	-19
0.525	3.675	+ 4	-15	-16	-16
0.665	4.635	+15	- 5	- 5	- 4
0.33	3.5	-	-18	-19	-14
0.475	3.5	-	- 2	- 2	- 2
0.525	3.5	-	+ 2	+ 3	+ 2
0.665	3.5	-	+15	+15	+16

Table 3.9: Discharge results
 (% deviation from origin discharge)

% Change in variable	Decrease 30%	Decrease 5%	Increase 5%	Increase 30%
Slope	-19	- 2	+ 3	+13
Channel friction	+35	+ 4	- 3	-17
Floodplain friction	+15	+ 2	- 1	- 9
Geometry	-28	- 4	+ 4	+27
Sinuosity	+14	+ 2	- 8	- 9

not sensitive to geometric variation in the channel. As noted above, however, the model is sensitive to the frictional aspects of the transverse circulation.

- iii) Sinuosity changes generate significant variability in the channel velocity results (Table 3.5). From equation 3.17 it can be seen that the sinuosity term is used to calculate channel length in both the frictional head loss and transverse circulation computations. For the main channel, therefore, the model can be interpreted as being sensitive to channel length.

On the floodplain within the meander width belt (area 1), Table 3.6 shows the velocity predictions are not sensitive to sinuosity variations. From equation 3.18 it can be seen that sinuosity is utilized to compute the flow path length and the angle of incidence of floodplain flow to main channel flow used in the calculation of the expansion and contraction head loss. From Table 3.6 it would seem reasonable to conclude that because of the linear flow path the velocity predictions are not affected by the length of the path, and it is not necessary to include the angle of incidence of floodplain flow in the modelling of expansion and contraction head losses. Table 3.6 also shows that the exact value of the Yen contraction loss coefficient need not be of concern to the modeller.

- iv) The effect of slope variations on velocity predictions were only significant where variation was large (+ 30%), seen in Tables 3.5 to 3.7. For the purposes of this sensitivity analysis the frictional slope (S_o) was assumed to be parallel to the bed slope, S , hence uniform flow was assumed. However, the sensitivity analysis tested the effects of frictional slope variation on the velocity and discharge predictions. The effects of different slopes in the main channel and floodplain areas are not directly included in the Ervine and Ellis model.
- v) The impact of variation in the depth of flow on the floodplain velocity results are shown in Table 3.8. Equation 3.17 shows that

the main channel depth is incorporated in the velocity computation as hydraulic radius, and analysis of intermediate computations in the analysis shows it is the hydraulic radius in the frictional head loss computation to which the velocity results are sensitive.

On the floodplain within the meander belt, equation 3.18 shows it is the ratio of floodplain to channel depth that is utilized to compute expansion and contraction head losses (see the lower four results on Table 3.8). However, the velocity predictions for floodplain area 2 are identical to those in floodplain area 1 and as the headloss in area 2 is entirely attributable to friction (equation 3.19), it would seem that the velocity variations in areal are due to the same frictional effects, and not due to expansion and contraction losses.

Tables 3.8 and 3.9 illustrate the effects of variability in the five groups identified on the discharge predictions computed using equation 3.20. Geometry is the only group to create additional influence on the discharge predictions, over those on the velocity results reported above. The geometry variables effectively weight the velocity results for each flow area based on their cross-sectional area, to give total discharge.

3.3.3 Conclusions

From the analysis of the results above, it is possible to make several conclusions:-

- i) The Ervine and Ellis scheme is highly sensitive to the Darcy-Weisbach friction factor.
- ii) The model is sensitive to the depth of inundation (incorporated in the computation of frictional headlosses) in all flow areas.
- iii) The sinuosity of the main channel is important in determining the length of the flow path and hence time to peak in a hydrograph.

- iv) The incorporation of headloss due to expansion and contraction of floodplain flow as it crosses the main channel is best achieved through the friction headloss computation.

3.4 Implications for the improvement of MILHY

The conclusions from the sensitivity analysis of the Ervine and Ellis scheme isolate friction as being the single most important factor in the prediction of discharge in two-stage channels. Friction is identified, therefore, as being the key to improving the conveyance capabilities of MILHY. The analysis showed that handling of frictional headlosses can successfully incorporate both boundary roughness effects and the effects of transverse currents in the meandering channels. The second area, and worthy of investigation in order to upgrade the predictive performance of MILHY, was the impact of the relatively longer, sinuous path length of the main channel over the floodplain.

Three key processes that need further investigation have, therefore, been identified; these are:

1. improvement of the handling of friction to incorporate boundary roughness and transverse circulations within the main channel
2. incorporation of turbulent shear stresses between the main channel and floodplain flow segments
3. different path lengths for main channel and floodplain areas to incorporate sinuosity

3.4.1 Incorporation of the effects of turbulence into MILHY

An objective identified by the sensitivity analysis is therefore to incorporate the effects of turbulence into the modelling of conveyance in MILHY. Two significant sources of turbulence have been identified as:

- 1) apparent shear stresses between floodplain and channel flow segments
- 2) transverse circulation stresses generated at meanders of the main channel

The relative importance of these two sources and the interaction between them is not clear from the literature although it is dependent on the depth of flow on the floodplain. Because the analysis of the Ervine and Ellis scheme suggests the effects of transverse circulations at meander bends could be successfully incorporated in modelling of boundary friction, it was decided to concentrate our investigation of the handling of turbulence modelling on the shear stresses between flow segments. This investigation is reported in Section 4. It is hoped that the incorporation of the transverse circulation effects can be investigated in the next eighteen months.

3.4.2 Incorporation of multiple routing pathways

As the analysis of the Ervine and Ellis scheme and Fread (1976) suggest, the different path lengths of the sinuous main channel and straight floodplain flows will affect the timing of a floodwave travelling downstream. At present, MILHY models a single pathway for floodplain and channel flows using a mean channel length and travel timetable. A priority, therefore, was to investigate alternative methods of incorporating these multiple pathways of flow through the reach. This investigation is reported in Section 5.

3.5 Logical development of a research scheme

In order to achieve the objectives of incorporating the two processes identified in Section 3.4, it was necessary to select and implement processes generally only modelled in hydraulically-based schemes. This raised a key issue in the MILHY3 project, which was how far can we successfully model channel hydraulics in a hydrological model and when does the user need to switch to a hydraulically-based model such as RMA-2? It seems that the user's decision on whether to use a hydrologically or

hydraulically-based scheme has been, in the past, based only on his experience, rather than on a clearly defined set of rules. In most applications, the user's experience is sufficient to correctly select hydrological models for initial passes at problems and ungauged applications, and hydraulic models for detailed engineering applications. However, there remains a 'middle-ground' of applications where data availability may be difficult or its quality poor, or where the user requires only reach outflow data but for a complex application. For these 'middle-ground' applications it is not clear if the user should pursue a hydraulically-based scheme with often extensive set-up and run times, or would be better selecting a simpler hydrologically-based scheme. The margin of error in either approach for these 'middle-ground' applications needs to be defined so that a series of operational rules may be developed.

The logic of the work reported here, therefore, is:-

- i) having identified the areas worthy of investigation in order to improve the downstream routing capability in Section 3, to
- ii) implement these improvements by selecting and modifying hydraulic processes into a hydrologic scheme - MILHY3, then to
- iii) test and validate MILHY3 against MILHY and MILHY2 on the River Fulda catchment, and finally to
- iv) develop a set of operational rules for the application of hydrological and hydraulically-based schemes by a comparative study between MILHY3 and RMA-2.

3.5.1 Implementation of research scheme

Having achieved the point aim in the research scheme of identifying and selecting areas worthy of investigation, the next stage of the research is to investigate how the selected two processes, momentum transfer between flow segments and short-circuiting of floodplain flows, may best be

incorporated into MILHY. These two processes are investigated individually in Sections 4 and 5 where alternative approaches are examined, the most appropriate selected and a series of initial tests run to check the validity of the improvements individually.

Once satisfied that the incorporation of these two processes improves the predictive capability of MILHY's downstream routing component when applied individually, the performance of MILHY3 is tested as a rainfall-routing model against MILHY2 and field data on the River Fulda catchment. This analysis is reported in Section 6.

Lastly, the comparative study between MILHY3 and RMA-2 is reported in Section 7.

3.5.2 Work identified for the next eighteen months

Section 3.4 indicated that there are other important processes and parameters worthy of further investigation that are beyond the scope of the three-year research period reported here. The key processes parameters identified were ranked according to their order of importance and the two most significant processes were implemented and validated. The investigation of the hydrology/hydraulic model trade-offs was not anticipated when the original research proposal was submitted, however it was felt that this issue was of importance for the MILHY project and of interest in many other areas.

It is hoped in the next eighteen months to continue the hydrology/hydraulic question by investigating the utility in linking these two types of models. This point is examined further in Section 7. In the next eighteen months it will also be possible to investigate the processes active in an in-bank meandering channel.

4. INCORPORATION OF MOMENTUM TRANSFER BETWEEN FLOODPLAIN AND CHANNEL SEGMENTS

The transfer of momentum between the main channel and floodplain flow segments was identified in section 3.4 as a process which it was felt would, if incorporated into MILHY's downstream routing scheme, make a significant improvement to the overall predictive capability of MILHY. The objective of the work reported in this section, therefore, was to investigate, implement and validate a method of incorporating momentum transfer between flow segments whilst maintaining MILHY's parsimonious data requirements.

4.1 The hydraulics of momentum transfer

In two-stage channels, the irregular cross-sectional geometry of the deep main channel, and its associated shallow floodplains, generate higher channel velocities in the main channel than those in the floodplain flow segments. This is due to the relatively greater depth of flow and smaller wetted perimeter of the main channel in comparison to the floodplain. Figure 4.1 illustrates the velocity isovels for a two-stage flume experiment conducted by Knight et al. (1983). The velocity isovels are dimensionless parameters because the observed values are divided by the mean velocity for cross-section, where $V = Q/A$. The difference in the flow velocity between the main channel and floodplain cause a transfer of longitudinal momentum generally from the main channel to the floodplain.

The physical mechanisms by which linear momentum is transported perpendicular to the direction of flow are:-

- 1) secondary currents
- 2) eddies generated in the mixing zones of stream tubes of differing velocities
- 3) eddies generated by flow along a boundary
- 4) molecular motion

Wright and Carstens (1970) ranked these processes on a scale of one to four in order of their effectiveness at transporting momentum. Figure 4.2 shows the first two processes listed above, and illustrates the position of the

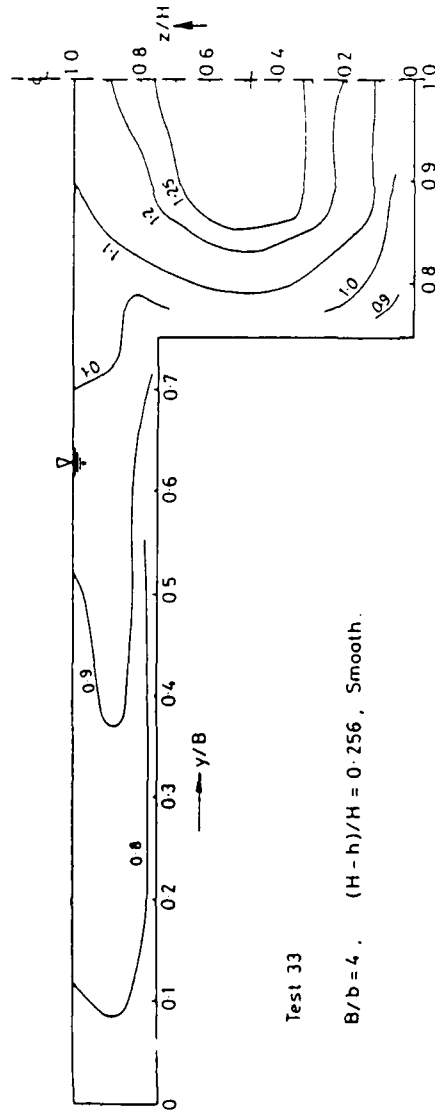


Figure 4.1 : Dimensionless isovels for a two-stage channel
(after Knight et al., 1983)

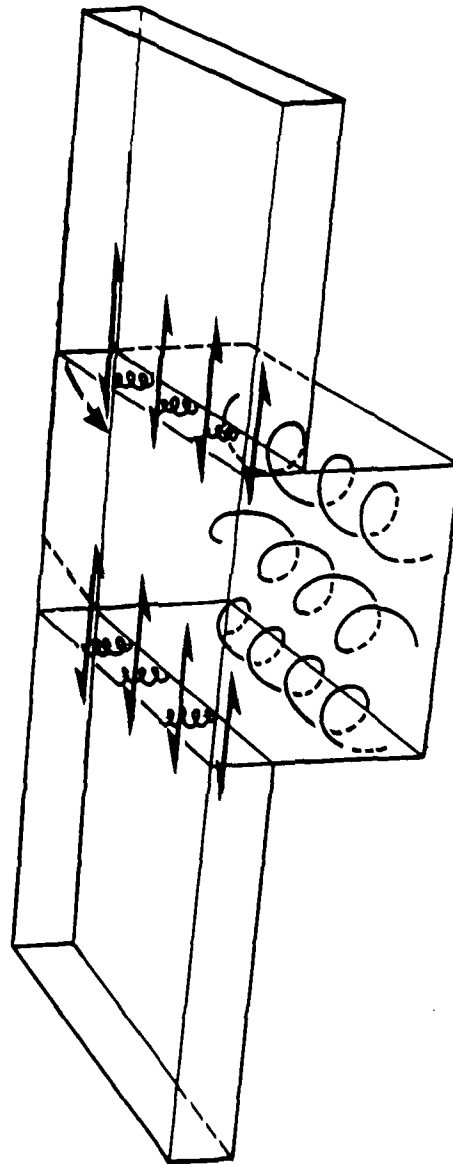


Figure 4.2 : Linear momentum transfer by secondary currents and turbulent eddies of the main channel/floodplain interface

eddies generated in the mixing zone between the floodplain and the main channel.

As suggested earlier in section 3.4, the dominant process in two-stage channels is the turbulent eddy in the mixing zones between the main channel and floodplain (Pasche and Rouve, 1985). Myers (1978) confirmed this when he observed that the shear stresses obtained in two-stage experimental flume channels were much greater than those exerted in the main channel.

The momentum transfer distorts the shear stress profiles on the beds of the main channel and floodplain, and increases the shear stresses on the floodplains near the junction with the main channel. Associated with the flow interaction are high shear stresses on the interfaces between the main channel and the floodplain regions, the average shear stress on these interfaces being known as the apparent shear stresses.

A great deal of research on the transfer of momentum in two-stage channels has been carried out in the last twenty-five years, starting with Sellin (1964) and Zheleznyakov (1965). Sellin (1964) was the first to identify the turbulence at the interface between main channel and floodplain by photographing the vortices generated by the turbulence in a flume study. Zheleznyakov found in both flume (1965) and field experiments (1971) that the momentum transfer mechanism decreased the overall rate of discharge for floodplain depths just over bankful. Wright and Carstens (1970) described the apparent shear stresses as a drag, retarding main channel flows and acting as a propulsion on the floodplain flows. Radojkovic (1976) pointed out the dependence of the shear stress on the velocity difference between the main channel whilst Rajaratnam and Ahmadi (1981) concluded that if the shear velocity were known, the logarithmic velocity distribution law can be applied to predict floodplain velocities and hence discharges. Recent research into the behaviour of two-stage channels, for example Holden and James (1989), has concentrated on quantifying the physical processes determining the rate of momentum transfer and collecting data which will allow the shear stress distribution to be modelled. In the United Kingdom, the Science and Engineering Research Council are funding a large flume-based research project taking place in four universities (Knight, University of

Birmingham, Sellin, University of Bristol, Wormleaton, Queen Mary College, London, and Myers, University of Ulster).

4.2 Modelling of momentum transfer

4.2.1 A theoretical approach

If a regular two-stage channel experiencing uniform flow is analysed, then the total retarding shear force acting on the wetted perimeter is equal to the gravitational force acting downstream. The gravitational component is given by:

$$F_g = w A_t S_o \quad 4.1$$

where w = weight of water per unit length of channel

A_t = total cross-sectional area

S_o = bed slope

The boundary shear force per unit length is given by:

$$F_b = \tau_c P_c + \tau_f P_f \quad 4.2$$

where τ_c and τ_f = average boundary shear stresses for the channel and floodplain solid boundaries respectively

P_c and P_f = wetted perimeters of the channel and floodplain

Equations 4.1 and 4.2 must balance for the two-stage channel cross-section but they must also balance for the individual floodplain and channel flow segments. However, if the flow segments are considered individually then part of the boundary shear force is provided by the apparent shear stress force acting on the boundary between the flow segments. Thus in the case of the main channel the total retarding force per unit length is given by:

$$F_{sc} = \tau_c P_c + \tau_{ai} P_{ai} = F_{bc} + 2F_a \quad 4.3$$

where τ_{ai} = apparent shear stress acting upon the assumed interface i
 P_{ai} = length of assumed interface i
 F_{bc} = main channel solid boundary shear force

Figure 4.3 illustrates these forces for a theoretical example where the apparent shear stresses are assumed to be acting on a vertical planar boundary where the channel and floodplain meet. Rewriting equations 4.1 and 4.2 for the channel segment only and combining them with equation 4.3 gives:

$$\tau_{ai} = \frac{1}{P_{ai}} (wA_{ci} \cdot S_o - \tau_c P_c) \quad 4.4$$

In any application A_{ci} , P_c and S_o are known from the geometry of the cross-section and a length for P_{ai} can be assumed. In the flume the average boundary shear stresses, τ_c may be measured and so τ_{ai} can be estimated using equation 4.4. The discharge for each flow segment can then be computed from the corrected retractive forces.

However, in an ungauged catchment, it is extremely unlikely we would have boundary shear stress data available and unlikely that we know or can estimate the length of the apparent shear stress boundary. We are not suggesting, therefore, that this type of analysis be incorporated into MILHY but investigation of the application of this method in flume experiments does provide a useful insight into the relationship between the cross-sectional geometry, apparent shear stress interfaces and accuracy of the discharge prediction.

4.2.2 Flume experiments investigating apparent shear stresses

Flume-based research programmes provide, at present, the only means of collecting data on the distribution boundary shear stresses which will enable us to understand and later model the processes active in two-stage channels. Field data of two-stage flood events are notoriously difficult and sometimes dangerous to collect. The variable nature of flood events means that flows are never steady enough to allow even reasonable measurement of the velocity fields, while field measurement of boundary

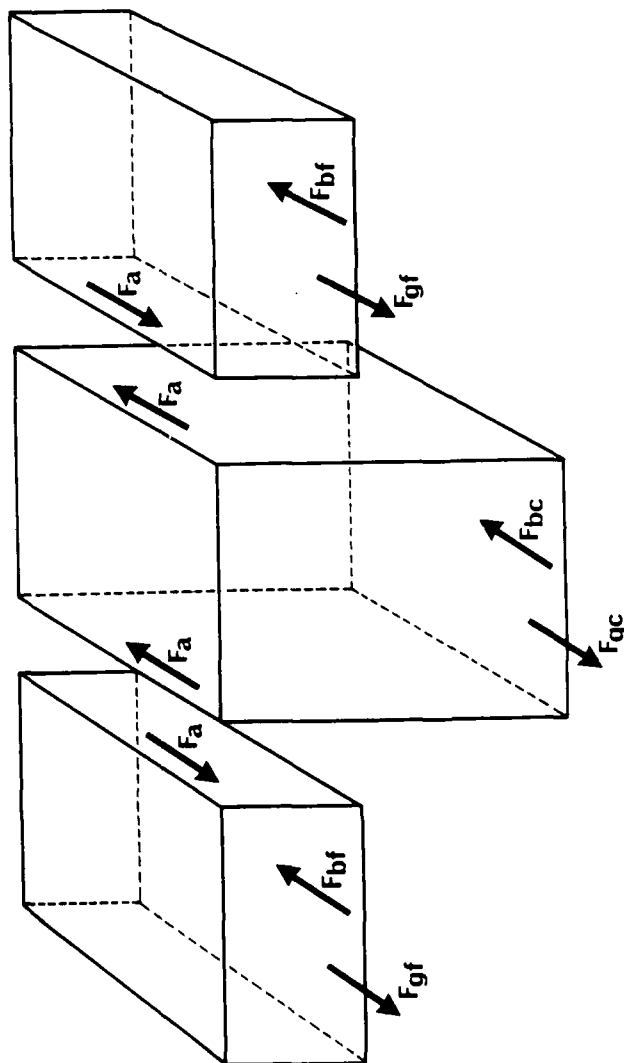


Figure 4.3 : Two-stage channel illustrating the gravitational boundaries and shear stress interfaces in each flow segment

shear stresses are almost impossible to collect. Reliance on flume-based investigations has therefore led to an extensive programme of modelling a variety of geometrical and roughness environments.

In these flume experiments the principal objective of the investigators is to develop a relationship between the stage and discharge in the main channel and floodplain flow segments. The investigators hope to achieve this objective by solving equation 4.4 using observed flume data to compute the apparent shear stresses from the solid boundary shear stresses. The boundary shear stresses are computed using either the Prandtl-von Karman velocity law, utilizing observed velocity data, or using Patel's (1965) relationship between head difference and boundary shear stresses. As noted earlier, however, and seen in equation 4.4, the value of the computed apparent shear stress is dependent on the length of the assumed interface over which the apparent shear theoretically acts. Figure 4.3 illustrates an assumed interface in a vertical plane, a method which has been utilized by Chow (1959) and Wright and Carstens (1970). Figure 4.4 shows the vertical plains and diagonal interfaces used by Wormleaton et al. (1980), and Yen and Overton (1973). and the horizontal interfaces utilized by Deuller et al. (1967).

Wormleaton et al. (1982) carried out a comparative investigation of the apparent shear stresses computed over the three types of planar interface. Their results were reported as an apparent shear stress ratio, that is the ratio of the apparent shear stress to the average shear stress including the assumed interface. As the apparent shear stress tends to zero, the ratio will also tend to zero, implying no shear on the interface. The results of Wormleaton et al. (1982) are shown on Figure 4.5 a, b and c for the vertical, diagonal and horizontal interfaces respectively, where the apparent shear stress ratio and an inundation ratio are compared. The inundation ratio is defined as the depth of flow on the floodplain divided by the depth of the main channel. The series A, B, C and D illustrate the effects of increasing the floodplain Manning's roughness from 0.011 for series A through 0.014 (B), 0.017 (C), to 0.021 series D.

Analysis of Figure 4.5 a, b and c shows that the apparent shear stress declines with increasing depth of flow on the floodplain in all three planar

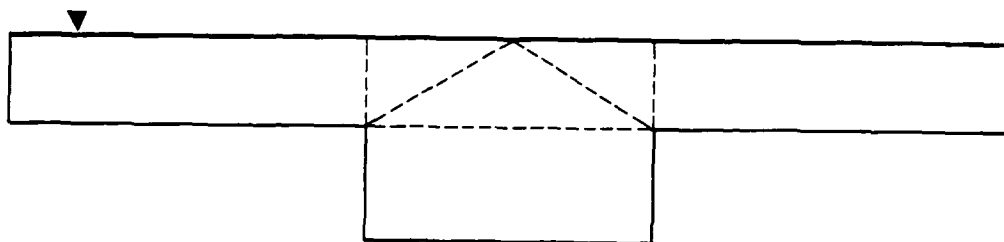


Figure 4.4 : Vertical, diagonal and horizontal apparent shear stress interfaces

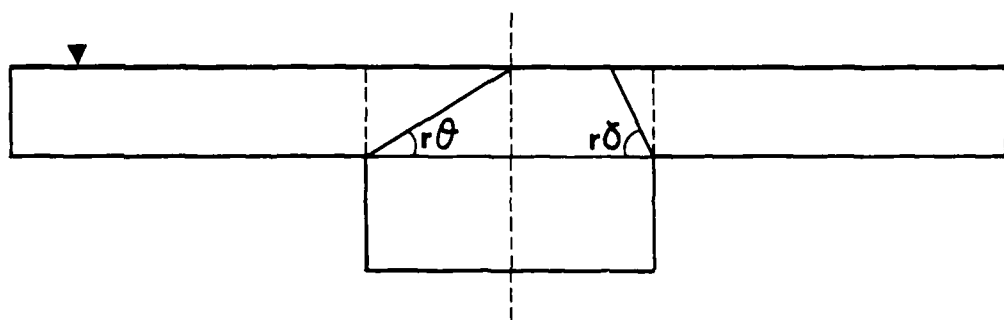


Figure 4.6 : Angle inclination of zero shear stress interfaces

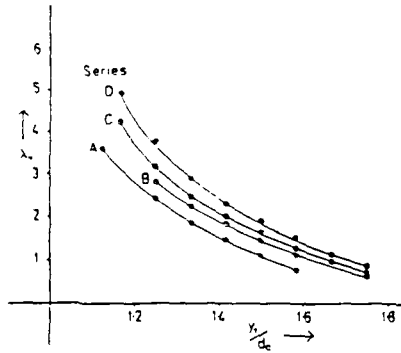


Figure 4.5a : Vertical interfaces

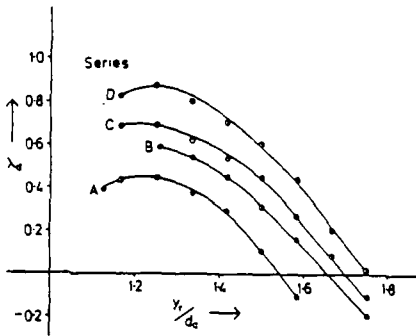


Figure 4.5b : Diagonal interfaces

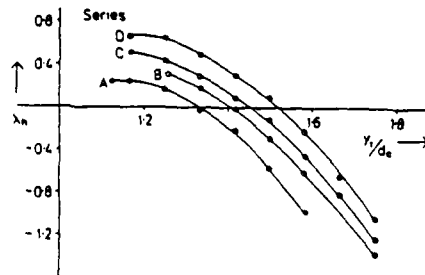


Figure 4.5c : Horizontal interfaces

Figure 4.5 : Apparent shear stress ratio versus depth ratio for three segment interfaces (after Wormleaton et al., 1982)

interfaces. The order of magnitude difference between the apparent shear stresses computed for the vertical interfaces and those computed on the diagonal and horizontal interfaces should also be noted. This shows that the vertical interface is much nearer to the turbulent eddies photographed by Sellin (1964). Analysis of the boundary stress distributions showed that the negative apparent shear stress ratios computed for the diagonal and horizontal interfaces at higher floodplain inundation depths indicate a transfer of momentum from the zone of flow above the main channel to the within-bank main channel zone.

Wormleaton et al. (1982) wary of the criticism that all their apparent shear stress values were computed using a single cross-sectional width, developed a relationship by regression analysis between geometric and velocity parameters for the apparent shear stress. This could then be compared with data collected by other authors often for very different applications and so utilize data from a wide variety of cross-sectional geometries. Wormleaton et al. (1982) give a final regression equation for the form of a vertical interface as:

$$\tau_{av} = 13.84 (\Delta V)^{0.882} \left(\frac{y_t}{d_c} \right)^{-3.123} \left(\frac{B_f}{B_c} \right)^{-0.727} \quad 4.5$$

where ΔV is the velocity difference between the floodplain and main channel flow segments, computed from the Manning equation (equation 3.19). Utilizing the data from 34 experimental set-ups the coefficient of determination for equation 4.5 was 0.983. Data collected by Myers (1978), Crory and Elsayy (1980) and Ghosh and Jena (1971) were found to conform closely with relationship 4.5.

Yen and Overton (1973) tackled the problem from an alternative perspective, using the measured boundary shear stress profiles to position an interface along which no shear would take place. The cross-section could then be divided up using these no-shear boundaries and the discharge computed easily as it would be directly related to the segment's cross-sectional area. Yen and Overton (1973) attempted to relate the angle of a zero shear interface, pivoting around the main channel/floodplain intercept (see Figure 4.5) to

observed discharge values. If this angle could then be related to the cross-sectional geometric parameters, then this method could be applied very simply to a wide variety of problems.

Yen and Overton's (1973) results showed that the angle of inclination of the zero shear stress plane varied with both the ratio of floodplain to main channel width, and the ratio of floodplain inundation to main channel depth. With a range of width ratios between 2.2 and 5.4 the angle of inclination varied by as much as 20° , with the angle increasing as the width ratio decreased. The angle of inclination varied with a depth ratio range from 0.2 to 1.8 by 60° with the angle increasing linearly from 15° to 50° , with the depth ratio up to a depth ratio of approximately 1.0 when the relationship becomes exponential. The angle of inclination of zero shear stress for a particular cross-section does not vary, therefore, when the depth ratio is above 2.

The results of Wormleaton et al (1982) reported in Figure 4.6 agree with those of Yen and Overton (1973) and show, therefore, that when the ratio of the floodplain inundation to main channel depth is approximately 2 or above, the two-stage channel may be considered as a single system. Below this ratio the distribution of the turbulent shear stresses has been shown to be complex where no one single position of the apparent shear stress interface or stress ratios can be adequately applied to describe the boundary shear stresses over a variety of cross-sectional geometries.

4.2.3 Implications of flume-based experiments for the prediction of the discharge capacity of two-stage channels

It was noted earlier that the main reason that the relationship between cross-sectional area and discharge does not hold for two-stage is the transfer of momentum between the main channel and the floodplain. The flume-based experiments reported in Section 4.2.2 attempt to quantify these momentum transfers by balancing the gravitational and retarding forces by the introduction of an apparent shear stress over a dividing interface between segments of flow. However, in order to compute the discharge capacity, we need to develop a relationship between easily measured geometric parameters and the stage/discharge rating curve. There are

several alternatives that can be used:-

- 1) We could use empirical relationships developed from flume experiments to predict the percentages of flow in each cross-sectional segment. These are developed from regression analysis of the computed apparent shear stresses on assumed interfaces. Examples include the relationships developed by Wormleaton et al. (1982) (reported earlier, see equation 4.5) and by Knight and Demetriou (1983).
- 2) We could attempt to divide the cross-section using the zero-shear interfaces, suggested by Yen and Overton (1973).
- 3) We could divide the cross-section using shear interfaces and make some assumption about the amount of momentum transfer across these interfaces.

Each of these alternatives are now considered. The first proposition to use empirically developed relationships seems attractive in that it would be simple to apply. However, the relationships have been developed using data collected in flume experiments which have had limited cross-sectional geometries. Table 4.1 shows the geometric parameters of the major flume investigations that have published this type of data. Comparison of the floodplain to main channel widths shows a maximum ratio of 3 where in the River Fulda catchment, flood inundation maps illustrate a ratio of up to 50. Similarly the maximum Manning's roughness applied to the floodplain is 0.022, whilst Chow (1959) suggests a typical grazed pasture to have a Manning's 'n' value of 0.03. To generate empirical relationships applicable to the sorts of two-stage channels typical in Europe, therefore, there is a need for further flume experiments with much wider and rougher floodplains. Until this is achieved, it would be inadvisable to extrapolate the existing relationships to geometrics and roughness outside those reported in Table 4.1.

The second alternative given is to divide the cross-section along zero-shear interfaces, as suggested by Yen and Overton (1973). As there is no momentum transfer across the zero-shear interface, the Manning equation will hold for

Table 4.1
 Cross-sectional geometric and roughness parameters for flume-based investigations
 into the transfer of momentum between the main channel and floodplain

Author	Main channel bankful width (m)	Floodplain widths (m)	Main channel depth (m)	Floodplain Inundation range (m)	Mannings 'n' channel	Mannings 'n' floodplain
Wormleaton, Allen & Hadjipanias (1982)	0.29	0.46	0.12	0.02 - 0.09	0.011	0.011-0.021
Myers (1984)	0.16	0.18, 0.30	0.08	0.01 - 0.07		Perspex
Crory & Elsayy (1980)	0.10, 0.15	0.36	0.10			
Chosh & Jena (1971)	0.20	0.15	0.10			
Knight & Demetriou (1983)	0.15	0-0.3	0.08	0.01 - 0.03		Perspex
Rajaratnam & Ahmadi (1981)	0.51	0.71	0.10	0.01 - 0.06	0.013	0.013
Prinos, Townsend & Tavoularis (1985)	0.51	0.38	0.10	0.05 - 0.12	0.011	0.011-0.022
Noutsopoulos & Hadjipanias (1983)	0.15	0.26 - 0.43	0.08	0.09 - 0.15	0.011	0.011-0.021
Smith (1978)	0.27	0.465	0.08	0.05 - 0.08	0.013	0.013
Asano, Hashimoto & Fujita (1985)	0.90 - 2.40	3.0	0.03 - 0.12	0.01 - 0.21	0.0091-0.0114	0.0098

each cross-sectional flow segment. Although Yen and Overton computed the angle of incidence of the interfaces (see Figure 4.6) for width ratios up to 5, the sensitivity of this angle to floodplain roughness, means the results cannot be reliably applied. Computing the area of flow segments based on the angle of inclination around the main channel/floodplain interface is also rather more difficult than if a vertical, horizontal or diagonal interface could be used.

However, it is important to note here that the zero shear interface has been applied widely for a number of years, as Lotter's (1933) technique, where the cross-section is divided vertically into a number of segments, and where the interfaces are ignored in computing the wetted perimeter of an interface. As Yen and Overton (1973) have shown, though, such interfaces are not vertical, but move from the inclined towards the horizontal as the depth of flow increases. Zero shear interfaces can be applied, therefore, for vertical, diagonal and horizontal inclinations by ignoring the assumed interface in the wetted perimeter computation and taking the solid boundaries only.

The third suggestion to compute the discharge capacity of the cross-section was to divide the cross-section using the shear interfaces, making an assumption about the amount of momentum transfer across these interfaces. In a similar way to the zero shear interfaces, shear interfaces have been applied in a great number of environments, using vertical, diagonal and horizontal inclinations. The assumption here is that the apparent shear stress is equal to the average shear stress (i.e. that of Wormleaton et al. (1982), apparent shear stress ratio is equal to 1, see Figure 4.5), so that the interface can be included as part of the wetted perimeter in the discharge capacity computation.

Wormleaton et al. (1982) computed the discharge for the zero-shear and shear interfaces for all three inclinations over a variety of floodplain roughnesses up to $n = 0.021$. Their results showed that, as expected, the computed discharge values converged to, or were smaller than, the observed values when the floodplain/channel depth ratio increased to 2, for all interface inclinations. However, the accuracy of the discharge prediction using these six techniques was considered only with variation in the depth

ratio and floodplain roughness; the width ratios were not considered.

The implication of the flume-based experiments to the computation of discharge in two-stage channels, is that no one single technique of incorporating turbulent exchange between the main channel and floodplain, is appropriate for all geometric and roughness environments. The flume experiments need to be extended to represent field environments with wider and rougher floodplains before a set of operational rules on the suitability of zero-shear or shear interfaces and their angle of inclination, can be developed.

4.3 Incorporation of momentum transfer into MILHY

Analysis of the flume-based experiments, in section 4.2, has shown that there is no single method of incorporating momentum transfer between flow segments that is appropriate for all cross-sectional geometries and roughnesses. For this reason, and because of the lack of comparative work on wide and rough floodplains, it was decided to incorporate a number of different methods into MILHY and test the accuracy of the discharge predictions against observed field data collected from the River Fulda catchment.

4.3.1 Selection of methods for incorporation into MILHY

Four methods of dividing the cross-section to incorporate momentum transfer were considered. These were:-

1. Vertical subdivision, with zero shear interfaces.
2. Vertical subdivision, with an apparent shear stress ratio = 1.
3. Diagonal subdivision, with zero shear interfaces.
4. Diagonal subdivision, with an apparent shear stress ratio = 1.

At present, method 2, that is vertical subdivision with an apparent shear stress ratio equal to 1, is incorporated into both MILHY and MILHY2. By application of these four different methods it should be possible to test the sensitivity of the generated rating-curve to the interface inclination

and apparent shear stress ratio. This sensitivity could then be compared to the impact on the rating curve of variation in the cross-sectional geometry and roughness parameters. If the analysis showed the rating-curve to be sensitive to the computational method, then further methods including horizontally inclined and Yen and Overton's (1973) angle of inclination could be incorporated and tested.

4.3.2 Incorporation of the four methods into MILHY

The four methods, identified above, of incorporating momentum transfer between the main channel and floodplain, are the same four methods utilized by Knight and Hamed (1984). Knight and Hamed (1984) tested the accuracy of the four identified techniques in predicting discharge by comparing the predicted results with those collected in flume experiments conducted by Knight and Demetriou (1983), reported in Table 4.1. For consistency, then, and to ensure the correct cross-sectional definitions were being applied to MILHY for each of the four methods, the equations of definitions reported in Knight and Hamed's (1984) paper were incorporated into MILHY. These equations are given in Table 4.2 whilst Figure 4.7 defines the cross-sectional geometry variables used. Analysis of the equations in Table 4.2 shows that the wetted perimeter of the interface is included in the main channel computation in methods 2 and 4, whilst being excluded in methods 1 and 3.

These four methods were then incorporated into the rating curve generation routine (subroutine CMPRC), introducing an option variable into the 'datal' dataset. These changes are recorded in the source code of MILHY3 which is given in Appendix 3. It is noted that the cross-section definitions reported in Table 4.2 are only incorporated for stage elevations above bankful. This is significant, especially for method 4, where the wetted perimeter of the main channel would be otherwise effectively extended above the stage level.

4.4 Sensitivity of the rating curve to interface inclination

There were several objectives in undertaking a sensitivity analysis of the

Table 4.2

Alternative geometric definitions to incorporate segment interactions
(after Knight and Hamed, 1984)

Method	Flood Plain		Main Channel	
	Area	Wetted Perimeter	Area	Wetted Perimeter
1	$(H-h)(B-b)$	$B-b + H-h$	$2bH$	$2b + 2h$
2	$(H-h)(B-b)$	$B-b + 2(H-h)$	$2bH$	$2b + 2H$
3	$(H-h)(B-b/2)$	$B-b + H-h$	$b(H+h)$	$2b + 2h$
4	$(H-h)(B-b/2)$	$B-b + H-h$	$b(H+h)$	$2b + 2h + 2((H-h)^2 + b^2)^{1/2}$

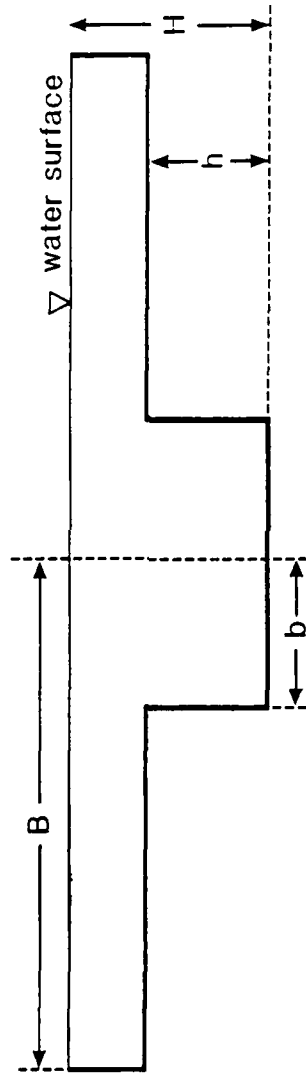


Figure 4.7 : Definition of cross-sectional geometry

rating curve. These were:

- 1) to establish whether any one method improved the accuracy of the rating curve in comparison to observed field rating curves, for a field cross-section
- 2) to establish whether there is a significant difference in the predicted rating curves generated by each of the four methods for wide floodplains with greater boundary roughnesses than those reported in Table 4.1.
- 3) to compare the difference in the computed rating curve attributable to the interface inclination method, with the difference due to variability in the cross-sectional geometry and roughness parameters

To answer these three questions, it was necessary to apply the four interface inclination methods to both field cross-sections, to achieve objective one, and hypothetical reaches, to achieve objectives two and three. Whilst the field cross-sections are similar to the theoretical cross-sections as they have broadly rectangular main channels and flat wide floodplains (see Figure 4.9) application of field cross-sections provided the only comparison to an observed rating curve possible. Objectives two and three can be achieved by comparison of the divergence in predicted rating-curve discharge between computation methods applied to hypothetical cross-sections.

4.4.1 Application of the four interface inclination methods

The cross-section at Bad Hersfeld on the River Fulda, West Germany, was selected in order to compare the accuracy of the four computation methods against a field rating curve. The rating curve at Bad Hersfeld was extended to out-of-bank conditions using data from gauged extreme events for floodplain inundation depths of up to 3.2 metres. This depth corresponds approximately to the 1 in 100 year event. At Bad Hersfeld the floodplains are symmetrical about the main channel with a floodplain to main channel width ratio (B/b) of 10. The bankful depth (h) is 4.1 m whilst the floodplains on either side of the main channel are pasture grazed with



Figure 4.9 : Cross-section on River Fulda at Mecklar, half way
between Bad Hersfeld and Rotenburg

cattle. The four interface inclination methods were applied for three sets of geometric and roughness environments and the discharge at increments of 0.5 m computed. The rating curve was also computed for the first two cases with the cross-section being treated as a single system, that is with no interfaces to divide the cross-section into segments. The rating curves produced from these three applications are reported in Tables 4.3 to 4.5.

A theoretical cross-section was established to achieve objectives two and three noted above, with a rectangular main channel and a floodplain rise from channel to valley side of only 0.1 metres. The floodplain to main width ratios considered were 10 and 20, as noted earlier. Flume experiments by numerous authors have investigated smaller width ratios. Wormleaton et al. (1982) reported that discharge predictions from all the interface inclination methods, vertical, diagonal and horizontal, converged on a common solution as the floodplain inundation depth to main channel depth (H/h) approached 2. To check this, discharge predictions were calculated for depth ratios (H/h) up to 2.2 were computed at 0.5m stage increments. As well as the four interface inclination methods, the rating curve was computed treating the cross-section as a single flow segment. Where friction or slope parameters varied between main channel and floodplain segments, a mean average between the two values was applied to the single segment case. This was true for both the hypothetical and Bad Hersfeld cross-sections. The hypothetical cross-section results are reported in Tables 4.6 to 4.10.

4.4.2 Sensitivity of the rating curve to the computational stage increment

Whilst the sensitivity analysis for the interface inclination methods was being set up, it was noticed that the discharge predictions were sensitive to the computational stage increment. The rating curve is computed at twenty evenly spaced elevation increments, these increments being generated from the minimum and maximum cross-sectional elevations. Figure 4.8 illustrates the impact of relatively small changes in the computational stage increment, from 0.29 to 0.61m, on the discharge values predicted for the Bad Hersfeld cross-section. The maximum difference in the predicted discharges between stage increment values occur at 1.5m above bankful where the discrepancy is approximately $150 \text{ m}^3 \text{ s}^{-1}$. The observed rating curve at

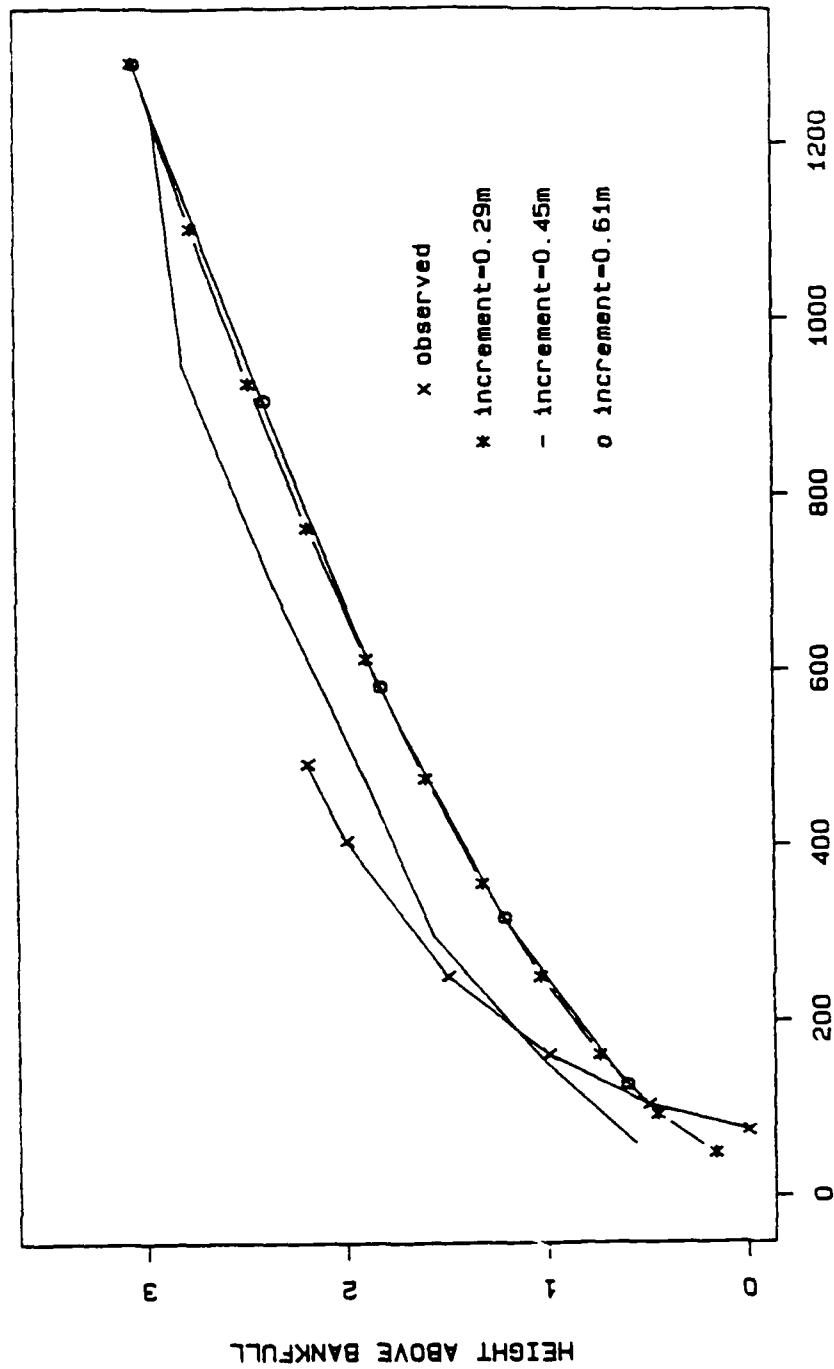


Figure 4.8 : Sensitivity of the Rating Curve to the Computational Stage Increment

this elevation gives a discharge value of $250 \text{ m}^3 \text{ s}^{-1}$. Figure 4.8 also shows that a decrease in the stage increment size does not necessarily improve the accuracy, as the rating curves for increment sizes of 0.29m and 0.61m are almost identical.

The maximum elevation in the field cross-sections of the River Fulda catchment are determined by the valley side. The computational stage increment therefore is computed from the height of the constraining side (valley) wall.

4.4.2 Results of the sensitivity analysis

The results of the sensitivity analysis of the computed rating curve to the interface inclination and variation in geometric parameters, are tabulated in Tables 4.3 to 4.10. Tables 4.3 to 4.5 show the results computed for the Bad Hersfeld cross-section and also record the percentage error of each of the interface inclination methods against an observed rating curve. Tables 4.6 to 4.10 show the results for a hypothetical cross-section, and the percentage error in these tables indicate the deviation from the MILHY solution as no 'observed' rating curve was available.

Table 4.3 contains the observed discharge values and the computed values from MILHY2 and interface inclination methods 1 to 4. Table 4.3 confirms that MILHY2 incorporates method 2, and in further tables, therefore, both are not shown. Manning's 'n' values of 0.035 for the main channel and floodplain were selected for the first run reported in Table 4.3. This value corresponds to the tabulated values suggested in Chow (1959). The channel and floodplain slopes were set at 0.0006, computed from the field rating curves from Bad Hersfeld and Rotenburg, the next gauging station downstream.

Results from the Bad Hersfeld station

Table 4.3 shows the discharge predictions from the four interface methods computed using the parameter values reported above. The mean average error of the discharge predictions over the observed figures was computed for each method over a range of inundation depths.

Table 4.3
Comparison of predictive accuracy of Interface inclination methods
1-4 for Bad Hersfeld, River Fulda

Height above bankful (metres)	Observed Q $\text{m}^3 \text{s}^{-1}$	MILHY2		Method 1		Method 2		Method 3		Method 4		Single segment	
		Q $\text{m}^3 \text{s}^{-1}$	Error %										
0.29	86	134	+ 55	118	+ 37	134	+ 55	163	+ 89	124	+ 44	67	- 22
0.78	134	232	+ 73	212	+ 58	232	+ 73	240	+ 79	197	+ 47	152	+ 14
1.27	205	411	+101	386	+ 88	411	+101	400	+ 95	352	+ 72	336	+ 64
1.76	321	650	+103	619	+ 93	650	+102	617	+ 92	563	+ 76	572	+ 78
2.25	490	950	+ 94	913	+ 86	949	+ 94	891	+ 82	833	+ 70	866	+ 77
2.74	675	1311	+ 94	1268	+ 88	1310	+ 94	1224	+ 81	1160	+ 72	1219	+ 81
3.22	830	1734	+109	1684	+103	1732	+109	1617	+ 95	1547	+ 86	1631	+ 97
Mean error		+ 90		+ 79		+ 90		+ 88		+ 67		+ 59	

B/b = 10
h = 4.1m
 n_{ch} = 0.035
 n_{fp} = 0.035
Sch = 0.0006
 S_{fp} = 0.0006

Table 4.4
 Comparison of the predictive accuracy of interface inclination methods
 1 - 4 for Bad Hersfeld, River Fulda, with variation in the floodplain roughness

Height above bankful metres	Observed $m^3 s^{-1}$	Method 1		Method 2		Method 3		Method 4		Single segment	
		Q $m^3 s^{-1}$	Error %								
0.29	86	113	+31	129	+50	155	+80	116	+35	47	-46
0.78	134	176	+32	197	+47	202	+51	158	+18	101	-24
1.27	205	281	+37	306	+49	291	+42	243	+18	224	+9
1.76	321	416	+30	447	+39	408	+27	355	+11	381	+19
2.25	490	583	+19	620	+27	555	+13	497	+1	577	+18
2.74	675	782	+16	825	+22	732	+8	668	-1	812	+20
3.22	830	1013	+22	1062	+28	939	+13	869	+5	1087	+31
Mean Error			+27		+37		+34		+12		+1

B/b = 10
 h = 4.1m
 n_{ch} = 0.035
 n_{fp} = 0.07
 n_s = 0.0525
 S_{ch} = 0.0006
 S_{fp} = 0.0006

Table 4.5

Comparison of the predictive accuracy of interface inclination methods 1 - 4 for Bad Hersfeld, River Fulda, with variation in the downstream main channel slope

Height above bankful metres	Observed Q $m^3 s^{-1}$	Method 1		Method 2		Method 3		Method 4		Single segment	
		Q $m^3 s^{-1}$	Error %								
0.29	86	53	-38	60	-30	76	-12	39	-56	51	-41
0.78	134	129	-4	137	+2	143	+7	61	-55	116	-13
1.27	205	282	+38	292	+42	293	+43	126	-39	257	+25
1.76	321	493	+54	505	+57	498	+55	273	-15	437	+27
2.25	490	763	+56	777	+59	761	+55	477	-3	661	+35
2.74	675	1092	+62	1108	+64	1082	+60	737	+9	931	+38
3.22	830	1481	+78	1500	+81	1462	+76	1056	+27	1246	+50
Mean Error			+35		+39		+41		-18		+17

B/b = 1.0
 h = 4.1m
 n_{ch} = 0.035
 n_{fp} = 0.035
 A_{ch} = 0.0001
 S_{fp} = 0.0006

Table 4.6
 Comparison of the predictive accuracy of interface inclination methods 1-4
 for a hypothetical reach

Height above bankful metres	MILHY2 $m^3 s^{-1}$	Method 1		Method 3		Method 4		Single segment	
		Q $m^3 s^{-1}$	Error %						
0.56	61	58	-5	42	-31	34	-44	33	-10
1.01	153	150	-2	127	-17	118	-23	131	-15
1.56	295	291	-1	261	-12	250	-15	275	-7
1.9	477	472	-1	433	-9	421	-12	460	-4
2.35	695	689	-1	641	-8	636	-10	679	-2
2.80	946	939	-1	880	-7	863	-9	931	-2
Mean Error			-2		-14		-19		-12

B/b = 10
 h = 2.4m
 n^{ch} = 0.035
 n^{fp} = 0.035
 S = 0.0005

Table 4.7

Comparison of the predictive accuracy of interface inclination methods 1 - 4
for a hypothetical reach, with variation in the floodplain roughness

Height above bankful (metres)	MILHY2		Method 1		Method 3		Method 4		Single segment	
	Q $m^3 s^{-1}$		Q $m^3 s^{-1}$	Error %						
0.56	53		51	-4	34	-36	26	-51	68	-28
1.01	107		103	-2	110	-26	70	-35	275	-157
1.55	185		181	-2	241	-20	137	-26	980	-114
1.90	284		279	-2	410	-16	225	-21	969	-151
2.35	401		396	-1	614	-14	380	-18	1432	-157
2.80	536		529	-1	850	-13	451	-16	1963	-166
Mean Error				-2		-21		-28		-19%

$B/b = 10$
 $h = 2.4m$
 $n_{ch} = 0.035$
 $n_{fp} = 0.07$
 $n_s = 0.0525$
 $S = 0.0005$

Table 4.8

Comparison of the predictive accuracy of interface inclination methods 1 - 4 for a hypothetical reach, with variation in the downstream main channel slope

Height above bankful (metres)	Milly2 m s^{-1}	Method 1		Method 3		Method 4		Stagile segment	
		Q $\text{m}^3 \text{s}^{-1}$	Error %						
0.56	35	34	-4	28	-21	24	-32	25	-30
1.01	121	119	-2	110	-9	106	-12	101	-17
1.56	254	252	-1	241	-5	236	-7	213	-16
1.90	427	425	-1	410	-4	404	-5	356	-17
2.35	635	633	0	614	-3	608	-4	526	-17
2.80	876	873	0	850	-3	843	-4	721	-18
<u>Mean Error</u>			-1		-8		-11		-19
B/b	=	10							
h	=	2.4m							
u_{ch}	=	0.035							
u_{fp}	=	0.035							
S_{ch}	=	0.0001							
S_{fp}	=	0.0005							
$S_{c'}$	=	0.0003							

Table 4.9

Comparison of the predictive accuracy of interface inclination methods 1 - 4 for a hypothetical reach with variation in the downstream main channel and floodplain slope

Height above bankful (metres)	MILHY2 Q $m^3 s^{-1}$	Method 1		Method 3		Method 4		Single segment	
		Q $m^3 s^{-1}$	Error %						
0.56	192	184	-4	132	-31	107	-44	103	-46
1.01	485	475	-2	403	-17	374	-23	413	-15
1.56	933	920	-1	824	-12	790	-15	870	-7
1.90	1508	1493	-1	1370	-9	1330	-12	1453	-4
2.35	2197	2179	-1	2026	-8	1980	-10	2148	-2
2.80	2990	2968	-1	2783	-7	2731	-9	2945	-2
Mean Error			-2		-14		-19		-13

B/b = 10
h = 2.4m
 n_{ch} = 0.035
 n_{fp} = 0.035
 S_{fp} = 0.005

Table 4.10

Comparison of the predictive accuracy of interface inclination methods 1 - 4
for a hypothetical reach with variation in the floodplain/main channel width ratio

Height above bankful (metres)	MILHY2 $m^3 s^{-1}$	Method 1		Method 3		Method 4		Single segment	
		Q $m^3 s^{-1}$	Error %						
0.56	77	74	-4	58	-25	50	-35	48	-38
1.01	254	251	-1	228	-10	219	-14	231	-9
1.56	531	527	-1	497	-6	486	-9	511	-5
1.90	891	886	-1	847	-5	834	-6	873	-7
2.35	1324	1318	0	1270	-4	1256	-5	1308	-1
2.80	1825	1818	0	1759	-4	1743	-5	1811	-1
Mean error			-1		-9		-12		-1
B/b	=	20							
h	=	2.4m							
n_{ch}	=	0.035							
n_{fp}	=	0.035							
S	=	0.0005							

Table 4.3 shows that all methods at all inundation depths overpredicted the carrying capacity of the cross-section. The average error shows that method 2, the method utilized by MILHY2, gave the worst prediction. The best overall prediction was given by the single segment method, however this was not so surprising as both the boundary roughness and slope variables were constant across the section.

Table 4.3 also shows that there was no consistent difference in predictive performance between the methods incorporating the shear face, methods 2 and 4, and the zero shear methods. Also worthy of note is that the percentage error increases with depth in all methods except method 3. It is important to remember here that the algorithm to reduce Manning's n as depth increases has been removed from MILHY3, for reasons specified in section 3.4.1.

Comparison of Tables 4.3 and 4.4 shows how increasing the floodplain boundary roughness can more than half the error of the predictions for all methods. The difference in mean average errors between computation methods is, however, the same as those in Table 4.3. This suggests that the carrying capacity computation is more sensitive to the boundary roughness value than the form of the main channel/floodplain interface.

Table 4.4 also shows that the percentage error does not increase with increasing floodplain inundation depth, as suggested by Table 4.3. In Table 4.4 the percentage errors values indicate that all four computation methods are converging to the observed discharge as the inundation depth increases and approaches the main channel depth. This suggests that a floodplain boundary roughness value of 0.07 corresponds more closely to the field conditions than the initial value used by 0.035. The logic behind this argument lies in that as floodplain inundation depth increases to the main channel depth, the two-stage channel behaves as a single system and therefore all of the computation methods should converge on a common solution. If they do not, as in Table 4.3, this suggests that the initial variable values used are not realistic.

Table 4.5 shows the effects of incorporating meandering in the channel by reducing the slope value used to 0.0001 from 0.0006. This value is

calculated from the ratio of the main channel length to the valley length between Bad Hersfeld and Rotenburg on the River Fulda. Comparison of Tables 4.3 and 4.5 shows that reducing the slope of the main channel improves the predictions of the carrying capacity in all computation methods. However, we are not looking to calibrate this particular applications, rather we are aiming to compare the effects of variation in the parameters against the method of computation. The results of this field application suggest that computation method utilized in MILHY2 (i.e. method 2) give in Tables 4.3 and 4.4 the poorest prediction of the carrying capacity of the cross-section. However, Tables 4.4 and 4.5 show that the prediction can be improved to much greater extent by more accurate selection of parameter values than by altering the computation technique.

Results from a hypothetical cross-section

Tables 4.6 to 4.10 report the predictions of the carrying capacity for a hypothetical cross-section, comparing methods one to four and discharges computed by treating the cross-section as a single segment. The percentage error values reported are computed from the MILHY2 predictions, which utilizes method 2. The percentage error values allow comparison of the relative sensitivity of the discharge predictions to variation in the computation method and parameters. The absolute accuracy of the techniques cannot be computed as this is a hypothetical application. It is not useful, therefore, to directly compare the percentage errors from the Bad Hersfeld section to the hypothetical application.

Analysis of Tables 4.6 to 4.10 shows that method 1 produces a very close approximation to the predictions produced from the MILHY2 computations, under all of the boundary roughness and geometry environments. In all cases, methods 3 and 4 rank second and third respectively in their closeness to the MILHY2 predictions. Methods 1, 3 and 4 under-predict the carrying capacity in comparison to the MILHY2 predictions in all five examples. Comparison of Tables 4.6 and 4.10 where the floodplain/main channel width ratio has been increased to 20 from 10, shows that this increase in the width ratio has made little impact on the comparative accuracy of the computation methods. There has been no radical change in the difference in

the mean average errors between the four computation methods.

Comparison of the hypothetical and Bad Hersfeld applications

Analysis of the two sets of results has shown that the method incorporated into MILHY2, method 2, gives the largest prediction of the carrying capacity of the cross-section in both the Bad Hersfeld and hypothetical sections. The Bad Hersfeld section results suggest that method 2 gives the worst prediction of the four methods, which all over-predict the carrying capacity. This suggests that all four methods do not introduce enough friction over the assumed interfaces between the main channel and floodplain to mimic the retarding effects of momentum exchange. Method 4 assumes a diagonal interface and an apparent shear stress ratio equal to one, and introduces the most additional boundary friction of the methods, hence producing the lowest prediction of carrying capacity (see Tables 4.3 to 4.10). This suggests that in the field apparent shear stress ratios on diagonal interfaces may be greater than one, rather than less than one as Wormleaton et al. (1982) found in Fig. 4.5b. Alternatively, these results suggest that the true position of the interface is between the vertical and diagonal, as apparent shear stress ratios on the vertical interface are very much greater than one (see Figure 4.5a). Apparent shear stress ratios of greater than one could be incorporated into the MILHY scheme by multiplying the wetted perimeter of the apparent interface in the main channel computation until the ratio was reduced to one.

4.4.4 Conclusions

From the analysis of the results above, it is possible to make several conclusions:

- 1) The three methods utilized to incorporate turbulent exchange between the main channel and floodplain, more accurately predict the carrying capacity of a cross-section than the technique used in MILHY2.
- 2) All four methods over-predicted the carrying capacity because they failed to introduce enough additional boundary friction to mimic the

effects of turbulent exchange. Method 4 introduced the most additional friction and therefore gave the best predictions.

- 3) Increasing the boundary roughness, Manning's 'n' for the floodplains was more effective at reducing the over-prediction of the carrying capacity of the section than increasing the wetted perimeter of the interface, or assuming an apparent shear stress ratio of one.

4.5 Implications for the improvement of MILHY

The initial sensitivity analysis, reported above, of the alternative methods of incorporating turbulent exchange, has shown that these simple redefinitions can improve the predictive capability of MILHY. Application of the techniques to wider and rougher floodplains than previously reported (see Table 4.1) and to cross-sectional field geometries which are only broadly rectangular has been successful. Therefore, these turbulent exchange routines are worthy of inclusion for validation of the whole MILHY3 scheme. As, however, these routines have only been tested against one field section in this analysis, it was felt that all the routines should be carried onto the final analysis, and not just the best method, method 4, identified in this analysis. Although it is not our intention to prove with any statistical certainty the most appropriate technique, as this would require possible hundreds of applications, we do intend to be able to suggest guidelines for these techniques. We anticipate that a combination of turbulent exchange routines and a multiple routing routine (reported in Section 5) may highlight a different exchange routine than the one selected here. It is also possible that in a rainfall, runoff and route application the turbulent exchange routine invoked may become unimportant. For these reasons, then, all four of the turbulent exchange routines are included in the sensitivity analysis reported in Section 6.

SECTION 5 : INCORPORATION OF MULTIPLE ROUTING REACHES

The sensitivity analysis of Ervine and Ellis (1987), reported in Section 3, found that the sinuosity of the main channel was important in determining the length of the flow path. In two-stage channels, therefore, multiple routing reaches provide a means of incorporating the differing path lengths of the sinuous main channel and relatively straight floodplain.

5.1 The behaviour of two-stage channel flow

In two-stage channels there is a tendency for floodplain flow to "short-circuit" the general more sinuous route taken by the main channel (Fread, 1976). The infrequency of out-of-bank flows means that flows taking the shortest path downslope do not develop the secondary flow system necessary for the development of meanders. Einstein and Shen (1964) suggested that the secondary flow system is initiated itself by shear along a rough bank. The shorter path length of the floodplain flow is exacerbated by the steeper gradient of the floodplain in comparison with the main channel, giving faster velocities and travel times for floodwaves passing downstream.

The accelerating effects of the path length and slope on floodplain flows are diminished, however, by effects of boundary friction. If floodplain flow depths are small then the hydraulic radius will also be small and hence velocities reduced. Floodplain boundary roughnesses also tend to be higher than those in the main channel because of vegetation and obstructions such as hedges.

5.1.1 Comparison of main channel and floodplain boundary roughness

As noted earlier in Section 3.1.3 the retarding effects of boundary roughness tend to decline as the hydraulic radius or stage increases.

This is particularly true for the broadly rectangular main channels found in the River Fulda catchment. On the floodplains, however, the situation is complicated by vegetation and man-made structures. As the floodplain inundation depth increases debris can become trapped in hedges and fences and the boundary roughnesses may increase. Klaassen and Zwaart (1974) showed that the spacing of hedges and trees is critical in computing the friction of floodplains.

When selecting Mannings 'n' values for the floodplain segments in the rating curve computation of MILHY, it is essential to consider not only the general land use but also the spacing and height of any hedges or fences.

5.1.2 Objective of investigating multiple routing reaches

The aim of incorporating multiple routing reaches is to separate the conflicting effects of the straighter pathway and higher boundary friction of floodplain flow, on the selection of the most appropriate Mannings 'n' value. By removing considerations of the sinuosity of floodplain flows, the selection of the correct 'n' value should be simplified. As the sensitivity of MILHY3 to the Manning 'n' value is anticipated, by improving the selection of a suitable value and improving the representation of the physical processes active in the two-stage channel, the predictive capability of MILHY should be improved.

5.2 Modelling alternatives

The optimal method of modelling the conveyance of a floodplain through a two-stage channel would be to use a two or even possibly three-dimensional finite element model. Such models allow for turbulent exchange between elemental areas and so predict a pattern of flow across the section. The amalgamation of these complex and time-consuming finite element models with simple hydrologic models, such as MILHY, is discussed further in Section 7.

The objective in this section is to develop a simple one-dimensional technique that can be incorporated into MILHY. Such a technique should therefore have -

- little additional data requirements
- low computer processor demands
- be capable of validation

These demands leave several alternative approaches available. These are:-

- 1) To develop a stage/reach length relationship. This approach was suggested by Perkins (1970), when he incorporated into a rainfall/runoff model a routine to increase reach length linearly from the main channel thalweg distance at bankfull to the shortest reach length dictated by the floodplain slope, at the maximum stage.
- 2) To develop an empirical adjustment to the roughness coefficients of the floodplain and main channel. This approach was suggested by Tingsanchali and Ackermann (1976), where Manning's 'n' value was weighted by a ratio of reach lengths between the actual floodplain distance and a schematized straight floodplain and main channel. Such that

$$n^* = n_f \cdot \frac{L_f}{L_{mc}}^{3/2} \quad 5.1$$

where n^* = adjusted Manning's 'n'
 n_f = Manning's 'n' floodplain
 L_f = reach length of floodplain
 L_{mc} = reach length of main channel

- 3) Replace the variable storage coefficient routing technique in MILHY, with a St. Venant technique utilizing a weighted four-point

implicit finite difference solution, modified by Fread (1976) to incorporate the differing path lengths of floodplain and main channel flows.

- 4) Separate floodplain and main channel flows and route using the existing routines in MILHY the flow downstream assuming no exchange of flow along the reach.

The simplest solution to apply is approach four, where each cross-sectional segment, used to develop the rating curve, is routed individually downstream. There are several disadvantages however:-

- i) flow has to be apportioned to floodplain or channel as the top of the reach, and these proportions are fixed throughout the reach. This implies the assumption that the cross-sectional geometry is fairly constant downstream;
- ii) there is no exchange of momentum between the main channel and floodplain along the reach;
- iii) floodplain flows cannot cross main channel flows.

Despite these disadvantages, approach four seemed to be a logical first step into tackling the problem of floodplain flows "short-circuiting" the main channel. Exchange of momentum between the main channel and floodplain has been incorporated at the valley-sections (see Section 4), and it was felt important at this stage to compare the sensitivity of the outflow hydrograph to the effects of variability in the turbulent exchange routines or the multiple routing of floodplain and channel flows. If the downstream "short-circuiting" effects were identified as being significant, then it would be appropriate to investigate Perkins approach as another simple alternative, or a more radical replacement of the routing subroutine with Fread (1976) St. Venant solution.

5.3 Incorporation of multiple routing into MILHY

The incorporation of multiple routing into MILHY proved to be a relatively simple matter, with changes in the source code being required mainly to facilitate the apportioning of flow across the cross-section. Each time step of the inflow hydrograph was apportioned into the cross-sectional segment according to the stage it reached at the cross-section nearest the top of the reach. It was necessary, therefore, to develop stage-rating curves and compute the percentage of total flow with stage for each segment. These computations are included in the CMPRC subroutine and are output to the results file. The inflow hydrograph is then apportioned in the ROUTE subroutine when the individual segment rating curves and percentage curves are recalled. For each segment, a TRAVEL TIME and ROUTE command are invoked and the outflow hydrographs are then added to give the total discharge across the segment.

This approach minimised the changes required in the source code as most of the multiple routing can be achieved by repetition of commands in the 'datal' dataset.

5.4 Application of multiple routing reaches

It was important at this stage to test the impact of multiple routing on the outflow hydrograph. The relative importance of the technique compared to other routine modifications and the sensitivity of the whole scheme to parameter variability is investigated in Section 6.

Multiple routing was applied, therefore, to a theoretical reach with rectangular cross-sectional geometry assumed to be constant downstream, and a reach from the River Fulda, between Bad Hersfeld and Rotenburg. A variety of inflow hydrographs were applied to the theoretical reach, in order to look at the impact of the depth of inundation on the travel time of the floodplain and the effects on the outflow hydrograph. The River

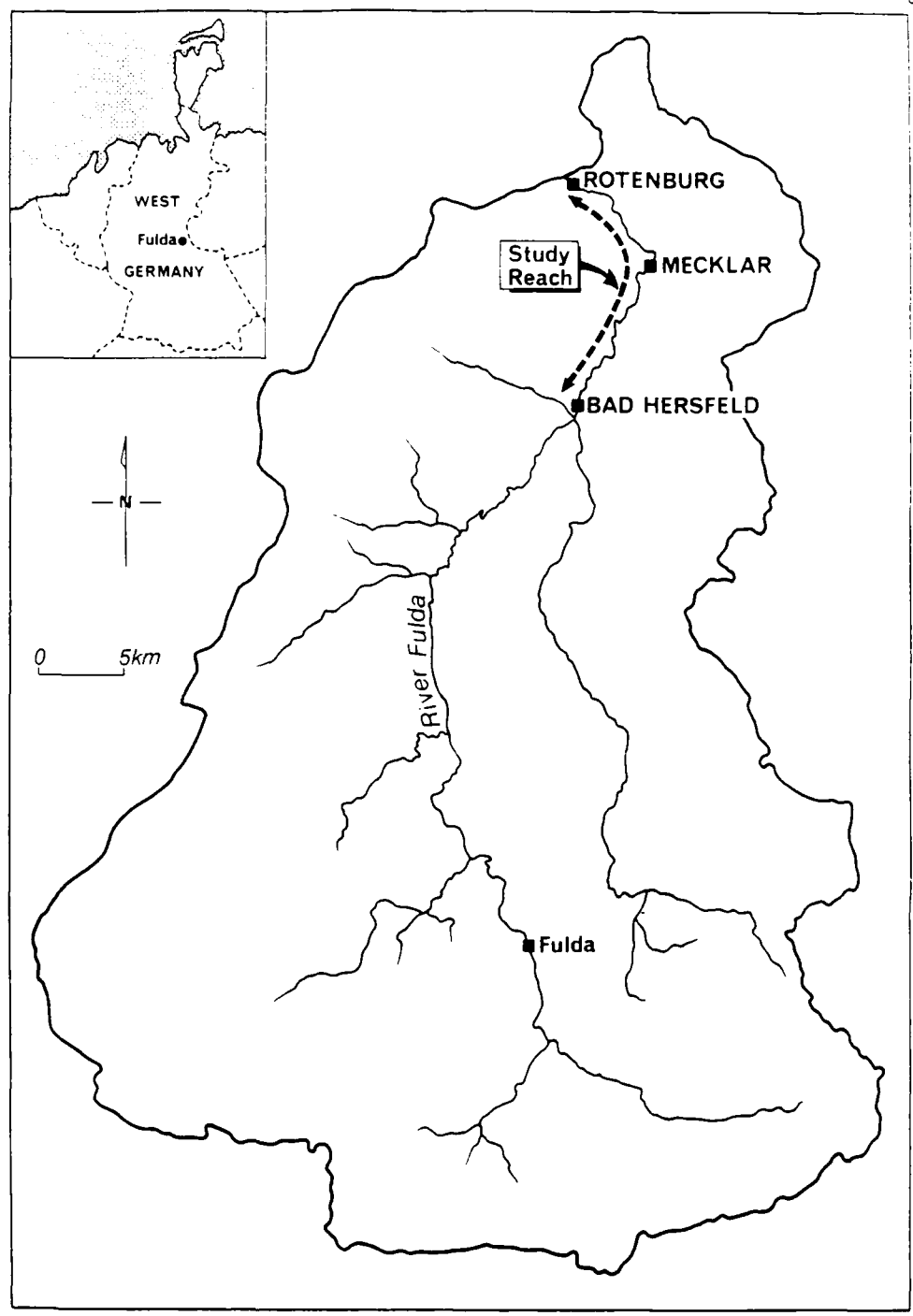


Figure 5.1 : River Fulda Catchment

Fulda, however, provided field data against which various roughness and routing lengths could be tested but with a limited number of observed flood in flow and outflow hydrographs. A 1 in 10 year event was available and enough flood frequency data was available to generate a 1 in 100 year event, assuming a similar shape as the 1 in 10 year event. The 1 in 100 year event could legitimately be used to compare the accuracy of the predicted peak stage and discharge.

All the simulations reported involve the routing of an input hydrograph from between two cross-sectional stations. The runoff contribution of the drainage area between the two stations is not considered. The results of these simulations are reported in Tables 5.1 to 5.3 and Figures 5.2 to 5.7. The tables show the time to peak, peak discharge and maximum floodplain inundation of the outflow (downstream) hydrograph.

5.4.1 Application to the Bad Hersfeld to Rotenburg reach

The results from the application of multiple routing reaches to the Bad Hersfeld to Rotenburg reach are found in Tables 5.1 and 5.2, and Figures 5.2 to 5.5. As reported earlier in Section 4.4.1, the cross-sectional geometry at Bad Hersfeld is broadly rectangular with the floodplains being symmetrical about the main channel. The reach from Bad Hersfeld to Rotenburg is approximately 24 km (15 miles) in length with a sinuous main channel; this can be seen on Figure 5.1. At Rotenburg the bankfull depth is 4.8 m as compared to 4.1 m at Bad Hersfeld, with a bankfull discharge of $180 \text{ m}^3 \text{ s}^{-1}$. The valley section is asymmetrical at Rotenburg with the left hand floodplain being approximately 300 metres wide whilst the right hand floodplain rises steeply. The bankfull width at Rotenburg is approximately 50 m as compared with 30 m at Bad Hersfeld. When multiple routing is invoked, therefore, the observed hydrograph at Bad Hersfeld is apportioned to floodplain and main channel segments according to the rating curve developed for the Bad Hersfeld cross-section. The travel time table is then developed for each cross-sectional segment using whichever of the two segments produces the smaller rating curve. The maximum floodplain inundation values reported in Tables 5.1 and 5.2 are computed at the downstream end of the reach, that is at Rotenburg.

Table 5.1

Bad Hersfeld to Rotenburg reach, 1 in 10 year event

	Time to Peak (hours)	Peak Discharge (m^3s^{-1})	Maximum Floodplain Inundation m
Observed	38	407	0.33
MILHY2	38	285	0.09
Multiple routing	40	330	0.17
Multiple routing floodplain length 5%	40	333	0.18
Multiple routing floodplain length 30%	40	352	0.21
Multiple routing floodplain 'n' 30%	38	355	0.22

Table 5.2

Bad Hersfeld to Rotenburg reach, 1 in 100 year event

	Time to Peak (hours)	Peak Discharge ($\text{m}^3 \text{s}^{-1}$)	Maximum Floodplain Inundation m
Observed	38	744	0.90
MILHY2	38	665	0.78
Multiple routing	40	634	0.73
Multiple routing floodplain length 30%	36	684	0.81
Multiple routing floodplain 'n' 30%	36	668	0.78

The 1 in 10 year event is shown in Figure 5.2, indicating a travel time of the peak discharge of approximately nine hours. The inflow hydrograph at Bad Hersfeld has been scaled up, in line with the flood frequency data available to provide the 1 in 100 year event and consequently the 1 in 100 year event has the same form as the 1 in 10 year event. At Bad Hersfeld the 1 in 100 year event corresponds to an increase in the floodplain inundation depth of approximately 1 m over the 1 in 10 year event.

Figure 5.3 compares the observed outflow hydrograph at Rotenburg with the outflow hydrographs produced by MILHY2 and the multiple routing technique. The greatest difference in the three hydrographs occurs in the over-bank section which is the area of particular interest. The corresponding time to peak, peak discharge and maximum inundation depths of these three hydrographs are recorded on Table 5.1. Both the figure and table show that the single routing technique used in MILHY2 effectively smooths the inflow hydrograph to too great an extent. This reduces the peak discharge and floodplain inundation depth. The effects of multiple routing are to sharpen up the hydrograph, thereby increasing the peak discharge and inundation depth. The multiple routing technique halves the MILHY2 errors in both the peak discharge and inundation depth. Table 5.1 also shows that the multiple routing technique produced a time to peak of 40 hours, two hours later than the observed peak. However, the observed inflow and outflow hydrographs were digitised at three hourly intervals and therefore errors of less than three hours can be effectively ignored.

As reported earlier in this section, the main objective of incorporating multiple routing reaches was to simulate the effects of the short-circuiting of floodplain flow, reducing the floodplain reach length. In the next simulation reported in Table 5.1, therefore, the reach length of the floodplain segments was reduced by 5%. This produced only very small changes in the outflow hydrograph in comparison with the multiple routing hydrograph shown on Figure 5.4. Analysis of the flood inundation maps available for the River Fulda indicated, however, that the floodplain reach length may be up to 30% shorter than the main

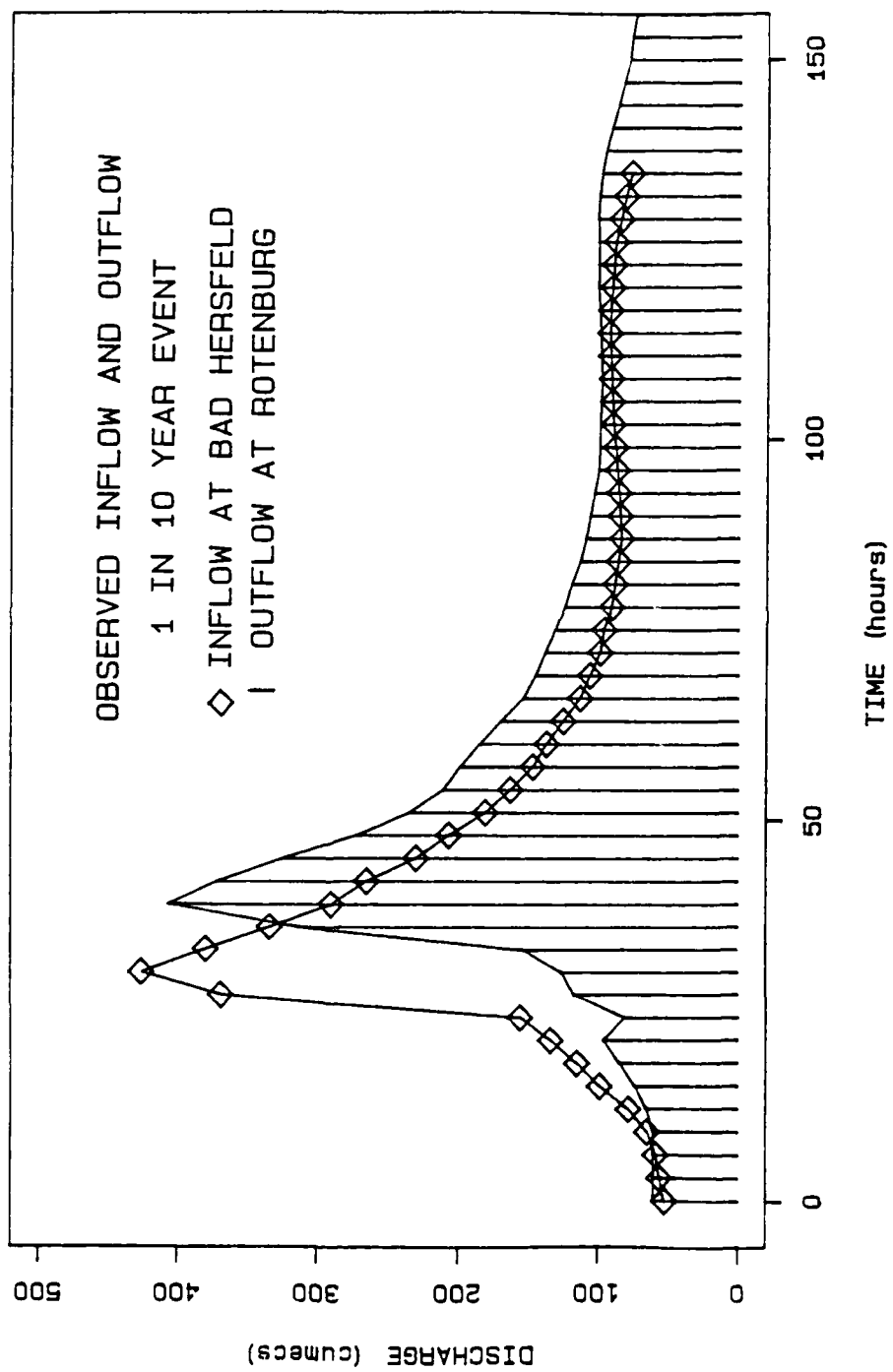


Figure 5.2

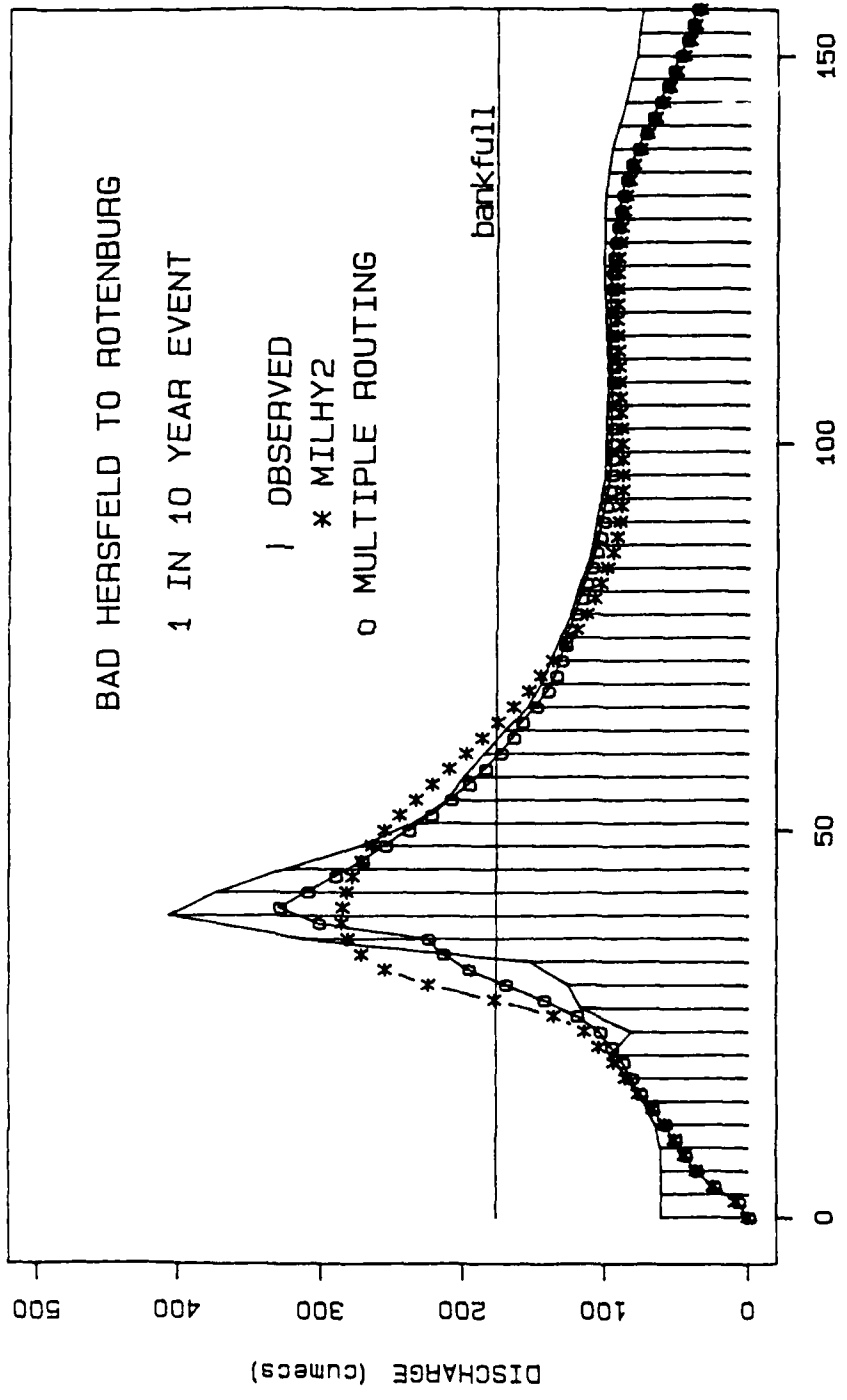


Figure 5.3

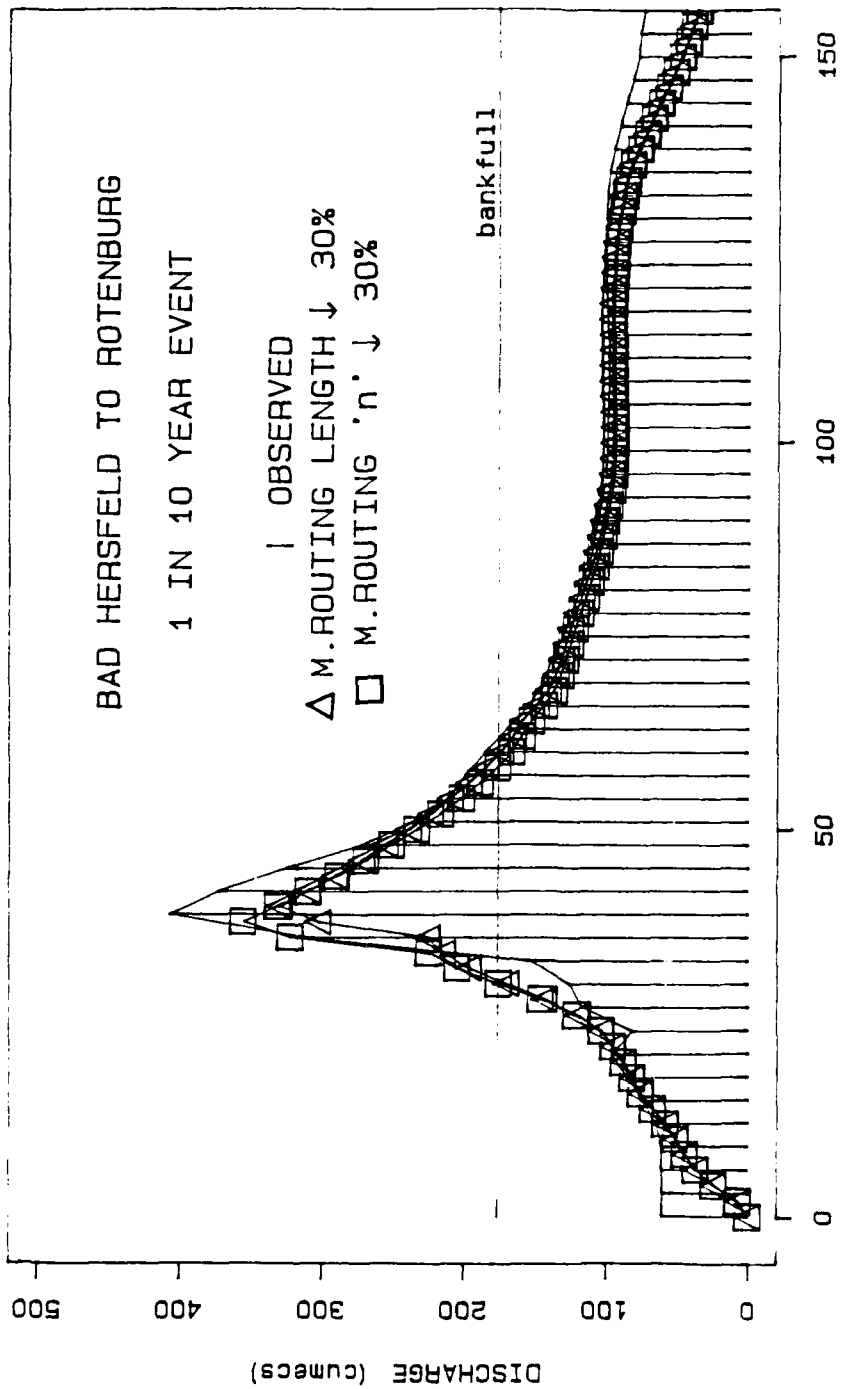


Figure 5.4

channel. The hydrograph produced by reducing the floodplain reach length by 30% is shown on Figure 5.4, indicated by the triangles. Comparison of Figures 5.3 and 5.4 shows that reducing the floodplain length by 30% makes a significant improvement on the prediction. Figure 5.4 shows as well, however, that a similar effect can be achieved by reducing the Mannings 'n' roughness coefficient by 30%. Chow (1959) showed that the effects of sinuosity of a channel can alter the 'n' value by up to 30%. As noted earlier, however, the aim of this investigation is to incorporate the processes active in two-stage channels and remove the reliance on empirical coefficients. The effectiveness of these new process 'modules' in improving the predictive capabilities of MILHY in comparison with the established techniques used is investigated in Section 6.

Table 5.2 and Figure 5.5 show the simulation results for the 1 in 100 year event on the River Fulda reach. In contrast to the 1 in 10 year event the MILHY2 prediction gives a higher peak discharge result than the multiple routing reach. The proportional difference between the MILHY2 and multiple routing technique is, however, much smaller in the 1 in 100 year storm being 4%, whereas the 1 in 10 year difference was 11%. This suggests that as the floodplain inundation depth increases the cross-section behaves as a single system. However, predicting the floodplain reach length or Mannings 'n' value has the same effects on the 1 in 100 year event as the 1 in 10 year event, the peak discharge is increased.

5.4.2 Application to a hypothetical reach

The aim of investigating the impact of multiple routing on a hypothetical reach was to look at the relative impact of the floodplain inundation depth on the outflow hydrograph. A hypothetical reach was set up with symmetrical rectangular cross-sections at upstream and downstream stations with a floodplain/main channel width ratio of 10. The main channel was a constant depth of 2.4 metres, so that the main channel capacity remained constant downstream. This meant that the proportion of flow on the floodplain was correct throughout the reach and, therefore,

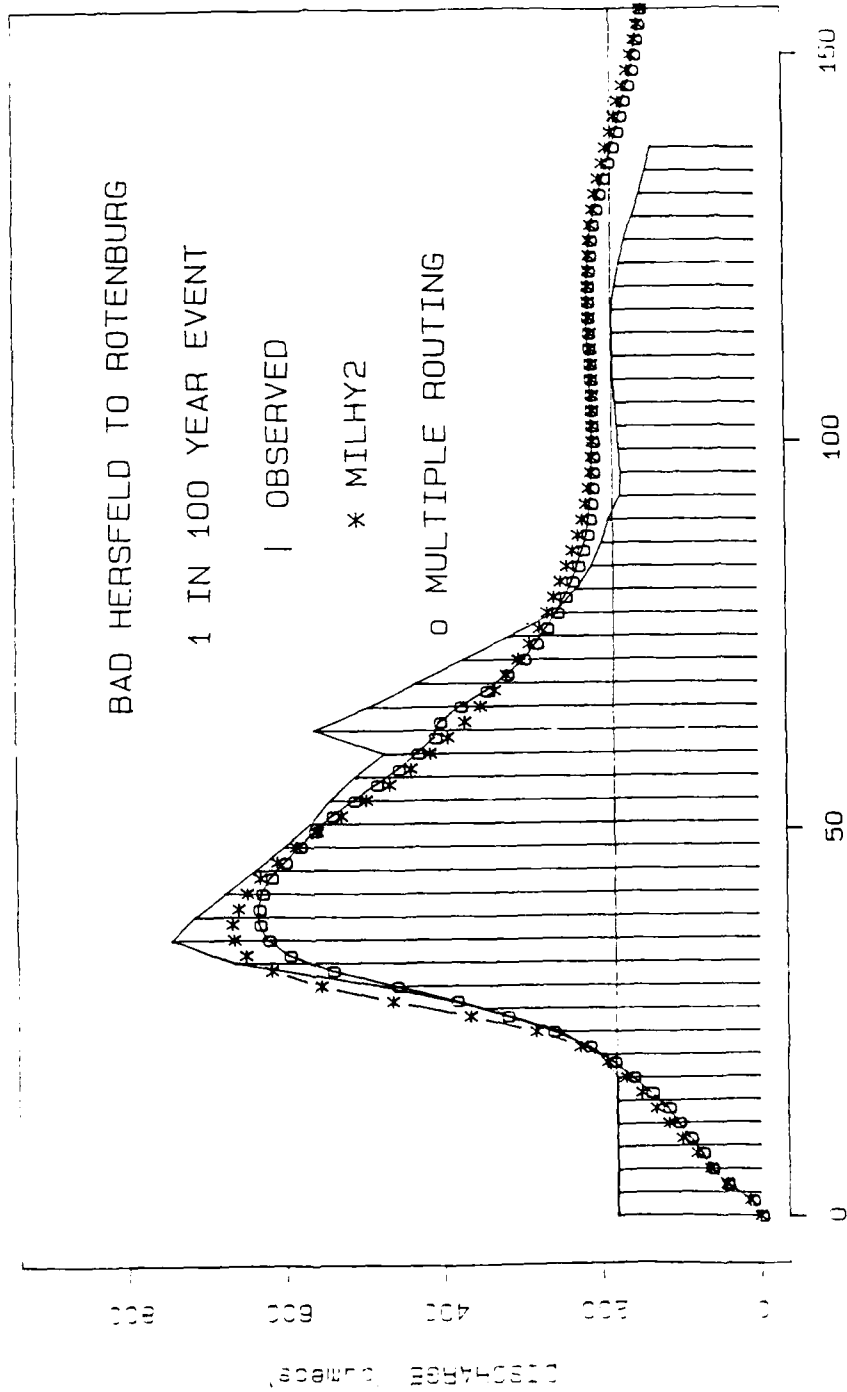


Figure 5.5

the analysis could concentrate on the effects of inundation depth.

Table 5.3 and Figures 5.6 and 5.7 summarize the results from this investigation into the impact of floodplain inundation on depth on the outflow hydrograph. In all these simulations the floodplain and channel reach length were held constant at 20 km. The seven inflow hydrographs were generated by scaling the 1 in 10 year observed hydrograph from Bad Hersfeld (see Figure 5.2). The scaling factor used for each storm is recorded in column two of Table 5.3. By using the same form of inflow hydrograph, it was hoped to be able to isolate the effects of the inundation depth on the time to peak of the outflow hydrograph.

The results in Table 5.3 are summarized on Figure 5.8 which plots the percentage error between the MILHY2 and multiple routing predictions of peak discharge. Negative errors occur when the multiple routing predictions are less than the MILHY2 prediction, positive errors occur when the multiple routing predictions are greater. Figure 5.9 plots the error between the MILHY2 and multiple routing technique when the floodplain routing reach length is reduced by 30%. Analysis of Figures 5.8 and 5.9 show that the predictions from the two techniques converge as the floodplain/main channel depth ratio increases to 1 (equal to a Wormleaton et al. (1982) depth ratio of 2). The maximum error between the two techniques occurs when the floodplain inundation depth is 0.3 of the bankfull depth.

5.4.3 Conclusions

1. The maximum impact of the multiple routing technique occurs when floodplain inundation depths are small.
2. At these small inundation depths (depth ratios 0.3) the utilization of multiple routing significantly improves the prediction of the peak discharge, errors are halved.
3. Reducing the floodplain routing length by 30% reduced the travel time of the peak discharge.

Table 5.3
Hypothetical reach

Storm	Multiple		Time to peak (hours)	Peak discharge ($\text{m}^3 \text{s}^{-1}$)	Maximum floodplain inundation m
1	1	MILHY2	36	309.8	1.16
		M. Routing	36	317.4	1.18
2	0.1	MILHY2	36	34.8	-
		M. Routing	36	32.8	-
3	0.2	MILHY2	42	57.2	0.09
		M. Routing	36	55.0	0.07
4	0.5	MILHY2	40	139.5	0.61
		M. Routing	38	126.9	0.56
5	1.5	MILHY2	36	536.0	1.68
		M. Routing	36	540.8	1.74
6	2	MILHY2	34	682.0	1.98
		M. Routing	34	685.0	1.99
7	3	MILHY2	34	1061.0	2.65
		M. Routing	34	1062.0	2.65

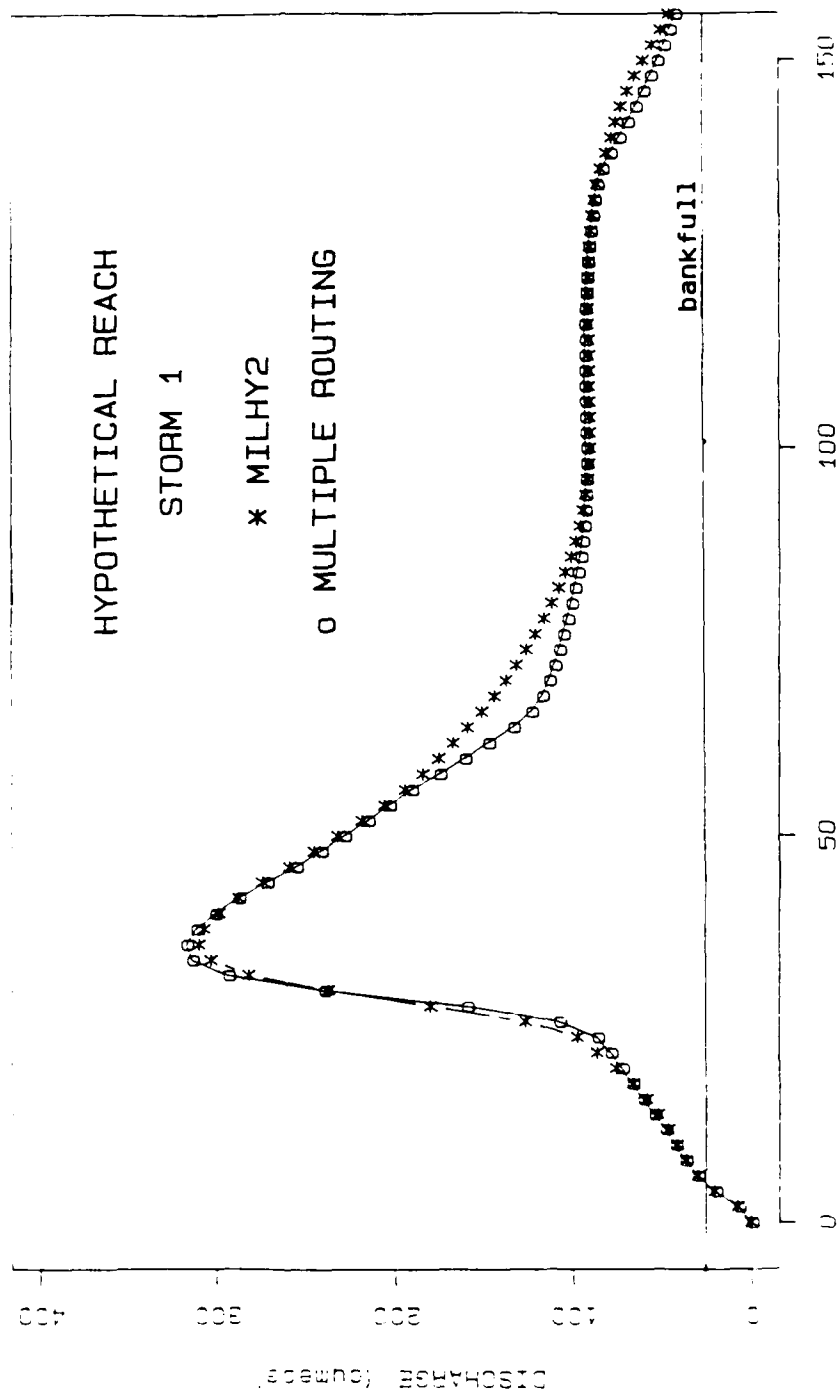


Figure 5.6

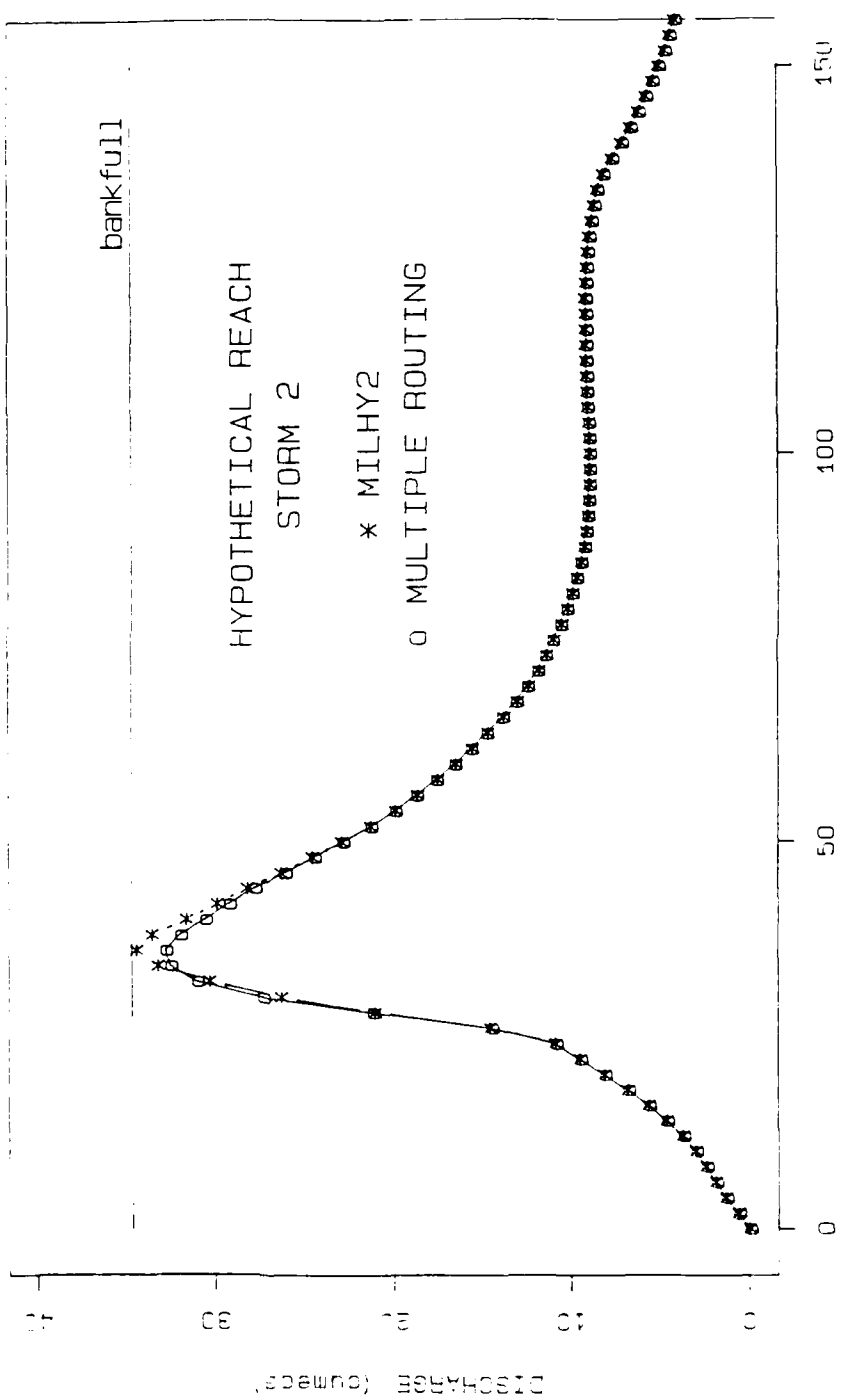


Figure 4.7

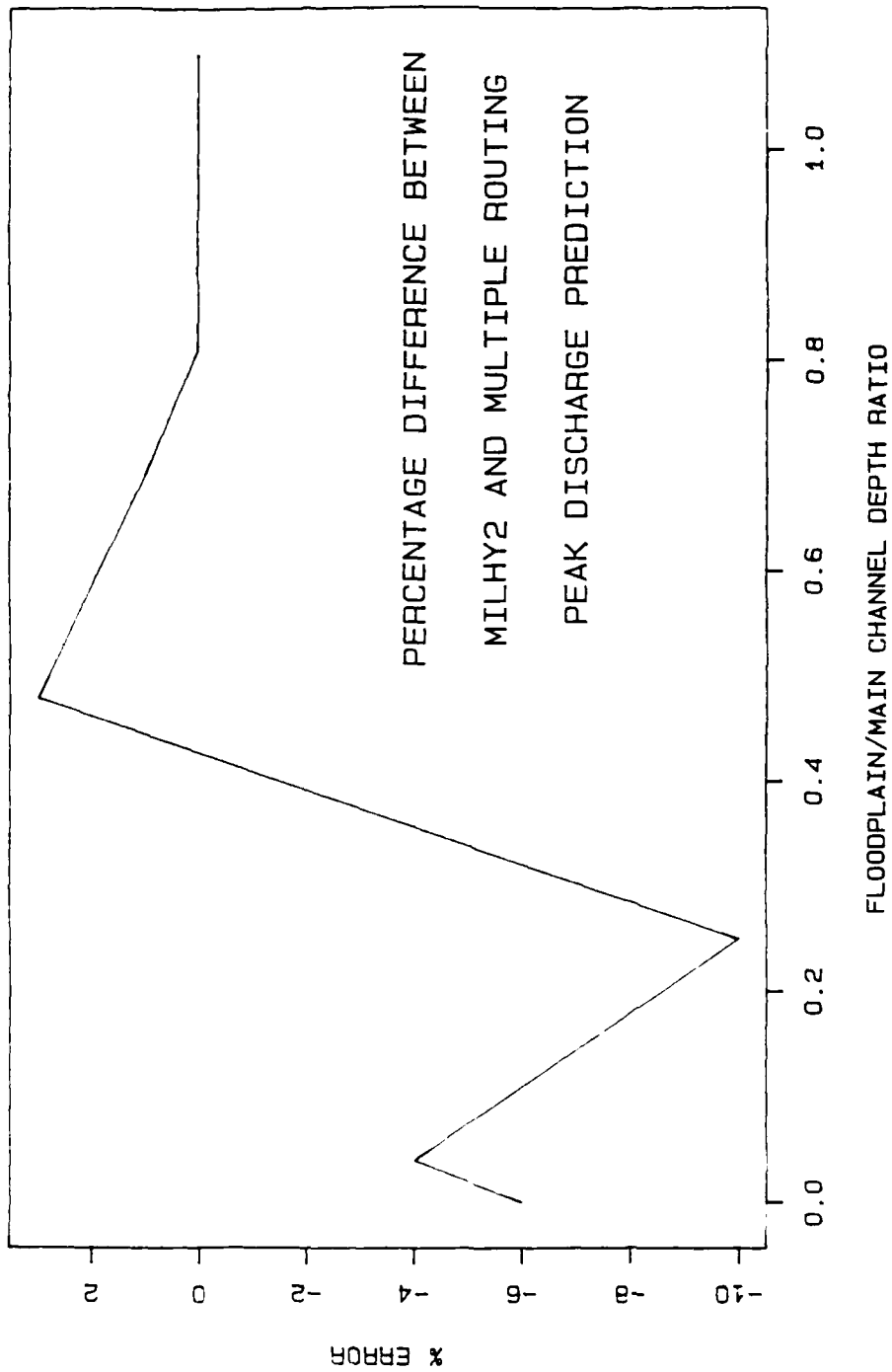


Figure 5.8

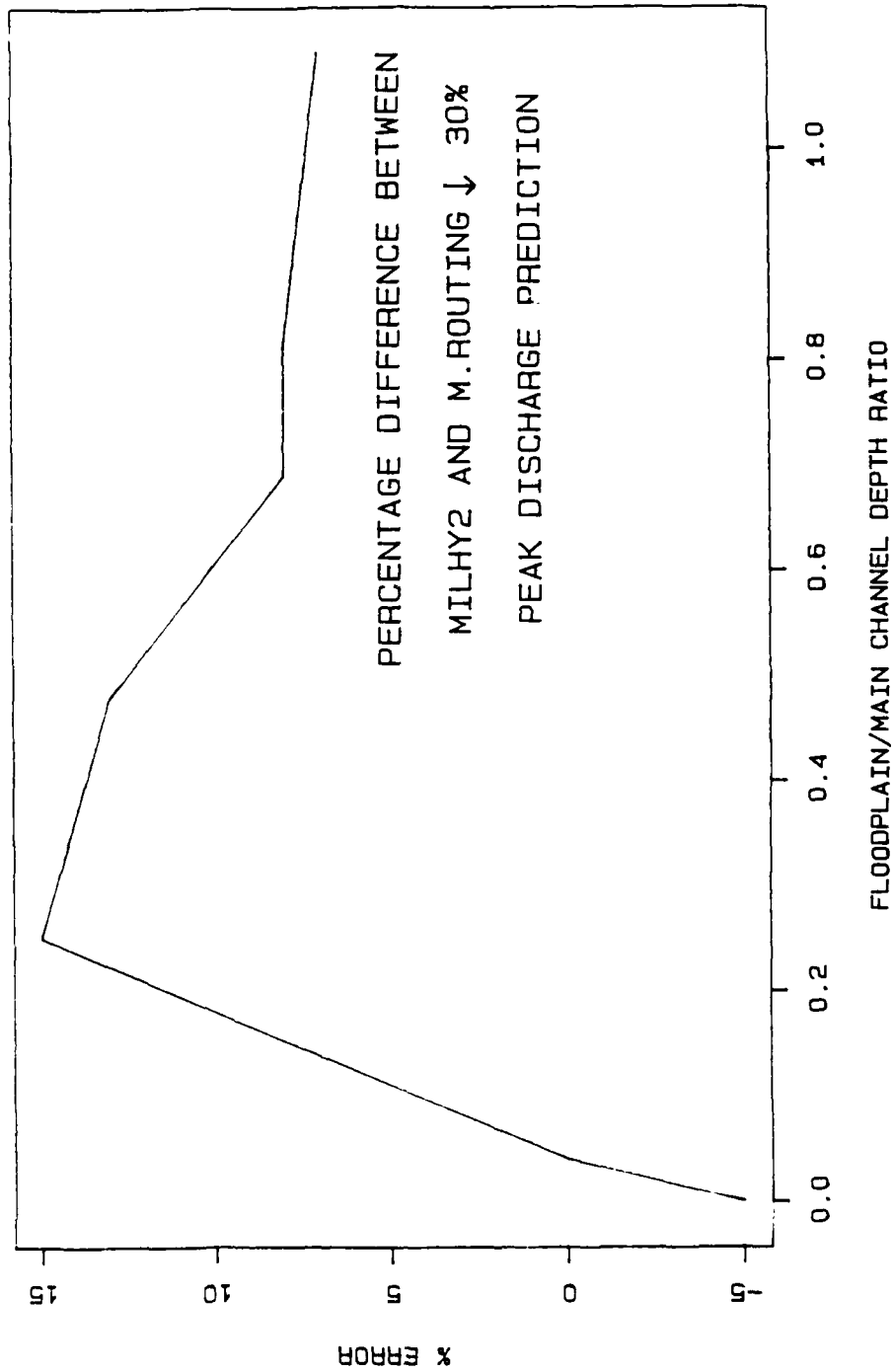


Figure 5.9

SECTION 6 : VALIDATION OF MILHY3

Before MILHY3 can be deemed to be operational the following questions must be answered:

1. Do the mathematical algorithms introduced represent the processes we are trying to model?
2. Are the mathematical algorithms robust?
3. Is the accuracy of the predicted outflow hydrograph a significant improvement over earlier versions of MILHY?
4. Is the resolution of each new submodel consistent with each other, with existing submodels and appropriate for ungauged applications?
5. Can a set of operational rules be developed for MILHY3?

The behaviour of the results reported in the initial analysis in Sections 4 and 5 suggests that the turbulent exchange and multiple routing algorithms are correctly modelling the effects of friction on the outflow hydrograph. These simulations prove that the algorithms are internally valid, that is that the outflow hydrograph does not change when the input parameters are held constant (Hermann, 1967), and that the algorithms are mathematically robust. Simulations also showed, although not reported here, that the coding of the turbulent exchange and multiple routing routines was correct, in that during in-bank conditions neither routine was invoked. Sections 4 and 5 have therefore satisfactorily verified the coding of the new submodels in answer to questions 1 and 2, and show that the new routines are modelling the processes they were designed to and are robust. The results also suggest that the new submodels are an improvement on the predictions made by earlier MILHY versions, although further testing is required to thoroughly establish this.

In the selection of the new algorithms the objective was to improve the predictive capability of MILHY by incorporating the representation of the active processes. However, the selection was made taking into consideration the limitations of the final objective of maintaining MILHY as an operational, ungauged model. These limitations were:

- (1) the data requirements of the new algorithms should be small; in particular field work should not be required
- (2) any additional demands made of the user in the establishment of the datasets should not require detailed hydrological knowledge of the physical processes or computer expertise
- (3) the computer demands, in terms of CPU and operating space, of the new routines should not limit the models portability to the IBM-PC level

In answer to question 4, posed above, these limitations reduce the risk of over-development in the resolution of modelling in a particular process area. The concentration of model resolution on the most important processes in an otherwise lumped model, improves efficiency but has inherent dangers. The dangers include limiting the portability of a model by increasing the quality and quantity of its data demands. It is felt therefore that the submodels developed in sections 4 and 5 are of a consistent resolution with each other, the existing submodels and the limitations of ungauged modelling.

Before a set of operational rules (question 5) can be developed, a series of applications must be made. It is to this question and to the quantification of the possible improvement in the predictive accuracy of MILHY that the rest of this section is directed. In the analysis of the applications that follow, all five of these questions will be investigated and the conclusions drawn from the results of sections 4 and 5 reassessed.

To answer the two outstanding questions posed at the start of this

section, several specific questions may be asked. These are:-

- (1) Is the outflow hydrograph more sensitive to variability in its parameters, or to the process submodels utilized?
- (2) What is the relative impact of the submodels introduced in MILHY3 in comparison with the infiltration algorithm introduced in MILHY2?
- (3) What is the impact on the outflow hydrograph of the conflicting effects of the new submodels?
- (4) What is the effect of the scale of the catchment on the three questions posed above?

To answer these and to complete the answering of the general questions asked earlier, it was felt necessary to undertake a sensitivity analysis of MILHY3. This analysis would compare hydrograph predictions made by MILHY3 and MILHY2 against data collected from a gauged catchment for out-of-bank conditions.

It is important to note at this point that the infiltration algorithm introduced in MILHY2 has only been applied to single subcatchments. Work by Anderson and Howes (1986) reported in Section 1 of this report, showed that the infiltration algorithm significantly improved the generation of the runoff hydrograph. The relative importance of this improvement in a large catchment, where several subcatchments are utilized, has not yet been tested.

6.1 Selection of a field site

From the objectives listed above, a list of prerequisites for the study catchment was developed.

6.1.1 Prerequisites of a study catchment

1. The catchment must be in a temperate region with a minimum of

forested areas.

2. The catchment must not exceed a maximum area of approximately 2500 km^2 (1000 sq.mi.), (Williams, 1975).
- 3.. There should be a minimum of man-made interferences with the hydrology of the catchment, such as reservoirs or land drainage schemes.
4. There should be intermediate gauging stations throughout the catchment, so that a suite of catchments can be developed.
5. The catchment must be subject to floodplain inundation.
6. The floodplains should be geometrically simple, bounded and preferably with a similar land-use type throughout the catchment.
7. Data should be easily available and reliable. The minimum requirements are:-
 - i) topographic maps
 - ii) soils classification maps
 - iii) cross-sectional geometries for a number of gauging stations in the catchment
 - iv) rating curves for these gauging stations
 - v) a number of storm hydrographs including out-of-bank events from each gauging station
 - vi) corresponding rainfall data for these storm events and the week preceding. Data must consist of a minimum of daily information from at least one rain gauge in the catchment
 - vii) flood frequency data to indicate the frequency and size of out-of-bank events

6.1.2 The River Fulda Catchment

These seven prerequisites limited prospective study catchments to the rural regions of Western Europe and areas of the U.S.A. From a short list of regions meeting the prerequisites, the River Fulda catchment in West Germany (see Figure 6.1) was selected, primarily because of the efficiency and rapid response to requests made to the relevant water authorities and meteorological offices. As well as the prerequisite data, the local authorities in the River Fulda catchment were able to provide:-

- i) an outline of the extent of floodplain inundation for a storm event in 1946, corresponding to the 1 in 200 year event
- ii) daily precipitation values for approximately 45 rain gauge stations (see Figure 6.2)
- iii) continuous rainfall data for two stations, Bad Hersfeld and Kunzell-Dietershausen
- iv) for one storm, the water-equivalent of snow, daily minimum and maximum temperatures, relative humidities and cloud cover
- v) long-profiles of two of the reaches, between Bad Hersfeld and Rotenburg, on the River Fulda, and between Marbach and Hermannspiegel, on the River Haune (a tributary of the River Fulda)

At this point, we would like to acknowledge the help and cooperation of the Water Authority, Wasserwirtschaftsamt, Fulda for the provision of the hydrological data and the Meteorological Office, Deutscher Wetterdienst Zentralamt, Offenbach, Frankfurt, for the meteorological records, collected during three visits to the catchment in the period November 1986 to June 1988. A copy of this raw data has been forwarded to the Environmental Laboratory, WES, Vicksburg, Mississippi, who kindly provided the soils classification maps.

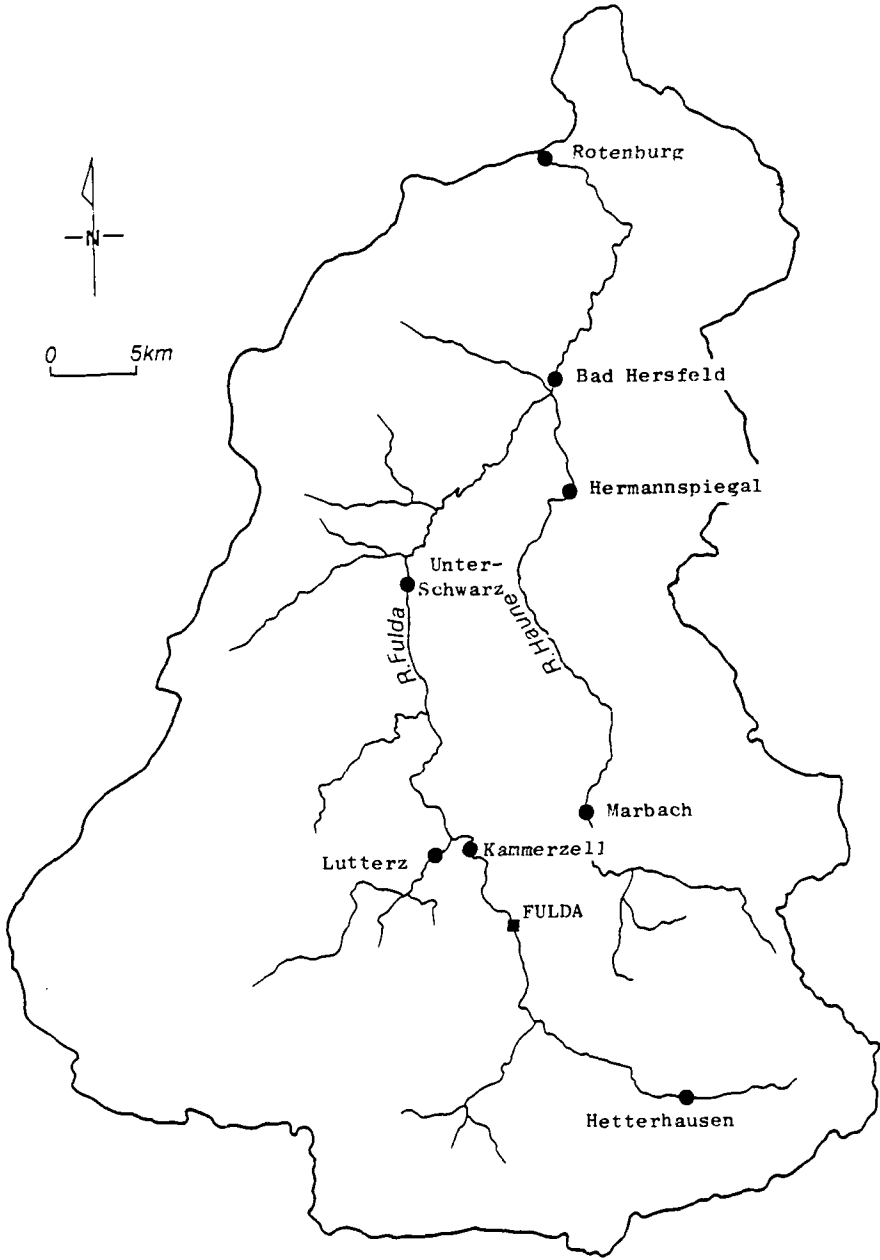


Figure 6.1 : River Fulda Catchment

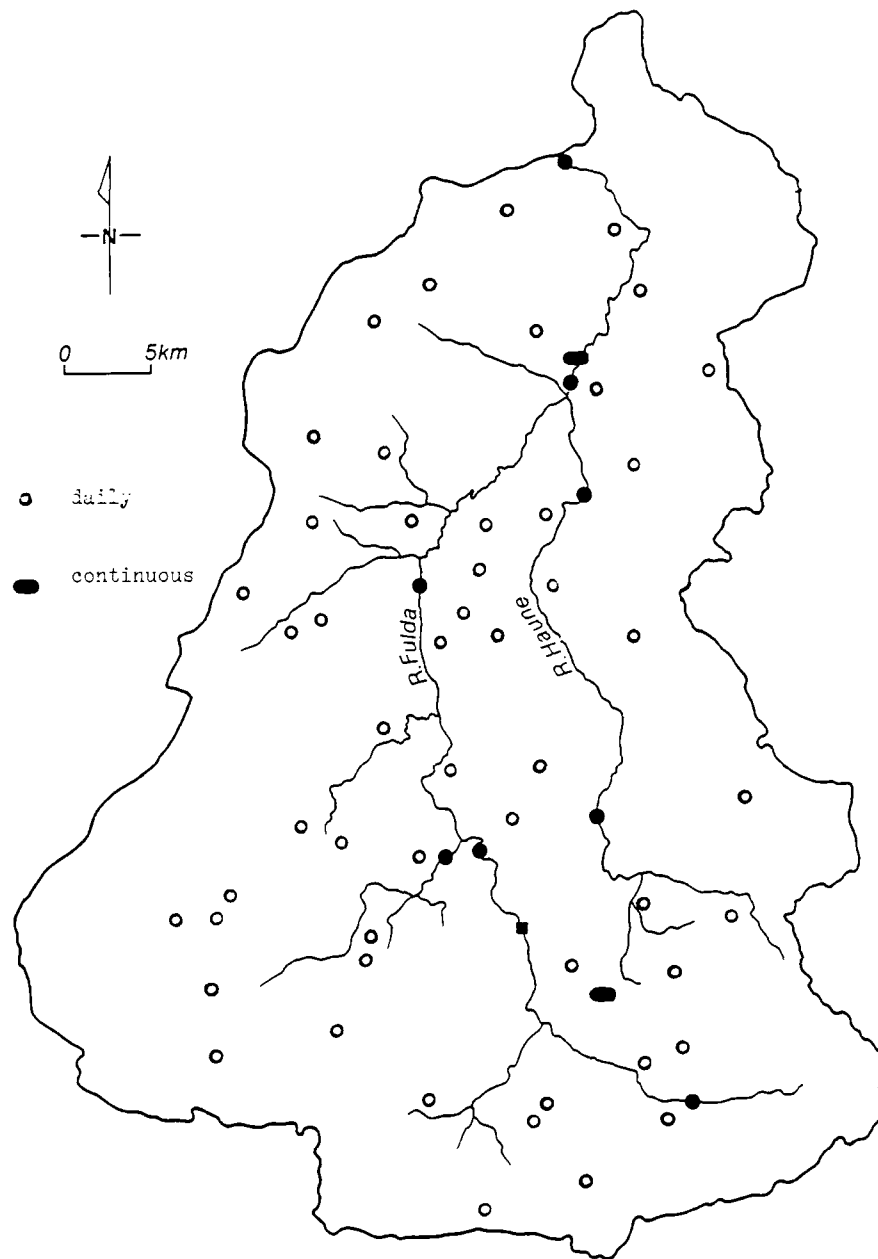


Figure 6.2 : Raingauge Network

6.2 Establishment of the River Fulda Catchment

The River Fulda catchment to Rotenburg consists of a drainage area of approximately 2523 km² (974 sq.mi.), drained by the River Fulda and its tributaries. The main tributary is the River Haune which joins the Fulda at Bad Hersfeld; in addition, the River Luder joins the Fulda at Lutterz. There are eight river gauging stations in the catchments, marked on Figure 6.1 for which six storm events have been collated. The positions of the gauging stations have enabled the division of the catchment into nine subcatchments depicted in Figure 6.3.

During the visits to the catchment, sketches were made and photographs taken that enabled the technical channel cross-sections to be extended across the floodplains. Estimates were also made during these visits of the Mannings 'n' roughness values of the channel and floodplain throughout the catchment. Figures 6.4 to 6.6 are photographs taken at Hetterhausen, Unter-Schwarz and Rotenburg, and show the topography and land-uses typical throughout the catchment. The photographs show that:-

- i) in the upper reaches the channel is tree-lined
- ii) the floodplains are extensive and flat
- iii) the floodplains throughout the catchment are vegetated by short grass
- iv) there are few obstructions on the floodplains, there are few fences, and the small villages tend to have been built clear of the areas subject to flooding
- v) the channel is broadly rectangular in cross-section
- vi) the channel is sinuous

Tables 6.1 and 6.2 collate some of the topographic dimensions of the subcatchments and the channel geometries at the gauging stations.

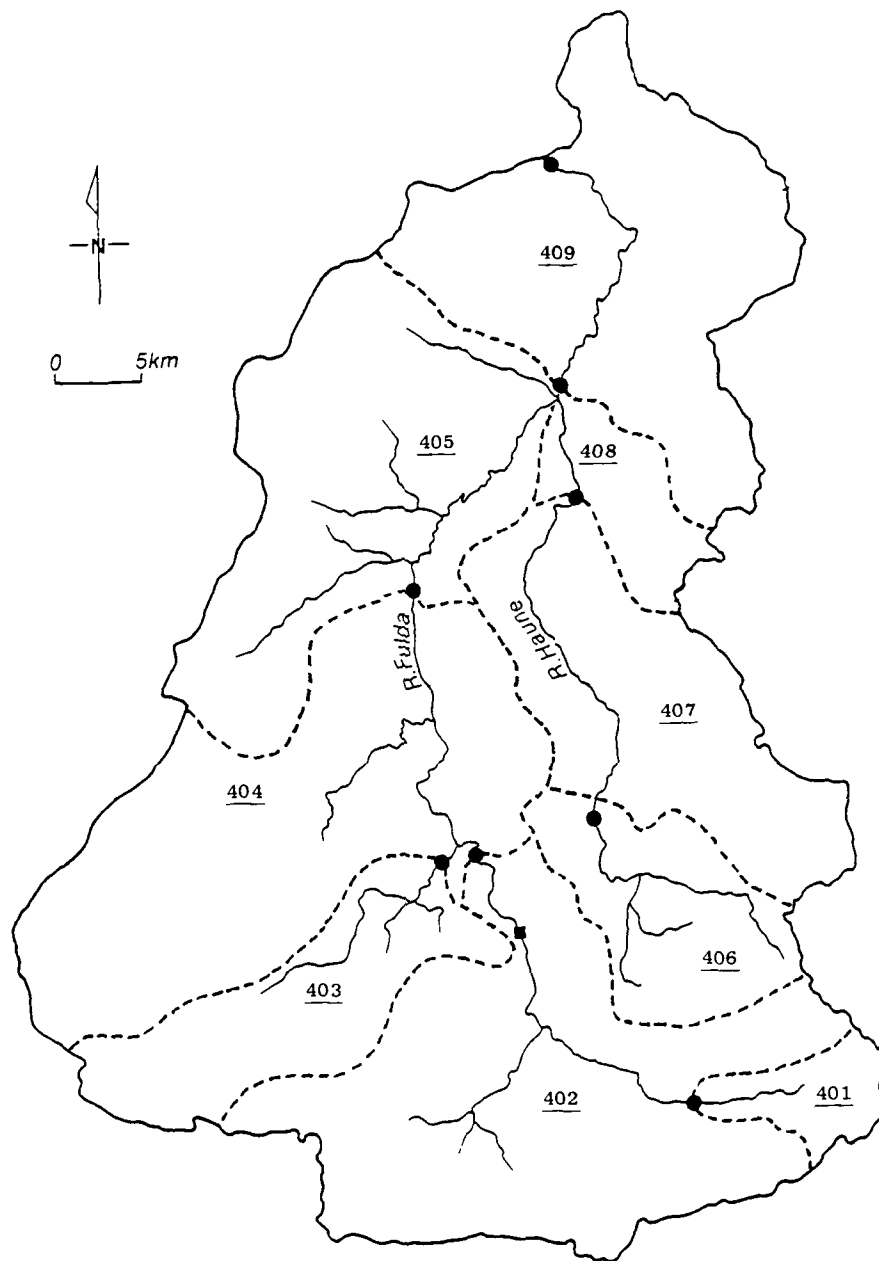


Figure 6.3 : River Fulda Subcatchments



Figure 6.4 : Hetterhausen



Figure 6.5 : Unter-Schwarz



Figure 6.0 : Rockbury

Table 6.1

Parameter Values for Subcatchments in the River Fulda Catchment

Subcatchment	Area km ²	Max. elev. m.	Min. elev. m.	Main channel length km.
401	56	838	365	14
402	506	550	232	36
403	182	700	232	25
404	469	775	216	27
405	394	416	193	33
406	148	700	265	24
407	274	610	209	34
408	90	518	193	9
409	403	391	179	24
Total	2523	838	179	227

Table 6.2

Parameter values for Gauging Stations in the River Fulda Catchment

Station	Bankfull depth m.	Bankfull width m.	Bankful capacity $m^3 s^{-1}$
Hetterhausen	2.3	17.0	26
Kammerzell	2.0	20.1	33
Lutterz	3.2	18.0	18
Unter-Schwarz	3.0	18.0	50
Marbach	2.3	8.0	10
Hermannspiegel	2.5	16.5	22
Bad Hersfeld	4.1	30.3	76
Rotenburg	4.8	50.0	179

Note: Cross-sectional geometrical data was not available for the Unter-Schwarz gauging stations. The figures that appear are estimates made during visits to the catchment.

The six storm events were identified as being discrete events, that is where the hydrographs rose and fell back to baseflow condition with a single seven day record. For each of these events, the daily rainfall totals for the three preceding weeks was collected in order to compute the antecedent conditions.

In order to compute the rainfall in each of the nine subcatchments, the theisson polygon technique was used to weight the daily rainfall total from each of the 45 rain gauges shown in Figure 6.2. Polygons of the area that could be associated with a particular raingauge were drawn as if the catchment were a peneplain.

Table 6.3 shows the percentage occurrence of each of the major soil groups in each of the nine sub-catchments. A certain amount of interpolation and generalization occurred during the computation of this table, as the pixel definition of the soils classification map (1 pixel = 100 metres) was a little detailed. The use of a graphics tablet attached to an IBM-AT, however, considerably speeded the computation of both the raingauge polygons and soils group areas.

6.2.1 Establishment of the Data Sets

Two data sets are required by MILHY3; 'data1' contains the program commands, hydrological commands and associated data, whilst 'data2' contains only data for the infiltration algorithm. The rules for setting up these data sets and examples of them are given in Appendix 2.

Data1

Figure 6.3 illustrates the division of the River Fulda catchment into nine subcatchments. In each of these subcatchments, a runoff hydrograph must be developed, and in all except the headwater subcatchments, this must be added to the flow routed through the subcatchment. In each routing reach, two cross-sections are developed, one at either end of the reach. In subcatchment 404, where the River Luder joins the River Fulda at its inflow, the Kammerzell cross-section is used.

Table 6.3

Soil Group Classification for the Sub-Catchments
on the River Fulda Catchment

Sub-catchment	UCSC Soil Classification System				
	Percentage occurrence of group				
	SC/SM	ML	CH	CL	G
401	54.6	11.6	11.3	10.5	12.1
402	45.6	10.3	5.2	27.7	11.4
403	25.0	2.9	4.0	59.9	7.9
404	36.6	2.7	15.2	33.0	12.0
405	65.8	4.1	4.7	8.2	17.3
406	50.1	13.4	9.8	21.4	5.4
407	46.4	8.4	25.2	15.5	4.6
408	41.0	-	15.2	34.7	9.2
409	86.5	-	4.8	-	8.6

- SC - Clayey sands or clayey gravelly sands.
 SM - Silty sand or silty gravelly sand.
 ML - Silts, sandy silts, gravelly silts.
 CH - Fat clays
 CL - Lean clays, sandy clays, or gravelly clays
 G - Gravels (grouped together)

The Curve Numbers for the generation of the runoff hydrograph using the SCS method were identified from tables in the Student Handbook on streamflow forecasting by James and Stinson (1981).

Data2

Each soils group in each subcatchment was represented by a single soil column, giving a total of 42 columns (see Table 6.3). The runoff generated by these columns was weighted by the percentage area of each subcatchment that a soil group occupied. For the six storm events identified during the establishment of the River Fulda catchment, a common theme was a period preceding each event of small low intensity showers. This enabled the fairly safe assumption that the soils were saturated at the beginning of each of the six identified events.

Each of the 42 soil columns was split into 3 layers, typical of well-developed soils, and a total of 10 cells were specified. The soils hydrological parameters were identified from the empirical charts and regression equations developed by Brakensiek and Rawls (1983), and reported in Anderson and Howes (1984).

To check that these data sets correctly represented the River Fulda catchment, a test simulation was established using a storm occurring in March 1986. During these trials two problems were identified. These were:

- i) during the application of the multiple routing technique, it appeared as if the addition subroutine, 'ADHYD', that sums two hydrographs, failed to be operating properly
- ii) the infiltration algorithm did not seem to be generating enough runoff in terms of the total volume of runoff throughout the storm

Investigation into the first of these problems identified a small bug in the original coding, that enabled one of the time intervals of the hydrographs being added to be overwritten if the time intervals of the

two hydrographs were different, and the identity number of the sum of the two hydrographs was the same as one of the hydrographs. This problem was only identified because of the complexity in the structure of the River Fulda catchment, and the large number of additions required. It is unlikely, therefore, that any previous work has been affected by this error. This bug has been rectified in the latest version of MILHY3, a copy of which is in Appendix 3.

The second problem to be identified, that the infiltration algorithm failed to produce enough runoff, was firstly blamed on the low precipitation intensity. The rainfall for each subcatchment was generated by:

- 1) Identifying the daily totals for each of the rain gauges in a subcatchment.
- 2) These totals were then weighted by the area of the Thiessen polygon associated with each raingauge.
- 3) The daily rainfall for each subcatchment was then divided into three time intervals of eight hours each according to known rainfall figures from a gauge at Fulda.
- 4) The hourly rainfall was then computed, assuming a minimum rainfall intensity of 1mm/hour, distributing backwards from the end of each of the thrice daily intervals.
- 5) The hourly totals were then cumulated.

However, this method and assumptions it was based upon, seemed reasonable, as the volume of precipitation over the River Fulda catchment was conserved. The runoff problem seemed to be a soils problem.

As noted earlier, the soil at the commencement of the simulation is assumed to be saturated, however in this example the simulation was started a more realistic three days prior to the start of the observed

outflow hydrographs, to allow some drainage. Analysis of the results from the infiltration algorithm showed that most of the precipitation was draining into the soil and very little was generating overland flow. These results focused attention on the firstly saturated hydraulic conductivity for each of the soil classification groups and, secondly, the occurrence of each of these soils groups.

A second trial simulation used the minimum saturated conductivity values recorded in the Brakensiek and Rawls (1983) tables for each of the soils group. This did not increase the volume of runoff generated, thereby identifying the soils classification maps as a possible source of error.

6.2.2 Soils classification problems

There are several feasible sources of error in the generation of the proportion of a subcatchment that a soil group contributes. These include:

1. Resolution. This includes the resolution of the soil surveyor's report, and the interpretive work carried out in the establishment of the data set. The resolution of the original survey will depend upon the purpose to which the map is aimed. Beckett and Webster (1971) point out that there is little practical purpose in having a resolution size less than the minimum land-use management area, usually a field.
2. Purity. This is the percentage area of each group that is occupied by that group. Beckett and Webster (1971) identify the level of purity many of the soil survey organisations attempt to work to, and this includes the USDA purity level of 80-90% (Simonsen, 1962), and the US Bureau of Reclamation purity level of 75%.

Analysis of the results from the infiltration algorithm simulations showed that it was only the clay groups (CH and CL, see Table 6.3) that

had a low enough saturated hydraulic conductivity to generate overland flow. Could we legitimately increase the percentage occurrence of these two groups, in line with the purity percentages reported above? Returning to the soils classification maps, closer analysis showed that the distribution of the clay grouped was heavily biased to the floodplain areas, where runoff could be expected to join the channel flow, due to the high water table and low slope angles. Without entering the field of "partially-contributing areas", and models such as VSAS-2 (Hewlett and Troendle, 1975), it would be impossible to quantify the importance of these contributing areas. However, it would suggest that in future applications the percentage area of soil groups with low hydraulic conductivities should be estimated more accurately at the expense of accuracy in other topographical zones of the catchment. Having completed the measurement of each soil group's extent in the River Fulda catchment, it was decided to experiment with the percentage area of the clay groups in the three headwater subcatchments.

Trials showed that increasing the occurrence area of the clay groups by 35% increased the runoff volume to match the observed hydrograph. The consistency of the level of increase required in the three subcatchments confirmed that we were investigating a real error and not merely calibrating the model. A 35% increase in the occurrence area of the clay groups meant that at least 15% of the error could be assigned to a resolution problem, accepting that the purity error accounted for up to 20% of the error. Looking at the soils classification maps and the complexity of soil crops in the valleys, a 15% error seemed very feasible. In the simulations reported in the rest of Section 6, therefore, the increased clay percentage occurrences have been applied.

6.3 Design of the sensitivity analysis

The main objectives of the sensitivity analysis are to investigate:

- 1) The sensitivity of the hydrograph to variation in MILHY3's parameters.

- 2) The sensitivity of the hydrograph to the submodels used in its development.
- 3) The interaction of the effects of the turbulent exchange and multiple-routing submodels.
- 4) The relative impact of the inclusion of infiltration algorithm in catchments where subcatchments are utilized.
- 5) The effects of scale.

It was first necessary, therefore, to identify all the parameters and submodels that make up MILHY3. Table 6.4 lists all the variables in three groups, spatial variables, temporal variables and physically-based parameters. The spatial and temporal variables describe the resolution of information in each submodel or process area, whilst the physically-based parameters describe the initial conditions and geometry of the catchment. Figure 6.7 describes the submodels contained in MILHY3 and shows the alternative pathways through these submodels.

Table 6.5 contains a list of all reported sensitivity analysis carried out on all versions of MILHY and HYMO. The table also gives the authors of these analysis so that the reader may refer to these texts, as the design of the sensitivity analysis reported here will avoid repetition of this work. As noted earlier, however, the simulations reported by Anderson and Howes (1984, 1986), and in Section 4 of this report, are single subcatchment applications. The sensitivity analysis reported here will consider the relative sensitivity of some of these variables in a multi-subcatchment application.

If we were to consider varying all the parameters listed in Table 6.4 in a statistically meaningful way, then a conservative estimate of the approximate number of simulations required would be 640, taking an impressive 6000 hours of CPU on the SUN workstation. The estimate ignores the ability of MILHY3 to incorporate stochastic variability in five of the soil parameters. It is important, therefore, to carefully

MILHY3
MODEL STRUCTURE

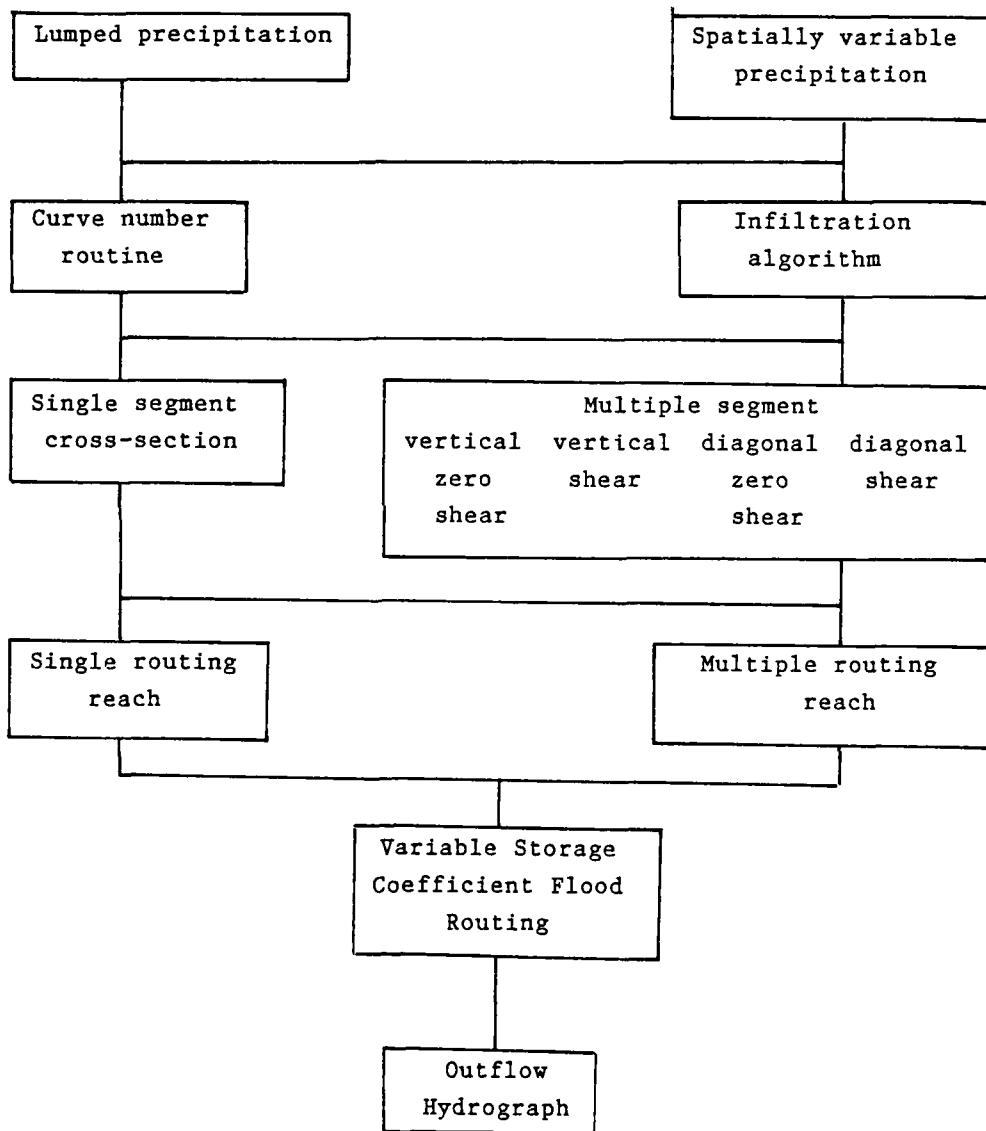


Figure 6.7 : MILHY3 submodel components

Table 6.4

Variables in MILHY3Spatial variability

Number of subcatchments
Number of rain gauges
Number of soil columns
Number of soil cells
Thickness of soil cells
Number of valley sections in reach
Number of segments in cross-section
Rating curve stage increment

Temporal variability

Rainfall time increment
Infiltration simulation iteration period
Routing time interval

Physically-based parameters

Initial soil moisture content
Saturated moisture content
Suction moisture curve
Saturated hydraulic conductivity
Surface detention capacity
Maximum evaporation
Watershed area
Watershed elevation
Main channel length
Cross-sectional geometry
Slope, channel and floodplain
Routing length
Mannings 'n', channel and floodplain
Reservoir outflow storage
Soil, crop, conservation and gradient factors
Precipitation - storm duration, intensity

Table 6.5

Sensitivity Analysis carried out on MILHY

<u>Author</u>	<u>Parameter or Variable</u>
Williams (1975)	Routing length Routing time interval
Anderson (1982)	Detention capacity
Anderson & Howes (1984)	Suction moisture curve Saturated moisture curve Saturated hydraulic conductivity Initial moisture content
Anderson & Howes (1986)	Watershed area Watershed elevation Main channel length Storm intensity Cell size Infiltration simulation increment
Anderson & Singleton (1987)	Precipitation, spatial variability
<u>Initial results</u>	
<u>this report:</u>	
Section 4	Number of segments in cross-section Rating curve stage increment Cross-sectional geometry Mannings 'n' Slope

select a series of simulations that will enable the sensitivity of MILHY3 to be ascertained with a fair degree of certainty. Interest has been directed in this project to the modelling of the frictional effects of over-bank flow or flow in two-stage channels. The sensitivity analysis will reflect this concentration and therefore focus in this area. The analysis will investigate the structure of MILHY3 in terms of its submodel components and explore variability in the physically-based parameters in the downstream conveyance submodels. These parameters will include the slope of the channel and floodplain, the routing length and Manning 'n' values for the channel and floodplain.

Having directed the sensitivity analysis to a manageable area of investigation, the next decision was to investigate alternative approaches available for exploring this area.

6.3.1 Alternative methods of undertaking a sensitivity analysis

McCuen (1973) defines sensitivity as:

"the rate of change in one factor with respect to change in another factor"

McCuen points out that it is the failure of researchers to appreciate the generality of this definition that has limited the application of the sensitivity analysis tool to the final verification of models. Several authors have identified the utility of the sensitivity analysis in all stages of the development of a model (McCuen, 1973, 1976; Miller et al. 1976; Hornberger and Spear, 1981). This is why an initial analysis was incorporated in the identification of most important processes in two-stage channels (Section 3) and in the development of the submodels to model these processes (Sections 4 and 5).

Jones (1982) identified two approaches to undertaking a sensitivity analysis, a deterministic and a stochastic methodology. A deterministic methodology involves making small changes in the input parameters and investigating changes these changes provoke on the model's output. A

stochastic approach involves selecting the input parameter values from a probability distribution of usually either the accuracy of the input values or the error bands to which the model internally operates. A stochastic analysis can usually, therefore encompass a wider range of input data values than a deterministic analysis, as the probability distributions can contain all physically realistic data input values. In a deterministic analysis the operator must usually either select input values systematically, or use his intuitive knowledge of the behaviour of the input parameters.

Work by Anderson and Howes (1984, 1986) has concentrated on a stochastic analysis of the soil input parameters of the infiltration algorithm. The difficulties of measuring these parameters in the field mean that a relatively large error band can be associated with the observed field values. A stochastic analysis was an ideal method of incorporating these error bands in an analysis of the effects of parameter variability on the model's output.

In the sensitivity analysis reported here, we are aiming to investigate the behaviour of the model's output with respect to the model structure and variability in certain parameters. As the model structure cannot be described by a probability distribution, this necessitates a deterministic analysis.

There are two methods of computing the sensitivity of a model to a parameter, known as the sensitivity function, in a deterministic approach. These are:

- 1) Differentiation: the model described as a function is parametrically differentiated with respect to each parameter. The mathematics of this approach has yet to be made portable enough to enable this approach to be widely used.
- 2) Factor perturbation: each parameter is incremented and the changes in the output quantified. This method was used by Smith (1976) and as noted earlier has extensive computing time requirements.

In the sensitivity analysis reported here, the factor perturbation technique was used in two separate approaches, for the model structure and for the parameter variability. As the number of feasible submodel combinations was relatively small (see Figure 6.7), it was possible to establish and execute a complete matrix of possible permutations. In investigating the sensitivity of MILHY3 to variability in the selected physically-based parameters, it was decided to attempt to utilize a technique previously only used to optimize the fit of parameters in calibrated models.

Although these optimization techniques are well-established, it seems that they have not been used as an alternative to the sometimes tedious development of factor perturbation matrices. It was hoped that, if successful, the intermediate values of the optimization scheme would provide a good indication of the sensitivity of the outflow hydrograph, as the scheme searched to find the 'best-fit' between an observed and a computed hydrograph. This would remove the necessity to initialise a great number of datasets and manually search through the results sets. A post-processor could search through the iterations of optimization scheme and find the parameter values that caused the greatest or smallest impact on the computed outflow hydrograph. Although there would not be any direct control over the parameter values selected by the optimization scheme, in a factor perturbation analysis the selection of values is usually subjective and therefore could just as easily overlook significant points. However, it must be noted that this investigation into the utility of optimization schemes is rather exploratory. The feasibility of using optimization schemes as an alternative to traditional factor perturbation techniques will depend upon:

- 1) the initialization period to set-up the scheme
- 2) computer demands
 - i) CPU
 - ii) disk storage

6.3.2 The optimization approach

As noted earlier, the technique of optimizing the fit of parameters in hydrologic models using a sensitivity analysis for the purposes of calibration, is well established. Applications have included Armstrong et al. (1980) and Ibbitt and O'Donnell (1971). McCuen (1973) identifies a range of techniques mostly based on the work of Cauchy (1847), who developed the method of converging the solution utilizing the rate of descent or gradient of an objective function of the model's output in response to parameter input variability.

A range of optimization techniques for minimising and maximising a function is available in the NAG (Numerical Algorithms Group) Library. Depending on the level of sophistication required and the availability of the derivatives of the function, an appropriate routine can be selected. A simple routine was selected for this exploratory investigation (e04jaf) which allows the user to select the upper and lower boundaries of each variable and did not require derivatives. The routine worked by developing a surface of values for a function (F) that describes the difference between a computed value and an observed value. The routine then searched for a minimum in this surface by selecting parameter values within the specified boundaries. A prerequisite, therefore, of this approach is that a function can be computed that adequately describes the difference, in this case, between an observed and computed hydrograph. The 'least squares' approach was identified as being a function already computed by MLHY3, in subroutine 'ERROR', and provided a simple test of the fit of the observed hydrograph. Figure 6.8 describes how the MLHY3 model, the function and optimization routine, e04jaf fit together schematically. In terms of the computer coding, MLHY3 is treated as a function called by e04jaf, which in itself is called by a short front programme which sets up the boundary conditions. Once the routine is running, it is difficult to interrupt as all the commands are issued by the library routine, e04jaf.

As this investigation was exploratory in nature and because of the concentration of the analysis on the downstream conveyance subroutines,

the infiltration algorithm and Curve Number routines were not included in the optimization scheme. The demands of the processor of the iterative nature of the optimization scheme, and storage of the results files was foreseen as a potential problem area, without exacerbation from the infiltration algorithm.

Setting up the optimization scheme, shown in Figure 6.8, proved a reasonable straightforward task, complicated only by the intermittent nature of the 'read' statements. The 'read' statements were rewritten, so that all commands and data was read in the 'front end' routine. All 'write' statements were edited out, bar the warning and failure statements, and the printing of the outflow hydrograph. The ability of MILHY3 to tolerate any set-up structure in the 'data1' dataset was retained, to permit the use of the multiple routing routine which is invoked using additional commands in the dataset.

MILHY3 then had to be fronted so that it appeared as a 'function' to the optimization routine (e04jaf). This necessitated the addition of several COMMON BLOCKS to ensure all the data was correctly passed from the initialization (front-end) routine. Lastly, all the parameters had to be defined as being 'double-precision' to enable them to be correctly incremented by e04jaf. It took about two weeks to set-up and test the optimization scheme, a similar period to the time taken to set up a whole series of datasets.

To test that the optimization scheme was working properly and reaching a minimum, for one particular application, three simulations were undertaken. In each of these simulations the initial parameter values were changed to check that the scheme was stopping at an absolute minimum. The initial conditions specified for all the variables were:

- 1) the upper boundary limits
- 2) the centre of the parameter limits
- 3) the lower boundary limits

OPTIMIZATION SCHEME

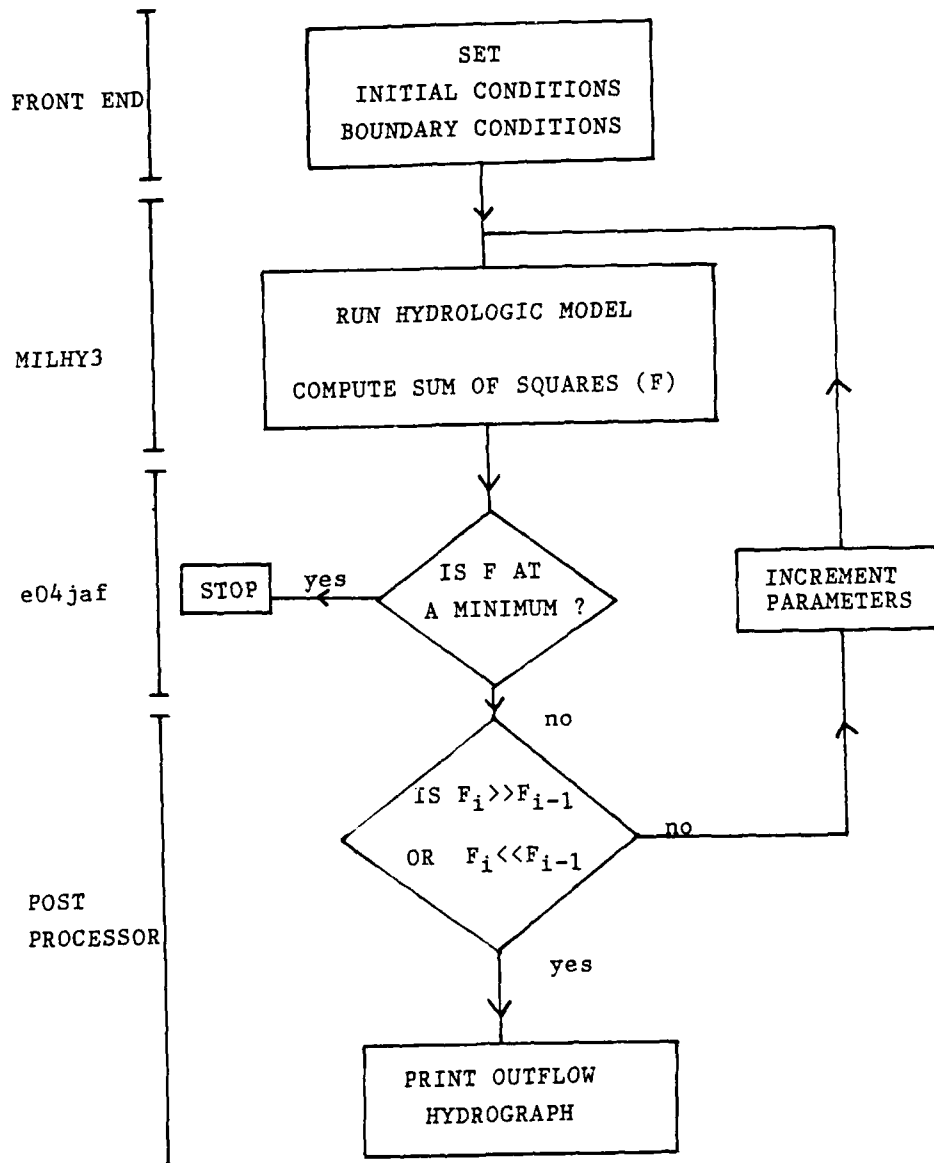


Figure 6.8 : Conceptual Optimization Scheme

The function values at which these three simulations stopped at was however, not the same. Analysis of the iterative solution showed that each of the simulations had got stuck in local minimums close to the initial conditions in each case, and that the predicted outflow hydrograph and parameter values at each of the local minimums were widely different. A closer examination of the parameter values as each simulation converged on its local minimum showed that the parameters were only changing from iteration to iteration by a very small amount, approximately 10^{-4} . The resolution of such parameter changes was too small to cause any change in the predicted outflow hydrograph, and hence there was no change in the sum of squares function and the solution converged. Three problems associated with the resolution of parameter variability were therefore identified:

- 1) that the simulation failed to converge on an absolute minimum
- 2) the parameter variability increments could not be resolved with the accuracy of data available in an ungauged catchment
- 3) the parameter variability increment caused no interpretable changes to the predicted hydrograph

As the objective of this investigation was to pinpoint parameter changes that did or did not cause a noticeable effect on the outflow hydrograph, the scheme was unsuccessful. That the scheme did not reach an absolute minimum was not so important as we were not attempting to calibrate the model. The reason for the failure to reach an absolute minimum was important, however, as it showed that the scheme was not searching within a wide enough range within the boundary limits. The cause of this problem was simple; it was the size of the parameter changes from iteration to iteration.

A solution was easily come by - a different optimization scheme, e04jbf, which allows the user to select the resolution of parameter changes. This scheme also allowed the maximum number of iterations to be specified and the likely size of the sum of squares at the absolute minimum to be

estimated. This potentially made the computing demands more controllable, a distinct advantage, the main disadvantage being that the scheme was more complex to set up. Having already made the program changes necessary in MILHY3, however, the bulk of the work was already done and the experience of setting up the previous scheme meant the changes to the new scheme took around a day to complete. The logic of the optimization set-up remained unchanged from e04jaf, shown in Figure 6.8.

Testing the new optimization scheme from a variety of initial conditions, resulted in solutions with a discrepancy well within the level of accuracy to which the parameters could be estimated. Initial investigation into the iterative results proved promising enough to encourage us to pursue the application of this optimization scheme, using data from the River Fulda dataset.

6.3.3 Application of the factor perturbation technique to the Fulda dataset

From the analysis of the possible approaches available reported above, it can be seen that the sensitivity analysis has been divided into two parts:

- 1) traditional factor perturbation techniques will be applied to investigate the effects of the model structure
- 2) exploratory optimization techniques will be used to investigate the effects of variability in the downstream conveyance parameters.

In the first section of the analysis, two events will be explored, an observed out-of-bank event occurring in March 1986, which has an occurrence interval of 1 in 10 years, and an observed in-bank event which occurred in June 1984. These two events will be simulated for the whole of the River Fulda catchment to Rotenburg, using the infiltration algorithm and the curve number routine. The four methods of

incorporating turbulent exchange and the multiple routing routine will also be used. Throughout these simulations, however, the only parameters that will change are those directly related to the storm event. In particular, the parameters involved in the downstream conveyance submodels will remain constant throughout.

In the second exploratory part of the sensitivity analysis, the optimization technique will be used to test the sensitivity of the outflow hydrograph to variability in five parameters. These are:

- i) floodplain Mannings 'n'
- ii) channel Mannings 'n'
- iii) floodplain slope
- iv) channel slope
- v) floodplain routing reach length

As this investigation is rather exploratory, a single storm event and one river reach length were selected for exploration. The storm event, as above, occurred in March 1986, and as in the initial analysis reported in Section 5, the reach between Bad Hersfeld and Rotenburg on the River Fulda has been selected.

The results from the investigation into the impact of model structure are reported in Section 6.4, whilst the optimization results are reported in Section 6.5.

6.4 Sensitivity of the outflow hydrograph to model structure

The objective of this analysis is to investigate the sensitivity of the outflow hydrograph to the submodels utilized to generate it. This analysis will also investigate the effects of catchment scale on the sensitivity of the hydrograph.

As noted earlier, two observed storms have been used, the first occurred in March 1986 and has a recurrence interval of 1 in 10 years. The second

storm occurred in June 1984 and has a recurrence interval in 1 in 1.5 years. For both of these storms, observed hydrographs were available for all of the stations shown in Figure 6.1, except for the outflow hydrograph at Rotenburg for the storm occurring in June 1984. Both of these storms are out-of-bank in the downstream half of the River Fulda catchment.

The precipitation data is used by the curve number routine in MILHY, and the infiltration algorithm in MILHY2 and 3 to generate Hortonian runoff excess. To this baseflow must be added. For the purpose of this sensitivity analysis the baseflow levels have been taken from the observed hydrographs, although we acknowledge that this would not be feasible in an ungauged catchment. There is potential, therefore, for the development of a submodel to generate baseflow conditions based on either the catchment characteristics or channel geometry data that is already derived.

6.4.1 Storm 1 : 1 in 10 year event

Figure 6.9 shows the precipitation pattern at Fulda and the observed flood hyetograph at Bad Hersfeld for the 1 in 10 year event. The precipitation patterns temporal distribution for all the subcatchments is based on this hyetograph, and the magnitude of the rainfall in each subcatchment is determined from the daily precipitation records of the stations shown in Figure 6.2. The minimum rainfall total for the event occurred in subcatchment 408 where 45 mm fell, the maximum occurring in subcatchment 403 where 75mm fell. The observed hydrograph shown in Figure 6.9 illustrates that the discharge peak occurred approximately 24 hours after the rainfall peak. The time to peak of the observed hydrograph is 30 hours from the simulation start time and the peak discharge is $426 \text{ m}^3 \text{ s}^{-1}$.

The predicted outflow hydrographs at Bad Hersfeld using the curve number and the infiltration algorithm are recorded in Tables 6.6 and 6.7 respectively. These tables summarize the characteristics of the hydrographs, noting the peak discharge, time to peak and equivalent

STORM1: 1 in 10 year event

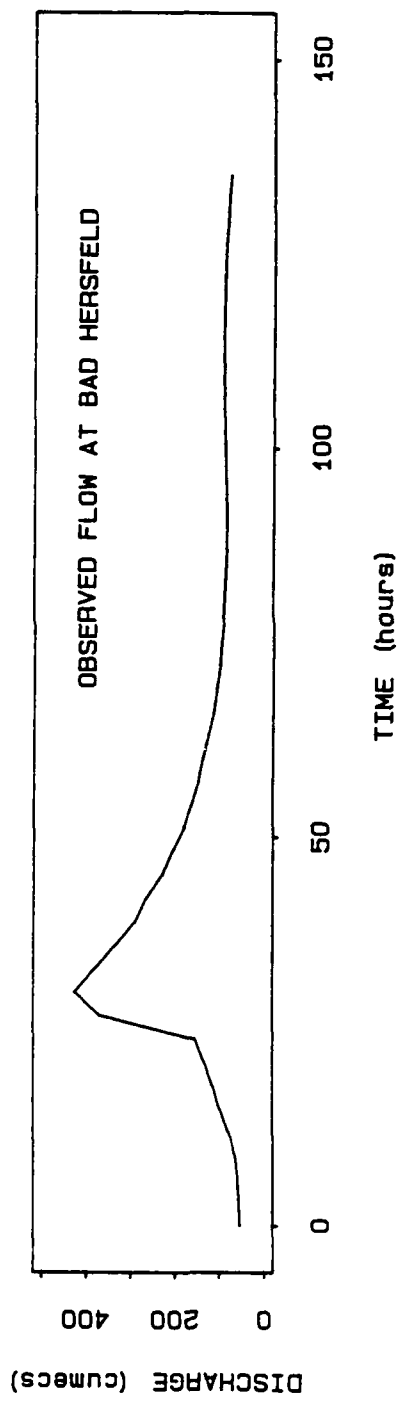
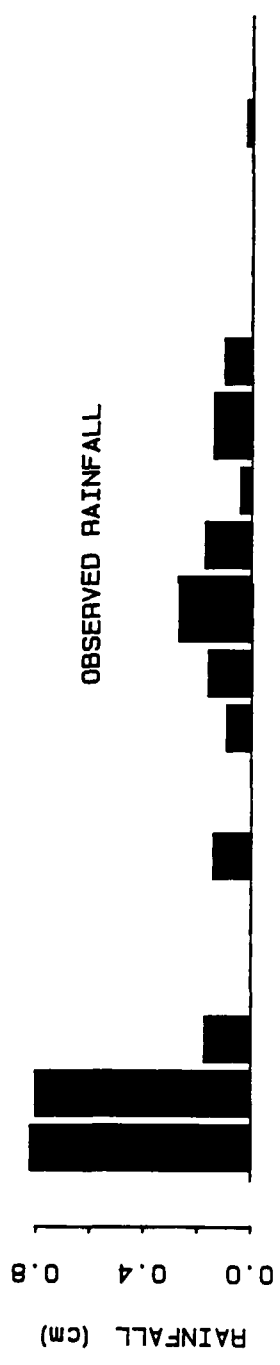


Figure 6.9

Table 6.6

Storm 1 : 1 in 10 year eventPredicted Outflow at Bad Hersfeld utilizing the
Curve Number Routine

Computation Method		Peak discharge $\text{m}^3 \text{s}^{-1}$	Time to peak hours	Runoff depth m
IT=1	MR=0	265	17.5	0.03
IT=2	MR=0	272	17.5	0.03
IT=3	MR=0	265	17.5	0.03
IT=4	MR=0	249	17.5	0.03
IT=1	MR=1	312	16.5	0.03
IT=2	MR=1	328	16.5	0.03
IT=3	MR=1	323	16.5	0.03
IT=4	MR=1	281	17.0	0.03

IT = turbulent exchange routine

MR = multiple routing - invoked = 1

- not invoked = 0

IT=1 vertical interface, zero shear

IT=2 vertical interface, apparent shear stress ratio = 1

IT=3 diagonal interface, zero shear

IT=4 diagonal interface, apparent shear stress ratio = 1

Table 6.7

Storm 1 : 1 in 10 year event

Predicted Outflow at Bad Hersfeld utilizing the
Infiltration Algorithm

Computation Method		Peak discharge $\text{m}^3 \text{s}^{-1}$	Time to peak hours	Runoff depth m
IT=1	MR=0	312	18.5	0.03
IT=2	MR=0	321	18.0	0.03
IT=3	MR=0	310	18.0	0.03
IT=4	MR=0	290	18.0	0.03
IT=1	MR=1	364	16.5	0.04
IT=2	MR=1	383	16.5	0.04
IT=3	MR=1	372	16.5	0.04
IT=4	MR=1	332	17.5	0.04

IT = turbulent exchange routine

MR = multiple routing - invoked = 1

- not invoked = 0

runoff depth, for all the turbulent exchange and multiple routing routine combinations.

Figure 6.10 illustrates the impact of the computation method on the predicted outflow hydrograph at Bad Hersfeld. MILHY invokes the curve number routine, whilst MILHY2 and 3 utilize the infiltration algorithm. MILHY and MILHY2 use the turbulent exchange method 2, and single routing reaches, whilst MILHY3 uses exchange method 3 and the multiple routing reach routine.

Comparison of Tables 6.6 and 6.7 shows that both the curve number and infiltration algorithm produce runoff depths comparable with the observed data for the drainage area up to Bad Hersfeld. Analysis of the runoff volumes generated at the intermediate stations (see Figure 6.1) shows that this is true for all the subcatchments. Tables 6.8 and 6.9 illustrate the runoff volumes for the station at Hermannspiegel, where the observed runoff volume is 0.028 metres.

Comparison of the curve number routine and infiltration algorithms prediction of the peak discharge rate at Bad Hersfeld and Hermannspiegel (Figures 6.10 and 6.11) shows that in both cases the infiltration algorithm produces higher peak discharges. This behaviour has been noted previously by Anderson (1982) and Anderson and Howes (1984), who showed that this behaviour occurred during high and low intensity storms. In this analysis it is worth noting that this behaviour is still visible after the hydrographs have been routed through up to four subcatchments. This re-emphasises earlier work by Anderson and Howes (1984, 1986) that illustrated the importance of the shape of the runoff hydrograph in determining the outflow hydrograph.

Analysis of Tables 6.6 to 6.9 shows that the peak discharge is the parameter most sensitive to the downstream computation method. The impact of the turbulent exchange and the multiple routing routines is related to the depth of flow on the floodplains. The outflow hydrograph at Hermannspiegel (shown in Figure 6.11) is routed from Marbach. The distribution of the inflow hydrograph at Marbach means, however, that

BAD HERSFELD STORM1: 1 in 10 year event

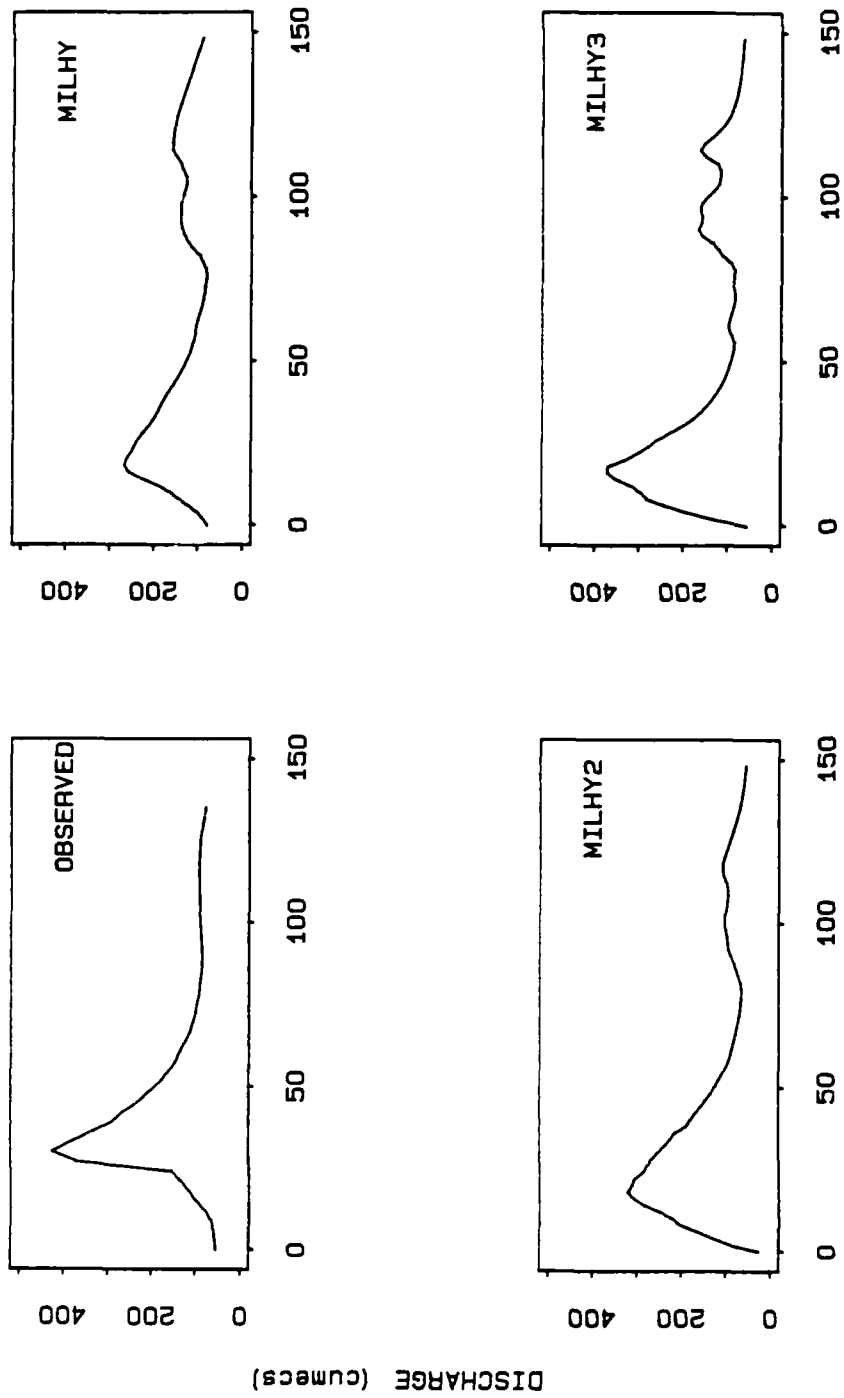
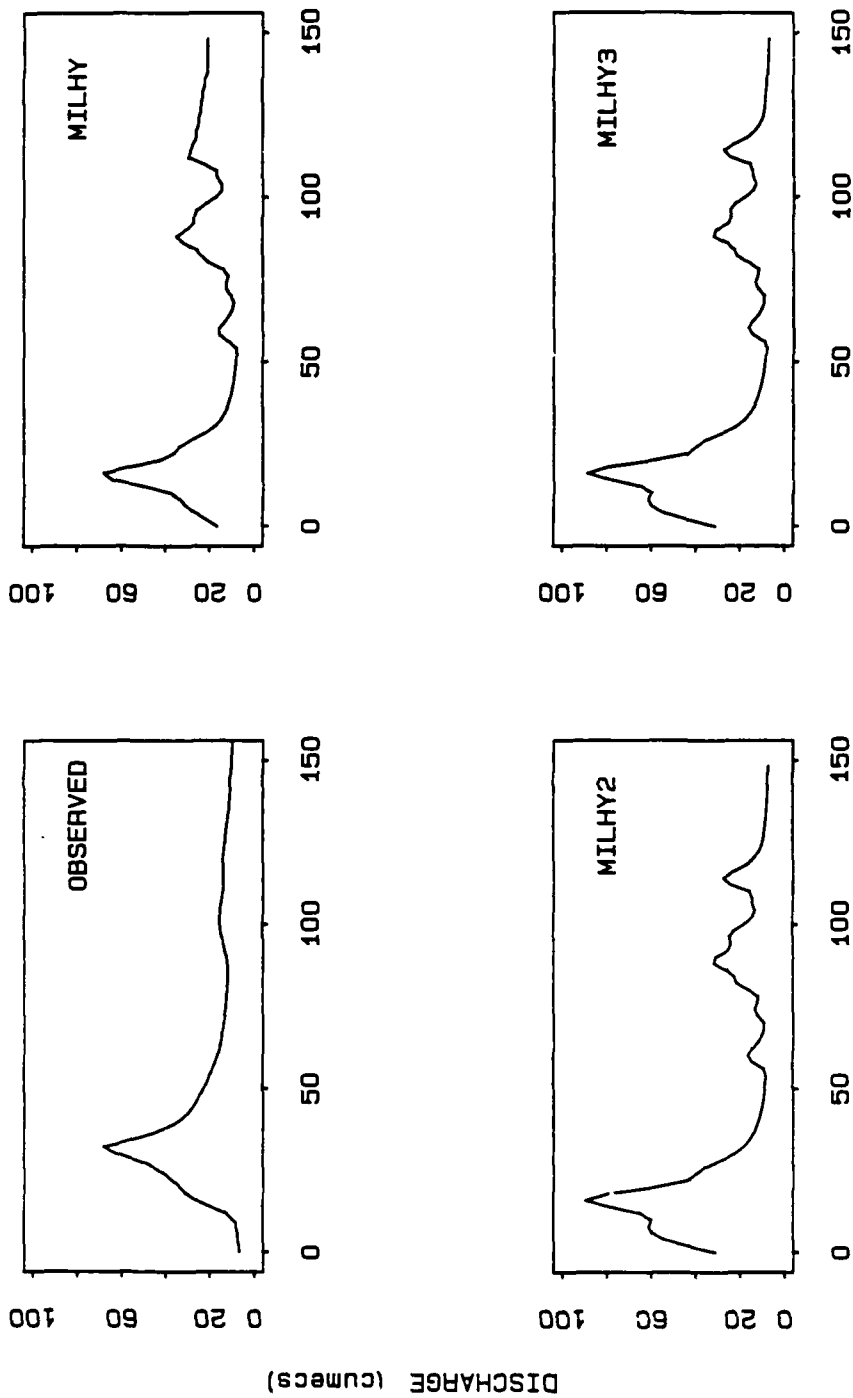


Figure 6.10

HERMANNSPIEGAL STORM1: 1 in 10 year event



TIME (hours)

Figure 6.11

Table 6.8

Storm 1 : 1 in 10 year eventPredicted Outflow at Hermannspiegel utilizing the
Curve Number Routine

Computation Method		Peak discharge $\text{m}^3 \text{s}^{-1}$	Time to peak hours	Runoff depth m
IT=1	MR=0	70	15.5	0.02
IT=2	MR=0	70	15.0	0.02
IT=3	MR=0	70	15.0	0.02
IT=4	MR=0	69	15.0	0.02
IT=1	MR=1	70	15.0	0.02
IT=2	MR=1	71	15.0	0.02
IT=3	MR=1	69	15.0	0.02
IT=4	MR=1	68	15.0	0.02

IT = turbulent exchange routine

MR = multiple routing - invoked = 1

- not invoked = 0

Table 6.9

Storm 1 : 1 in 10 year event
Predicted Outflow at Hermannspiegel utilizing the
Infiltration Algorithm

Computation Method		Peak discharge $\text{m}^3 \text{s}^{-1}$	Time to peak hours	Runoff depth m
IT=1	MR=0	89	16.0	0.03
IT=2	MR=0	90	16.0	0.03
IT=3	MR=0	90	16.0	0.03
IT=4	MR=0	89	16.0	0.03
IT=1	MR=1	90	16.0	0.03
IT=2	MR=1	90	16.0	0.03
IT=3	MR=1	89	16.0	0.03
IT=4	MR=1	87	16.0	0.03

IT = turbulent exchange routine

MR = multiple routing - invoked = 1
 - not invoked = 0

only three data points at the peak of the hydrograph are assigned to the floodplains. The impact on the turbulent exchange and multiple routing routines is therefore minimal. At Bad Hersfeld, the impact of the new routines is more pronounced. Tables 6.6 and 6.7 show that the turbulent exchange techniques that assume zero shear, methods 1 and 3, produce very similar results and the methods that assume an apparent shear stress ratio of 1 produce smaller discharge predictions. These results are as expected, as the methods that assume zero shear do not incorporate the shear surfaces between segments in out-of-bank flow and therefore the type of division has nominal effect. The methods that incorporate the shear stresses surfaces would be expected to have lower discharge predictions, as the larger wetted perimeter reduces the hydraulic radius and hence the discharge using the Manning equation. The discharge discrepancy between turbulent exchange remains relatively constant, irrespective of the absolute discharge.

All of the simulation methods predicted the time of the hydrograph peak too early. This can be related to the rainfall data which was derived from records taken at eight hour intervals.

6.4.2 Storm 3: 1 in 1.5 year event

Figure 6.12 shows the hydrograph for subcatchment 402 and the observed discharge hydrograph at Bad Hersfeld for the 1 in 1.5 year event. The precipitation data for each subcatchment was derived from hourly data available for the station at Bad Hersfeld. The spatial variability was generated from the daily records, and showed a minimum total precipitation in subcatchment 403 of 58 mm, and a maximum in subcatchment 406 with 71 mm. In contrast to the 1 in 10 year event, this event is characterized by a double peak in the rainfall event, the effects of which can be seen in the observed hydrograph. In both of these peaks, the discharge peak occurs approximately 30 hours after the precipitation peak.

The results from the curve number and infiltration algorithm simulations are given in Tables 6.10 and 6.11 for Bad Hersfeld, and 6.12 and 6.13 for

STORM3: 1 in 1.5 year event

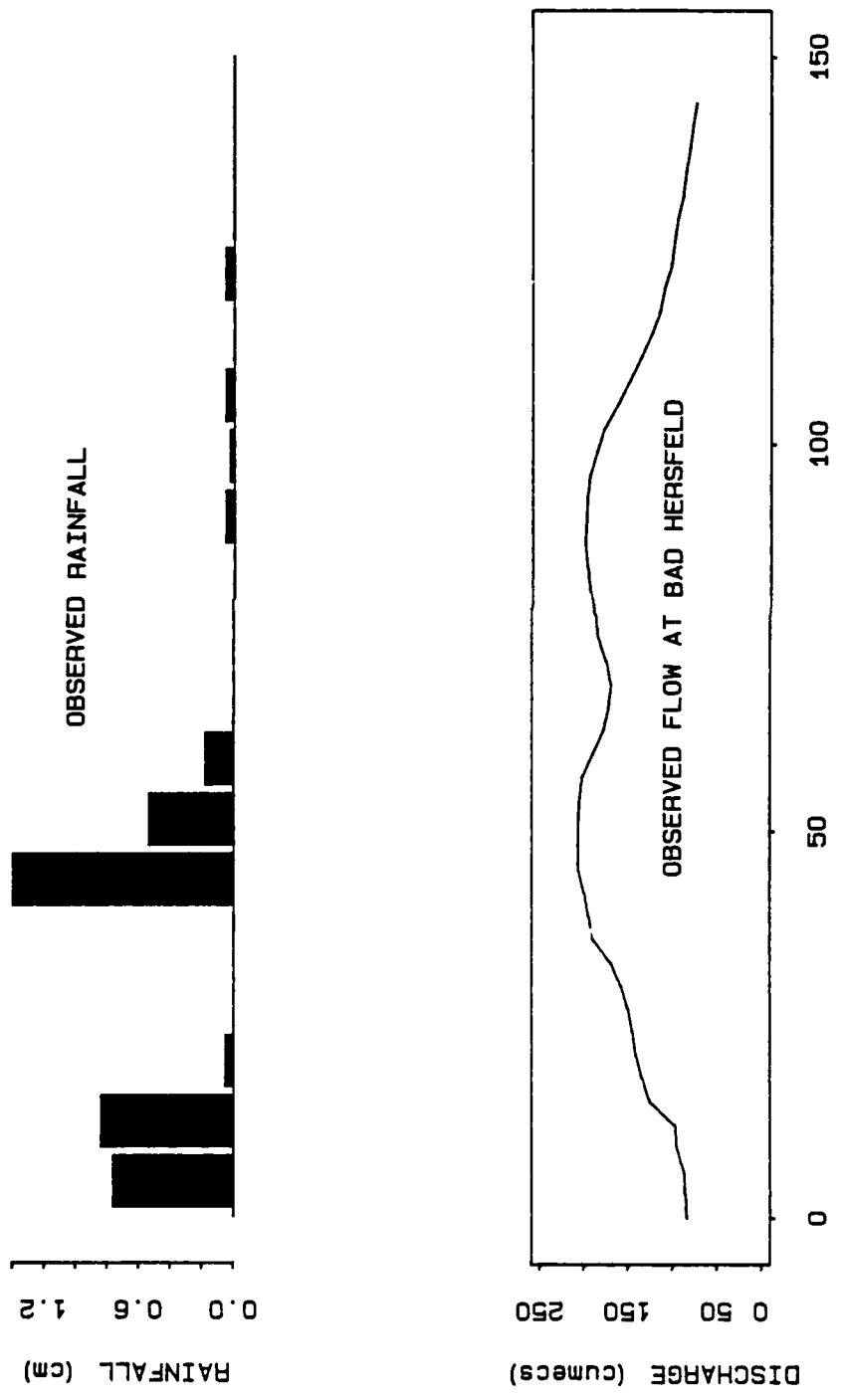


Figure 6.12

Table 6.10

Storm 3 : 1 in 1.5 year event
Predicted Outflow at Bad Hersfeld utilizing the
Curve Number Routine

Computation Method	Peak discharge		Time to peak		Runoff depth m	
	$\text{m}^3 \text{s}^{-1}$		hours			
	1	2	1	2		
IT=1	MR=0	238	355	19.5	55.5	0.04
IT=2	MR=0	242	359	19.5	55.0	0.04
IT=3	MR=0	235	361	19.5	55.0	0.04
IT=4	MR=0	224	353	19.5	55.5	0.04
IT=1	MR=1	262	364	19.0	54.5	0.04
IT=2	MR=1	273	383	19.0	54.0	0.04
IT=3	MR=1	273	377	19.0	54.5	0.04
IT=4	MR=1	224	352	19.5	55.5	0.04

IT = turbulent exchange routine

MR = multiple routing - invoked = 1

- not invoked = 0

Table 6.11

Storm 3 : 1 in 1.5 year event
Predicted Outflow at Bad Hersfeld utilizing the
Infiltration Algorithm

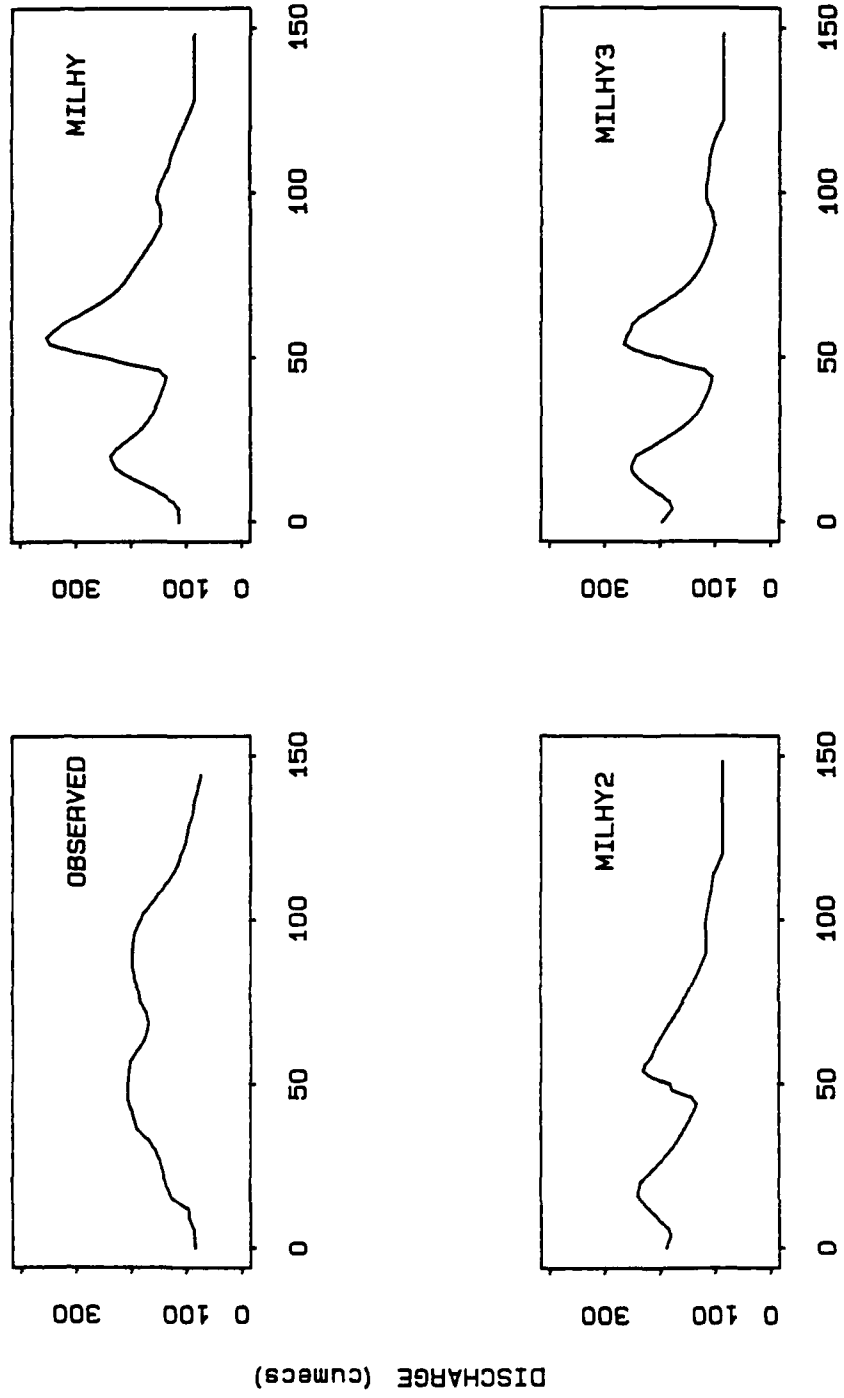
Computation Method		Peak discharge		Time to peak		Runoff depth
		$\text{m}^3 \text{s}^{-1}$		hours		m
		1	2	1	2	
IT=1	MR=0	236	238	16	55.0	0.04
IT=2	MR=0	241	232	16	54.5	0.04
IT=3	MR=0	238	235	16	54.5	0.04
IT=4	MR=0	229	235	16	54.5	0.04
IT=1	MR=1	240	255	16	54.0	0.04
IT=2	MR=1	249	269	16	54.0	0.04
IT=3	MR=1	253	266	16	54.5	0.04
IT=4	MR=1	226	234	16	54.0	0.04

IT = turbulent exchange routine

MR = multiple routing - invoked = 1

- not invoked = 0

BAD HERSFELD STORM3: 1 in 1.5 year event



TIME (hours)

Figure 6.13

HERMANNSPIEGAL STORM3: 1 in 1.5 year event

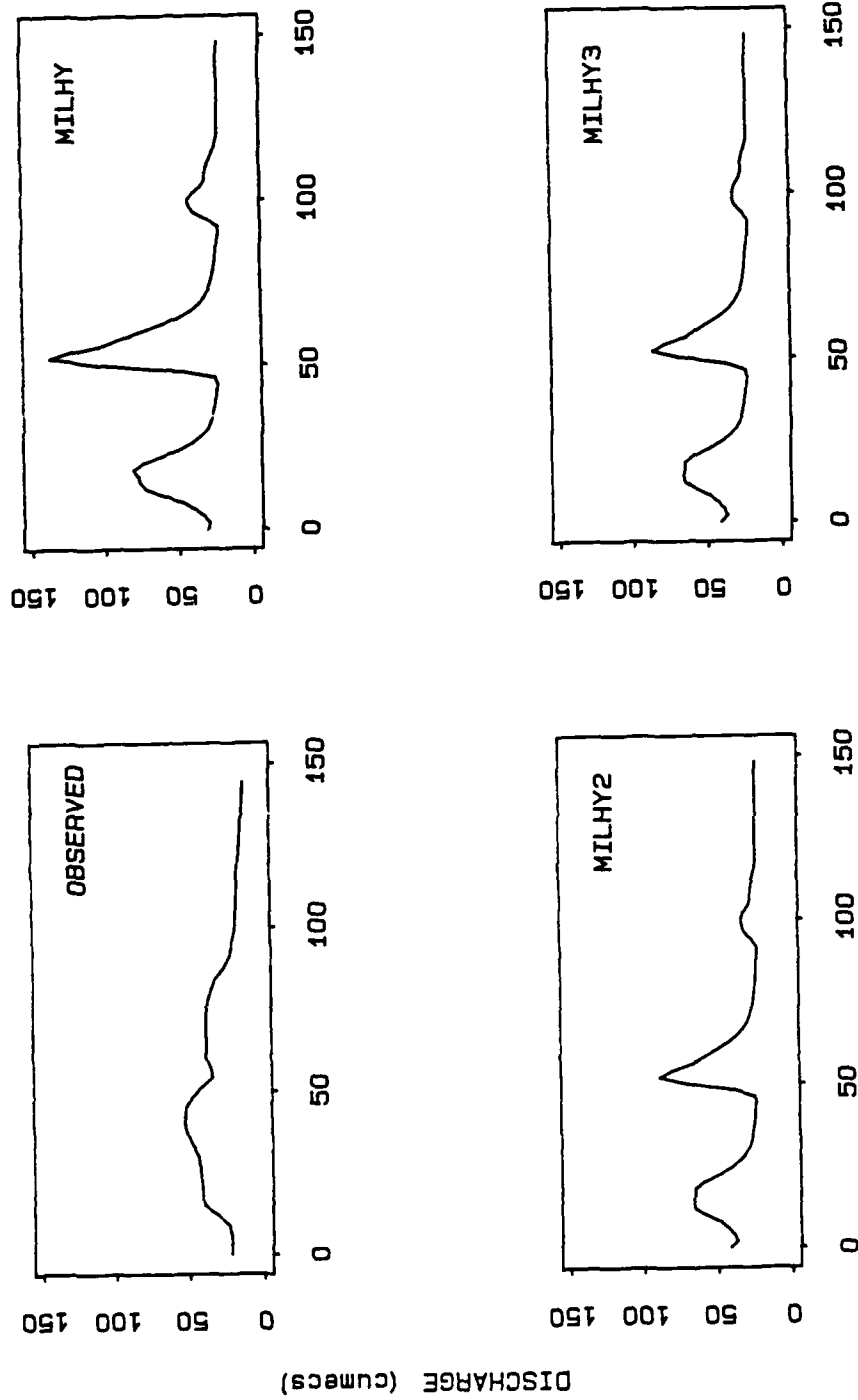


Figure 6.14

Table 6.12

Storm 3 : 1 in 1.5 year event
Predicted Outflow at Hermannspiegel utilizing the
Curve Number Routine

Computation Method		Peak discharge		Time to peak		Runoff depth
		$\text{m}^3 \text{s}^{-1}$		hours		m
		1	2	1	2	
IT=1	MR=0	81	138	18.0	52.0	0.05
IT=2	MR=0	81	139	18.0	52.0	0.05
IT=3	MR=0	81	138	18.0	52.0	0.05
IT=4	MR=0	81	135	18.0	52.5	0.05
IT=1	MR=1	81	138	18.0	52.0	0.05
IT=2	MR=1	81	140	18.0	52.0	0.05
IT=3	MR=1	81	132	18.0	52.0	0.05
IT=4	MR=1	81	134	18.0	52.0	0.05

IT = turbulent exchange routine

MR = multiple routing - invoked = 1

- not invoked = 0

Table 6.13

Storm 3 : 1 in 1.5 year event
Predicted Outflow at Bad Hersfeld utilizing the
Infiltration Algorithm

Computation Method		Peak discharge		Time to peak		Runoff depth m
		$m^3 s^{-1}$		hours		
		1	2	1	2	
IT=1	MR=0	67	88	13	52	0.05
IT=2	MR=0	67	88	13	52	0.05
IT=3	MR=0	67	89	13	51	0.05
IT=4	MR=0	66	88	13	52	0.05
IT=1	MR=1	66	88	13	52	0.05
IT=2	MR=1	66	89	13	52	0.05
IT=3	MR=1	67	87	13	52	0.05
IT=4	MR=1	66	84	13	52	0.05

IT = turbulent exchange routine

MR = multiple routing - invoked = 1

- not invoked = 0

Hermannspiegel. These tables record the peak discharge and time to peak of both of the peaks and the runoff depth of the simulation. The results are summarized in Figures 6.13 for Bad Hersfeld and Figure 6.14 for Hermannspiegel.

Comparing the curve number and infiltration algorithm simulations (MILHY and MILHY2), in all the subcatchments the curve number routine generates far too large a discharge in the second peak. In the infiltration algorithm, the effects of the second stage of the precipitation on the discharge are negated by the preceding dry period during which drainage occurs. In the infiltration algorithm, therefore, some of the precipitation is absorbed by the soil columns before saturated conditions reoccur and overland flow is predicted. This more complex storm therefore shows the superior predictive capability of MILHY2 over MILHY, in multiple and single subcatchment applications.

Analysis of the impact of the turbulent exchange and multiple routing routines, shows as in the 1 in 10 year the peak discharge is the hydrograph most sensitive to any change in the computation method. The impact at Hermannspiegel is negligible because the upstream hydrograph is in-bank. At Bad Hersfeld the greatest impact is generated by the multiple routing routine.

6.4.3 Comparison of the two storms

Figures 15 and 16 illustrate the impact of the multiple routing and turbulent exchange routines on the predicted outflow hydrograph at Bad Hersfeld for both of the storms. It is interesting to compare the effects of these routines individually and their impact when operating together which is illustrated by the MILHY3 simulations in Figures 6.10 and 6.13. The turbulent exchange method (IT) used throughout this analysis is method 3 (diagonal interface with zero shear stress), as the results recorded in Tables 6.7 and 6.11 show this method seems to have the greatest impact on the peak discharge.

Figure 6.16 shows that the impact of the turbulent exchange method 3, has no noticeable impact on the predicted hydrographs of either storm, when

MULTIPLE ROUTING

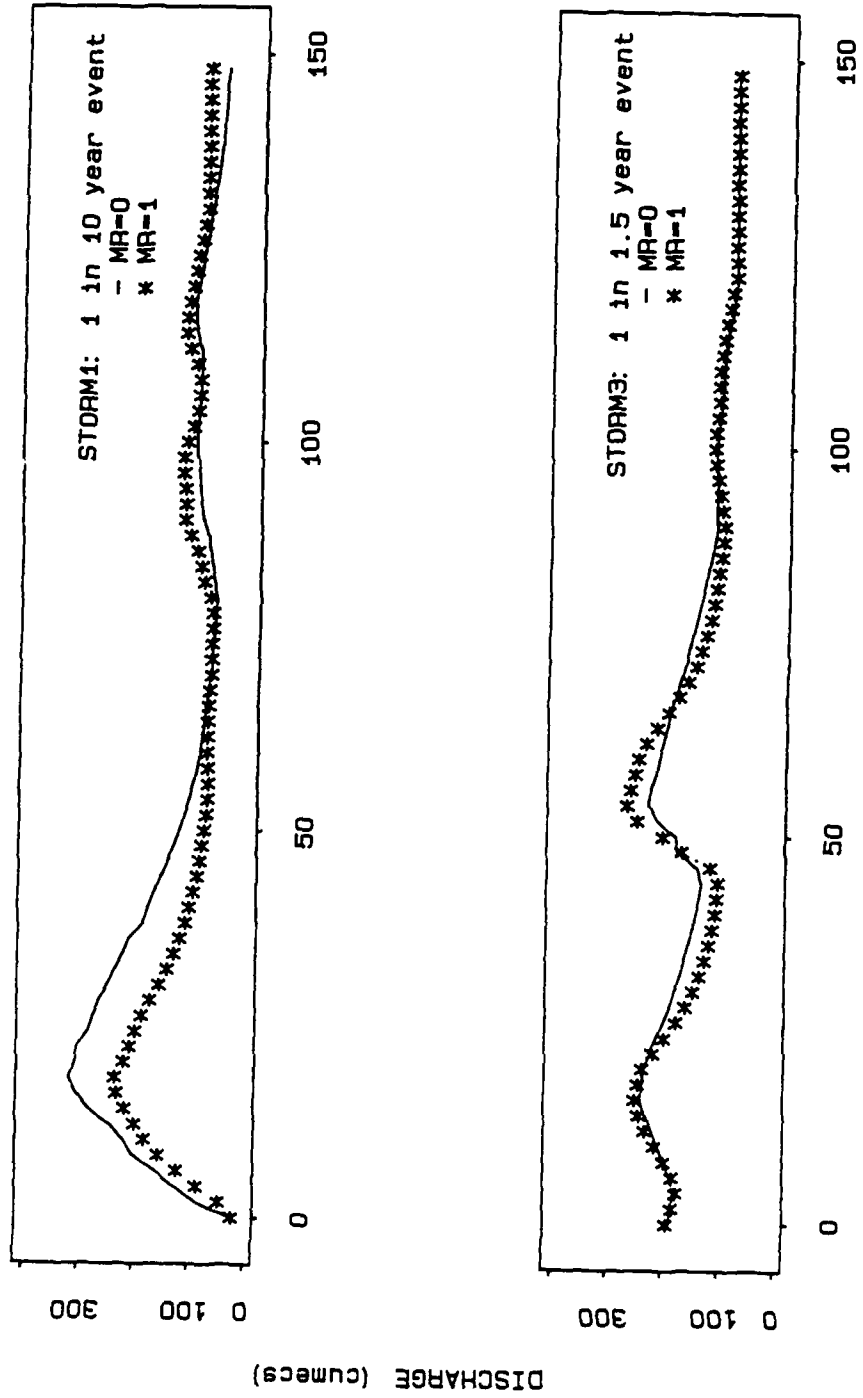


Figure 6.15

TURBULENT EXCHANGE

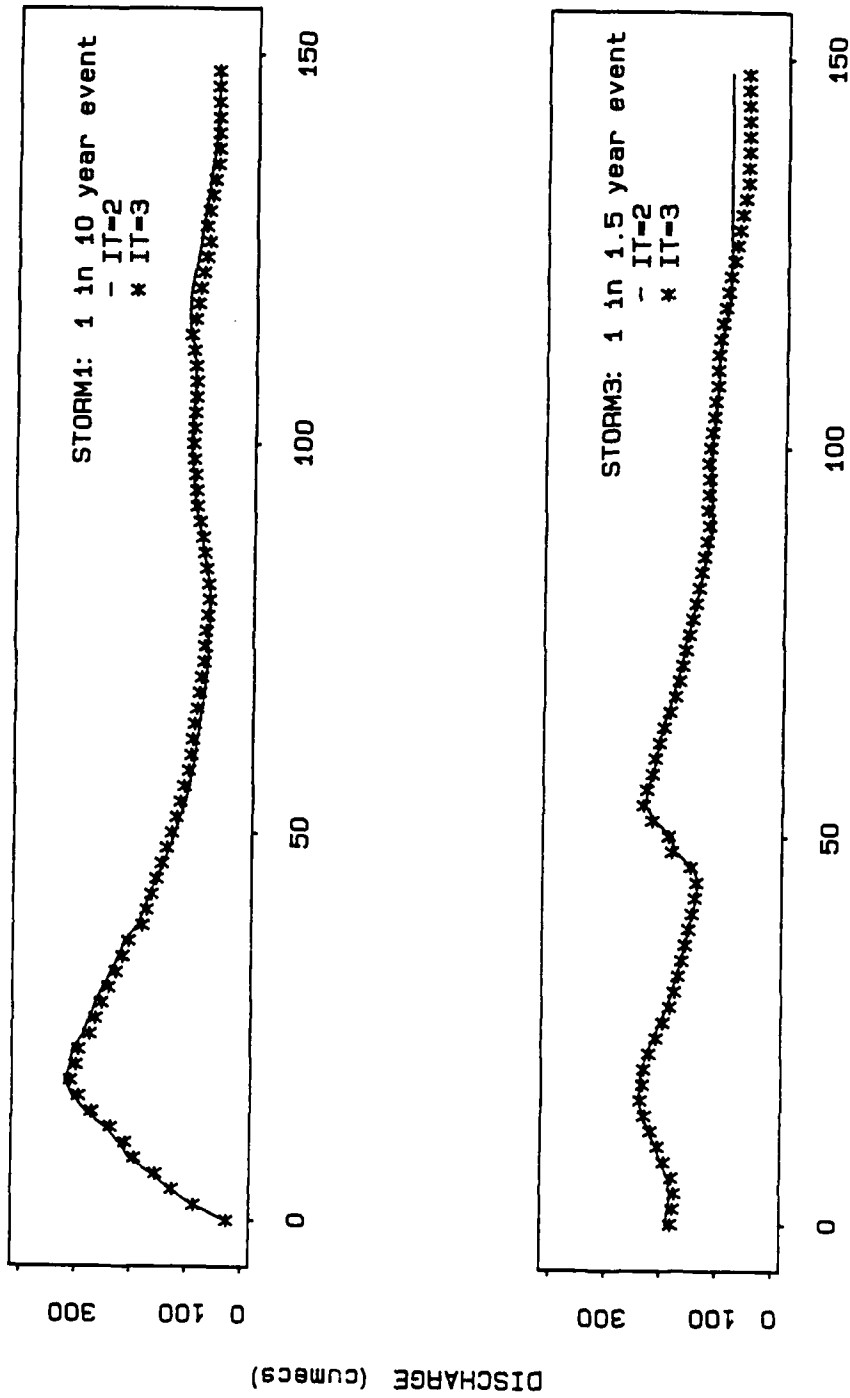


Figure 6.16

applied without the multiple routing routine. Figure 6.15 shows, however, that the multiple routing routine has a significant effect on the hydrograph, and that the routine's impact varies between the two storms. In Storm 1 the main peak of the hydrograph is reduced whilst the minor peaks on the recession limb are accentuated. In Storm 2, by contrast, the recession from the first peak is steepened and the second peak is significantly accentuated.

Taking each of the storms in turn, in Storm 1 it is important to appreciate that floodplain flow only occurs from Unter-Schwarz to Bad Hersfeld on the River Fulda. The inflow hydrographs at Unter-Schwarz for the simulation with multiple routing routine are identical to that without the routine, and that the inflow from the Haune is channel flow only and therefore can be ignored. Comparison, therefore, concentrates on the travel time tables for the Unter-Schwarz to Bad Hersfeld reach for the two simulations. At the main peak of the hydrograph of around $350 \text{ m}^3 \text{ s}^{-1}$, in the application without multiple routing the time taken for the peak to travel the length of the reach is 13 hours. In the multiple routing application, however, 45% of this peak is apportioned to the floodplain where the travel time is approximately 19 hours. The remaining 55% is assigned to the main channel where the travel time is only 5 hours. This difference in travel times means that the peak of the hydrograph is flattened out. In the later minor peaks, the effect of the division of floodplain and channel flows is rather different. Looking at two points on the inflow hydrograph, the travel time without multiple routing is 11.4 hours, with multiple routing the floodplain travel time is 55 hours, and the main channel travel time is 6 hours. However, as only 4% of the flow is assigned to the floodplain, with multiple routing the flow arrives earlier and the peaks are more accentuated. Storm 1 shows, therefore, that the effects of the multiple routing routine on the outflow hydrograph is determined by the percentage of flow that is assigned to the floodplain.

Storm 3 confirms this conclusion as where 15% of the flow is assigned to the floodplain, the multiple routing prediction is more attenuated. Where floodplain flows account for 10% or less of the total discharge,

the hydrographs less attenuated, as the multiple routing channel time is significantly lower than the joint channel/floodplain travel time.

The predicted hydrograph at Bad Hersfeld for the application of both the multiple routing and turbulent exchange routines (MILHY3) are shown in Figures 6.10 and 6.13 for Storms 1 and 3 respectively. Comparison with Figures 6.15 and 6.16 shows that the hydrograph for Storm 1 is significantly different from those produced by the multiple routing and turbulent exchange routines alone. The Storm 3 hydrograph exactly matches the hydrograph from the multiple routing routine. It would seem, therefore, that the effects of applying both routines varies according to the storm.

In Storm 1, the MILHY3 prediction seems particularly strange as when compared to the MILHY2 solution, MILHY3 predicts the main peak as being earlier and attenuates it less. This contrasts with Figure 6.15, where the multiple routing routine increases the attenuation of the peak. Analysis of the rating curves and travel time tables generated by MILHY3, and those from the simulation shown in Figure 6.15, showed that it was the travel times that control the attenuation of the hydrograph. When the routines are applied together, the travel times are reduced and more flow is assigned to the floodplain. The turbulent exchange generated small changes in the rating curve and changes in the travel time that have no impact on the hydrograph when applied on its own, hence Figure 6.16. When applied with the multiple routing routine, these small changes become significant. For example, at the fifth hour of the simulation, for IT=2, MR=1, 18% ($39 \text{ m}^3 \text{ s}^{-1}$) of the total discharge was in the left floodplain, this water has a travel time of 70 hours. In contrast, when IT=3, MR=1 (MILHY3) 26% ($58 \text{ m}^3 \text{ s}^{-1}$) of the discharge was in the left floodplain, the travel time was 60 hours.

In Storm 3, however, there are no noticeable differences between the multiple routing and multiple routing with turbulent exchange solutions. Although there are differences in the travel time tables between these two techniques, these differences do not become significant as a much greater proportion of the hydrograph is out-of-bank.

6.4.4 Conclusions

From the analysis of the March 1986 and June 1984 storms it is possible to conclude that:-

- 1) The infiltration algorithm still makes a considerable improvement in the predictive capability of MILHY when several subcatchments are applied.
- 2) The multiple routing routine has a significant impact on the predicted hydrograph. When floodplain inundation accounts for approximately 15% or more of the total discharge, then the multiple routing routine increases the attenuation of the floodwave. When floodplain flows account for less than 10% of the total discharge, the multiple routing routine decreases the attenuation of the floodwave.
- 3) The turbulent exchange routine makes no significant impact on the predicted discharge hydrograph.
- 4) When the multiple routing and turbulent exchange routines are applied together, then changes invoked by the turbulent exchange routine becomes significant. When 15% or more of the discharge is assigned to the floodplain, the floodwave attenuation is reduced.
- 5) For cases where the floodplain accounts for 15% or more of the discharge, then the joint application of the multiple routing and turbulent exchange routines improves the predictive capability of MILHY.

6.5 Optimization results

As noted earlier, this investigation into the utility of optimization techniques as sensitivity tools is rather exploratory, and therefore a single reach and storm are used. The reach used is between the gauging

stations at Bad Hersfeld and Rotenburg on the River Fulda, and has been described in Section 4.4.1. An observed hydrograph of the 1 in 10 year event occurring in March 1986 was specified as the upstream inflow, and the computed outflow, assuming no inflow from the intervening drainage area, was compared with the observed hydrograph at Rotenburg.

Two methods of computing F, the function that describes the difference between the computed and observed hydrographs, were used, to see if this had any impact on the range of parameter values the optimization technique would select. The techniques were:

- i) ordinary sum of squares 6.1

$$OF2 = \sum_{i=1}^n (q_m i - q_m c)^2$$

- ii) absolute error divided by variance 6.2

$$OF7 = \frac{\sum_{i=1}^n (q_m i - q_m c)^2}{\sum_{i=1}^n (q_m i - \bar{q}_m)^2}$$

where q_m - observed peak discharge
 q_c - computed peak discharge
 \bar{q}_m - mean observed discharge

Both of these methods of analysis are incorporated in the subroutine "ERROR", which remains unchanged from the version incorporated in MILHY2.

The upper and lower boundary limits for the five parameters identified earlier are reported in Table 6.14, which also includes the initial

Table 6.14

Initial Conditions, Boundary Conditions and Variable Increments
for the Optimization Simulations

	Initial Conditions	Boundary Upper	Limits Lower	Variable Increments
Floodplain Mannings 'n'	0.05	0.16	0.025	0.01
Channel Mannings 'n'	0.035	0.1	0.025	0.01
Floodplain Slope	0.0006	0.001	0.0001	0.0001
Channel Slope	0.0007	0.001	0.0001	0.0001
Floodplain routing reach length (m)	21951	23750	16860	1525

values for the values at the start of each simulation, and the variable increment intervals.

The number of iterations, MAXCAL, was set randomly at 500. All of the simulations reached this maximum without satisfying the optimization routines rules for a minimum, and consequently failed. Investigation into the results files, however, showed that the routines rules for a minimum were very stringent and for the level of accuracy required in this analysis, an effective minimum was reached at around 400 iterations.

As the computing demands of this approach were foreseen as being a major drawback in the utility of the technique, a close eye was kept on the CPU and size of files produced. Output at each iteration was restricted to the parameter values and the function (F) value, and the post-processor added the computed outflow hydrograph approximately every tenth iteration. CPU demands for a single reach varied from 400 to 800 seconds for 500 iterations. Trial simulations for the whole Fulda catchment, utilizing the curve number routine to generate runoff, took up to 6000 seconds of CPU. For applications where CPU demands are small, therefore, the optimization technique is an efficient method of undertaking multiple simulations. With the utilization of the infiltration algorithm, the CPU demands for the Fulda catchment would become excessive, as each simulation iteration would take 9 hours of CPU.

The results files proved to be more of a problem as the files were very large. Sizes ranged from 12 kbytes to 2.9 mega bytes, files too large to edit. Clearly the post-processor needs to be more selective in the iteration results it saves. Because of the size of the results files the results presented here represent only a small selection of the most important points.

The presentation of the results has been structured in order to answer several questions. These are:

- i) to which of the five parameters is the hydrograph most sensitive?
- ii) does the computation method affect this sensitivity?

- iii) do the parameters interact to increase or decrease the sensitivity of the hydrograph?

In much of the analysis presented, the relative error and absolute error are used to compare the differences between the computation methods. The relative error is dimensionless and is defined as:

$$RE = \frac{x_c - x_i}{x_i} \quad 6.3$$

where x_c - computed value of x
 x_i - value of x under initial conditions

6.5.1 Sensitivity to parameter variability

Tables 6.15 to 6.19 show the absolute (AE) and relative error (RE) for the peak discharge, time to peak and sum of squares for five of the computation methods and all five of the variables. The errors shown are computed for one increment step above and below the initial conditions.

Analysis of these tables show the asymmetrical sensitivity of the three indicators, peak discharge, time to peak and sum of squares, around the initial conditions. For example, Table 6.15 shows that the sensitivity of the peak discharge to variation in the floodplain Mannings 'n' value is markedly different for values greater than the initial conditions than values less than the initial conditions. This asymmetrical effect is particularly noticeable for the variation in Mannings 'n', both in the floodplain and channel (see Tables 6.15 and 6.16), suggesting that the sensitivity of the hydrograph to variation in 'n' is not linear.

Tables 6.15 to 6.19 show the sensitivity of the hydrograph to a one incremental step in the mid-point between the upper and lower boundary limits for all five variables. Table 6.20 shows an example of the relative errors generated from a one increment step increase in each of the parameters at the boundaries and compares these with the mid-limit

Table 6.15

Errors from one increment step variation in floodplain Mannings 'n'

Increment	Computation method		Peak discharge		Time to peak		Sum of squares OF2	
			$\frac{AE}{m^3 s^{-1}}$	RE	AE hours	RE	AE	RE
+1	IT=2	MR=0	-125	0.01	0	0.00	62941	0.00
	IT=3	MR=0	-115	0.13	0	0.08	62951	0.31
	IT=1	MR=1	-107	0.01	+9	0.00	124796	0.12
	IT=2	MR=1	-127	0.10	+9	0.07	105431	0.12
	IT=3	MR=1	- 88	0.03	0	0.00	86893	0.08
0	IT=2	MR=0	-121		0		63177	
	IT=3	MR=0	- 72		-3		91568	
	IT=1	MR=1	-110		+9		111038	
	IT=2	MR=1	- 95		+6		94106	
	IT=3	MR=1	- 79		-3		94782	
-1	IT=2	MR=0	-123	0.01	0	0.00	68801	0.09
	IT=3	MR=0	- 71	0.00	-3	0.00	92675	0.01
	IT=1	MR=1	- 71	0.13	+6	0.06	92118	0.17
	IT=2	MR=1	-102	0.02	+3	0.07	70169	0.25
	IT=3	MR=1	- 70	0.03	-3	0.00	106950	0.13

Table 6.16

Errors from one increment step variation in channel Mannings 'n'

Increment	Computation method		Peak discharge		Time to peak		Sum of squares OF2	
			$\frac{AE}{m^3 s^{-1}}$	RE	AE hours	RE	AE	RE
+1	IT=2	MR=0	-138	0.06	0	0.00	68270	0.08
	IT=3	MR=0	- 91	0.06	-3	0.00	74276	0.19
	IT=1	MR=1	-143	0.11	+9	0.00	85134	0.23
	IT=2	MR=1	-103	0.03	+9	0.07	107817	0.15
	IT=3	MR=1	- 82	0.01	-3	0.00	91518	0.03
0	IT=2	MR=0	-121		0		63177	
	IT=3	MR=0	- 72		-3		91568	
	IT=1	MR=1	-110		+9		111038	
	IT=2	MR=1	- 95		+6		94106	
	IT=3	MR=1	- 79		-3		94782	
+1	IT=2	MR=0	-105	0.06	0	0.00	68694	0.09
	IT=3	MR=0	- 96	0.07	-3	0.00	73639	0.19
	IT=1	MR=1	- 96	0.05	+3	0.13	70847	0.36
	IT=2	MR=1	- 58	0.12	+3	0.07	68635	0.27
	IT=3	MR=1	- 73	0.02	-3	0.00	107051	0.13

Table 6.17

Errors from one increment step variation in floodplain slope

Increment	Computation method		Peak discharge		Time to peak		Sum of squares OF2	
			$\frac{AE}{m^3 s^{-1}}$	RE	AE hours	RE	AE	RE
+1	IT=2	MR=0	-120	0.00	0.0	0.00	63421	0.00
	IT=3	MR=0	- 72	0.00	-3	0.00	92115	0.00
	IT=1	MR=1	-105	0.02	+9	0.00	109250	0.02
	IT=2	MR=1	- 89	0.02	+6	0.00	92953	0.01
	IT=3	MR=1	- 75	0.01	-3	0.00	98774	0.04
0	IT=2	MR=0	-121		0.0		63197	
	IT=3	MR=0	- 72		-3		91568	
	IT=1	MR=1	-110		+9		111038	
	IT=2	MR=1	- 95		+6		94106	
	IT=3	MR=1	- 79		-3		94783	
-1	IT=2	MR=0	-123	0.01	0.0	0.00	62997	0.00
	IT=3	MR=0	-112	0.12	0.0	0.08	63756	0.30
	IT=1	MR=1	- 99	0.04	+9	0.00	124144	0.12
	IT=2	MR=1	-110	0.05	+3	0.07	104471	0.11
	IT=3	MR=1	- 83	0.01	-3	0.00	90447	0.05

Table 6.18

Errors from one increment variation in channel slope

Increment	Computation method		Peak discharge		Time to peak		Sum of squares OF2	
			AE $m^3 s^{-1}$	RE	AE hours	RE	AE	RE
+1	IT=2	MR=0	-117	0.01	0.00	0.00	63290	0.00
	IT=3	MR=0	-107	0.10	0.00	0.08	66138	0.28
	IT=1	MR=1	-112	0.01	+9	0.00	107855	0.03
	IT=2	MR=1	-100	0.02	+6	0.00	90519	0.04
	IT=3	MR=1	-78	0.00	-3	0.00	96431	0.02
0	IT=2	MR=0	-121		0.0		63177	
	IT=3	MR=0	-72		-3		91568	
	IT=1	MR=1	-110		+9		111038	
	IT=2	MR=1	-95		+6		94106	
	IT=3	MR=1	-79		-3		94782	
-1	IT=2	MR=0	-126	0.02	0.00	0.00	63223	0.00
	IT=3	MR=0	-78	0.02	-3	0.00	84485	0.08
	IT=1	MR=1	-103	0.02	+9	0.00	110171	0.01
	IT=2	MR=1	-121	0.08	+9	0.07	108635	0.15
	IT=3	MR=1	-80	0.00	-3	0.00	93286	0.02

Table 6.19

Errors from one increment step variation in floodplain routing reach length

Increment	Computation method		Peak discharge		Time to peak		Sum of squares OF2	
			AE m^3s^{-1}	RE	AE hours	RE	AE	RE
+1	IT=1	MR=1	-114	0.01	+9	0.00	114505	0.03
	IT=2	MR=1	-100	0.02	+6	0.00	96189	0.02
	IT=3	MR=1	- 82	0.01	-3	0.00	91338	0.04
0	IT=1	MR=1	-110		+9		111038	
	IT=2	MR=1	- 95		+6		94106	
	IT=3	MR=1	- 79		-3		94782	
-1	IT=1	MR=1	-106	0.01	+9	0.00	106985	0.04
	IT=2	MR=1	-111	0.05	+9	0.07	91810	0.02
	IT=3	MR=1	- 76	0.01	-3	0.00	98741	0.04

Table 6.20

Relative error in peak discharge from one increment variation
at the boundaries and mid-way

Variable	Relative Errors		
	Upper Boundary	Mid-range	Lower Boundary
Floodplain Mannings 'n'	0.053	0.10	0.01
Channel Mannings 'n'	0.003	0.025	0
Floodplain slope	0.083	0.019	0.058
Channel slope	0.083	0.014	0.03
Routing reach length	0.029	0.014	0.011

values. This particular example compares the relative errors in the peak discharge for one computation method and is typical of the tables derived for other computation methods.

Table 6.20 shows that at both the upper and lower boundaries the outflow hydrograph is most sensitive to slope. In the mid-ranges, the hydrograph is most sensitive to Mannings 'n'. For MILHY applications significant inundation therefore is important to define Mannings 'n' as accurately as possible; this is especially true in the floodplain. Table 6.20 also shows that the outflow hydrograph is not sensitive to relatively small changes in the floodplain routing length, except when slopes are steep (1×10^{-3}).

6.5.2 Sensitivity variations associated with the computation method

The computation method of the optimization scheme incorporates two sources of variation:-

- 1) the structure of MILHY3, specifically in this case which of the turbulent exchange routines has been used and whether the multiple routing routine has been invoked
- 2) the factor (F) used to quantify the differences between the observed and computed hydrographs

Section 6.4 investigated the sensitivity of the outflow hydrograph to variations in MILHY3's structure for two storms in the River Fulda catchment. Here the impact of the model structure on the sensitivity of the hydrograph to parameter variability is investigated. Tables 6.15 to 6.19 compare the relative errors for three measures of hydrograph fit, for a range of model structures. If the sensitivity of the model to variation in the five physically based parameters were not affected by the model structure then we would expect the relative errors for all the computation methods to be the same. The fact that there are variations suggests that certain computational techniques increase the sensitivity of the model to parameter change. This problem is particularly

noticeable in the sensitivity to variation in floodplain Mannings 'n' and in the channel Mannings 'n' with the introduction of the multiple routing routine.

The second question raised in this section is: does the function (F) utilized to describe the fit of the predicted affect the utility of using optimization techniques as part of a sensitivity analysis? Analysis of the results showed that the exact function value did not influence the routine's selection of parameter values; only the relative function value between simulations was used. The solutions from both functions converged on minimums for which the five parameter values were very close. We accept, however, that this may not be the case if a radically different function were applied.

6.5.3 Conclusions

The optimization results have shown that:-

- 1) Optimization schemes provide a viable alternative to traditional factor perturbation sensitivity analyses provided that:
 - (a) the CPU demands of the model can be met
 - (b) a satisfactory function can be found to describe the fit of the hydrograph
- 2) The sensitivity of MILHY3 in two-stage applications is dominated by:-
 - (a) slope when slopes are $\gg 1 \times 10^{-3}$
 - (b) floodplain Mannings 'n' when slopes $\gg 1 \times 10^{-4}$
- 3) Slopes need to be defined to an accuracy of 1×10^{-4}
- 4) Mannings 'n' values need to be defined to an accuracy of at least 1×10^{-2}

- 5) The short-circuiting of floodplain flow is only significant if the floodplain slope is $\leq 1 \times 10^{-3}$ and the floodplain routing length is at least 10% shorter than the main channel routing length.

Conclusions

In answer to the specific questions posed at the start of Section 6, it is possible to conclude from this analysis that:-

- 1) The sensitivity of the predicted outflow hydrograph to variation in its parameters and process submodels is dependent on the magnitude and duration of the out-of-bank event.
- 2) All out-of-bank events are sensitive to the inclusion of the multiple routing routine. Larger out-of-bank events are sensitive to the joint application of the turbulent exchange and multiple routing routine, where MILHY3 significantly improves the accuracy of the predicted hydrograph over MILHY2.
- 3) MILHY is sensitive to variations in slope $\geq 1 \times 10^{-3}$ and floodplain Mannings 'n' variations of $\geq 1 \times 10^{-2}$.
- 4) Variability in the predicted hydrograph can be attributed to the slope parameter when slopes are ≥ 0.001 , and Mannings 'n' when slopes < 0.001 and ≥ 0.0001 .
- 5) The introduction of the infiltration algorithm is still the most important improvement in the predictive capability of MILHY.

7. FLOODPLAIN MODELLING

7.1 Introduction

The preceding chapters have been concerned with the establishment and implementation of MILHY3. As we have discussed, such a scheme would appear to have significant advantages over the earlier versions of MILHY. Notwithstanding this, however, the MILHY schemes only provide for the estimation of stage at subcatchment or routing reach outflow points.

Considerable benefit would accrue if, firstly, more within-reach information were available in a predictive context, and, secondly, if the method to generate this was eventually compatible with the MILHY3 capability outlined above.

One of the objectives of the current research was, therefore, to establish whether an existing finite element method (FEM), in the form of RMA-2, could be implemented at a sufficiently large reach length (15-30 km). As we will outline below, this scheme is capable of generating detailed out of bank, within reach predictions of stage and hence inundated area. We sought, therefore, to attempt the implementation of the scheme on the River Fulda and to undertake initial validation tests.

7.2 Existing Applications of Finite Element Methods for River Reach Studies

Two dimensional horizontal finite element numerical models have been applied to certain classes of river channel problems. Applications have included detailed analyses of flow patterns near structures such as bridges (Tseng, 1975; King and Norton, 1978), river confluence studies (Gomez, 1979; Su et al., 1980), estuary studies (Boltz and Netsch, 1981), and river and floodplain modelling (Samuels, 1985). In addition, studies have compared finite element and finite difference methods, for example, in the context of tidal studies (e.g. Tielke and Urban, 1981). In all these classes of problems finite element models have been used as

alternatives to physical models and the scale of interest has been small, e.g. reaches of river a few river widths long. An exception has been some estuary studies that were of large scale (e.g. tens of miles); some of which utilized a "hybrid" (numerical plus physical) modelling technique (McAnally et al., 1984a & 1984b). Moreover, in a review of the application of finite element methods to river channels, Samuels reports that in only two studies (Lee, 1980 and Zielke & Urban, 1981) is the river channel resolved separately from the floodplain.

7.3 Large Scale Floodplain Modelling with Finite Element Methods

From the above review of model applications, the lack of attention to large scale floodplain modeling is evident. This is the primary focus of this chapter and is drawn from two separate research needs:

- (i) to establish the accuracy of finite element modelling at larger river reach scales (of the order of 16-32 km) and appropriate operational rules for such applications
- (ii) to explore the feasibility of using finite element modelling (at this larger scale) to effectively extend the record of a gauged catchment to include extreme events which may not be available. These large events may be needed for the purposes of assessing the accuracy of simpler hydrologically based forecasting models. The proviso here is that the finite element method is considered to be capable of providing accurate predictions ((i) above) that can be equated with known 'gauged' data where extreme event data is unavailable.

7.4 Model Selection

The numerical model known as RMA-2 (King and Norton, 1978) was selected for use in this study and all the runs necessary for the project were undertaken by Dr D M Gee at the Hydrologic Engineering Center, Davis, California. This model solves the depth integrated Reynolds equations for two-dimensional free-surface flow in the horizontal plane using

using the finite element technique. It can be applied to both steady and unsteady flows. The finite element formulation of RMA-2 allows boundary roughness and solution resolution to vary spatially to accurately reflect topography. It also provides for a wide variety of boundary conditions, including stage hydrographs, discharge hydrographs, and rating curves. Recent research has produced schemes that allow elements to be either wet or dry; that is, to have a horizontally moving flow boundary.

RMA-2 has proved a useful tool for solving a wide variety of complex flow problems where the traditional one-dimensional assumption that the flow path and distribution can be determined a priori is questionable. Most applications, however, have been to either large estuaries (McAnally, et al., 1984a; McAnally et al., 1984b, MacArthur et al., 1987) or to the prediction of local flow patterns near structures (Gee, 1985).

The ability of RMA-2 to allow dry areas within the solution domain during the simulation of an unsteady flow event such as a flood wave led us to select it for testing on a floodplain problem where flow is initially within the channel, spreads into the overbank areas as the flood arrives, and returns to the channel as the flood recedes. The two-dimensional solution relieves the engineer of having to construct cross sections that are perpendicular to the flow for all flows, as is required in a one-dimensional analysis.

The version of RMA-2 (version 4) used in this study contains a new approach to the wetting/drying problem. Previously, an element instantaneously became dry once the depth at any node in that element became zero or negative, and similarly with wetting. This resulted in relatively large changes in cross-sectional area as overbank elements were brought into the solution. The new approach is based upon the concept of "marsh" elements that gradually wet and dry. This is accomplished through a pseudo-porosity that operates on the flow carrying capacity of an element as the depth changes (King, 1987). The application described herein is the first practical application of the marsh element option.

7.5 Research Design

In exploring the capability of finite element models (such as RMA-2) to operate on large scale floodplain applications, there are two principal approaches that could be taken to the overall research design. Firstly, a single reach study could be undertaken utilizing accurate field and recorded data, or, secondly, hypothetical reaches could be established and estimated parameter values used. It was felt desirable in this case to select the former approach because we wished to eventually explore the relative effect of field parameter values on the model result, in relation to the geometrical definition of the application as well as the model structure. This opportunity would have been denied if hypothetical reaches were used. We do, however, acknowledge that since we only utilize the model on one study reach, our conclusions, while hopefully appropriate to other floodplains with similar characteristics, must be interpreted within this framework. As will be evident from the following sections, the model set-up and subsequent computation time requirements prevented a greater number of study reaches from being established under this research project.

The study reach selected for the RMA-2 application was that of the Bad Hersfeld-Rotenburg section of the River Fulda in West Germany. This is a 24 km reach that is described in the following section, and is of a topographic type that is typical not only of the region, but many other river systems in Europe.

With any field application data limitations may subsequently become evident. In particular, in that we were seeking to examine the potential of finite element schemes to model large-scale floodplain inundation, we were particularly interested in high magnitude extreme events. While 1 in 10 year events may be available in terms of observed hydrographs, 1 in 100 year, or larger, events may not be. These flows are of interest in the current context because of the associated extreme inundation areas. It is likely, therefore, as in this application, that high magnitude events need to be generated from smaller events by application of accepted flood frequency techniques. This in no way represents

a criticism of the overall approach we have adopted, in that for hypothetical reach studies, totally hypothetical events would be used with 'unknown' recurrence intervals. In the context of data acquisition, available hydrographs and related gauging information was obtained from the Fulda River Authority.

Four simulations were undertaken with RMA-2 using two overbank roughnesses for each of two flood hydrographs. To develop the larger of the two hydrographs an observed 1 in 10 year flood was scaled up to a 1 in 100 year flood. Both floods were modelled using field estimated values of Manning's n . To enable an evaluation of model sensitivity, prediction susceptibility to parameter change and possible error in field estimation of roughness, the two overbank roughness conditions were considered to be essential to the research design.

7.6 Study Reach

Having established that the study was to be based upon a natural river reach, the River Fulda between Bad Hersfeld and Rotenburg was selected (figure 5.1). The reach is some 15 miles (24 km) long with a slope of 0.0008 (a 50 ft., or 15 m., drop in elevation). The floodplain is typically 0.6 miles (1 km) wide. From figure 2, it can be seen that the floodplain itself has a very shallow slope orthogonal to the river (typically 0.0001), and is bounded by steep hills, often forested. The floodplain land use is typically grazed pasture. Field estimates of Manning's n were undertaken throughout the reach using the photographic definition of roughness type identified in Chow (1959). Figure 6.6 illustrates channel and floodplain conditions that dominate the majority of the reach and illustrates an important category of flood inundation problem in comparatively sinuous rivers, especially where, as in this case, both settlements and transportation routes are located within the floodplain area. Roughness was assessed as 0.045 for the floodplain and 0.035 for the channel. There were, however, a number of sections within the reach where somewhat rougher floodplain conditions were evident, as shown in figure 4.9. These latter floodplain areas were assessed as having a Manning's n of 0.07.

Channel cross-sectional data, rating curve and hydrographs are available for the Bad Hersfeld and Rotenburg sections and were used in the RMA-2 application detailed below. At bankfull, the channel is about 13 ft. deep and 98 ft. wide (4m by 30m) at Bad Hersfeld and is 18 ft. deep and 164 ft. wide (5.5m by 50m) at Rotenburg.

Available maps of inundation show the whole floodplain to have been inundated in 1946. However, no record of the flood hydrograph for this event was found.

7.7 System Schematization

RMA-2 utilizes a finite element network composed of both triangular and quadrilateral elements. Ground elevations are defined at the corners of the elements and assumed to vary linearly between corner nodes. In this study, the channel was represented by a strip of two elements wide (figure 7.1) producing a triangular cross section. Overbank areas were represented by much larger elements. The lateral extent of the network was determined by a bluff line, beyond which none of the simulated flood events would extend.

Manning's roughness coefficients may be varied spatially in RMA-2 applications. For this study, two roughnesses were used in each simulation, one for the channel elements and another for the overbank elements. The resulting finite element network was composed of 860 elements and 2660 nodes. The ratio of maximum to minimum element sizes was about 200 to 1. This variability in resolution demonstrates the flexibility of the finite element method for use in large scale floodplain modelling.

The times simulated were 21 hours for Storm 1 and 34 hours for Storm 2. These times covered the rising limb of the hydrographs and a portion of the recession limb. All results reported herein were accomplished using a 0.5 hr. time step. No over-attenuation due to this relatively large time step was observed. One simulation of Storm 1 was performed using

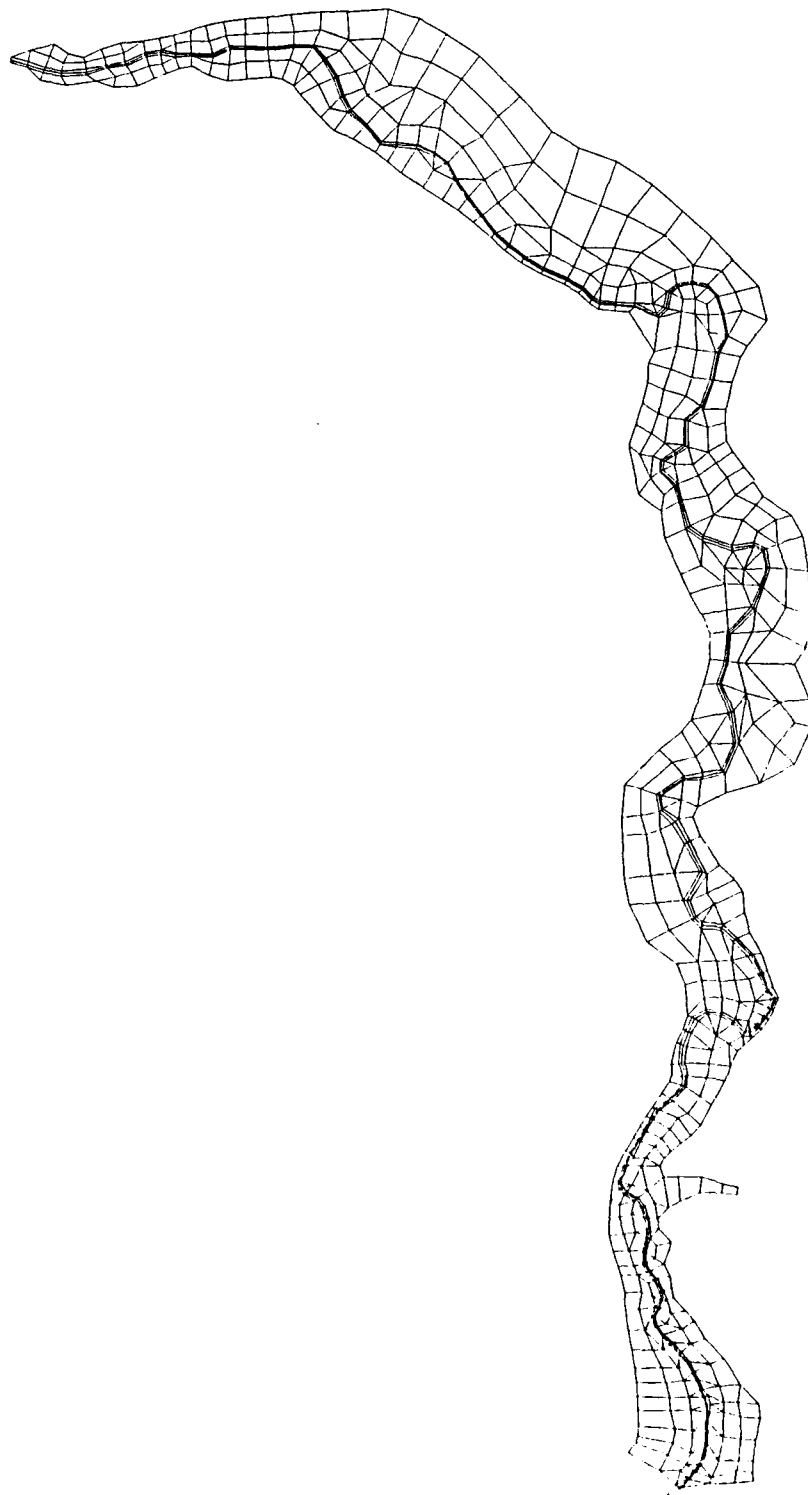


Figure 7.1 : Finite element network for River Fulda application

FIGURE 7.1
RIVER FULDA
MAY 1988

an 0.25 hr. time step, yielding results the same as those with the 0.5 hr. time step. Further investigations need to be done regarding the selection criteria and sensitivity of results to various time steps for use of this implicit finite element model for floodplain inundation studies.

7.8 Computational Aspects

Although this is not a very computationally intensive problem for the simulation of steady flow conditions, the dynamic simulations performed (consisting of 40 to 60 time steps) utilized significant computational resources. Each simulation took several hours of central processing time on a Harris 100 super microcomputer at H.E.C. Although contemporary desk top computers equal or exceed the processing speed of this computer, the results indicate that engineers contemplating two-dimensional floodplain modelling on this scale for dynamic flow events should carefully plan their studies to minimize the number of situations to be modelled and utilize steady flow simulations wherever possible. It should be pointed out here that traditional floodplain inundation mapping is accomplished using semi-empirical discharge routing with steady, one-dimensional computation of water surface elevation to define inundated areas.

7.9 Results

As discussed above, two storms were applied to the study reach. Storm 1 was an event commencing 31 March 1986, which produced a 1 in 10 year flood event at the downstream station (Rotenburg). Continuously recorded stage hydrographs were available for this storm at both Bad Hersfeld and Rotenburg. Using RMA-2 in association with the mesh illustrated in figure 7.1, Storm 1 was simulated using values of Manning's n for the channel of 0.035 and for the floodplain of 0.045. The results of this simulation are illustrated in figures 7.2a and 7.2b. From these results, it is evident that there is under-prediction of the stage at the upstream location (figure 7.2a) and over-prediction of stage by about 1 ft. (0.3m) at the peak stage at the downstream station (figure 7.2b). These results indicated that the channel plus floodplain conveyance was too efficient. A second simulation was performed based upon the floodplain condition

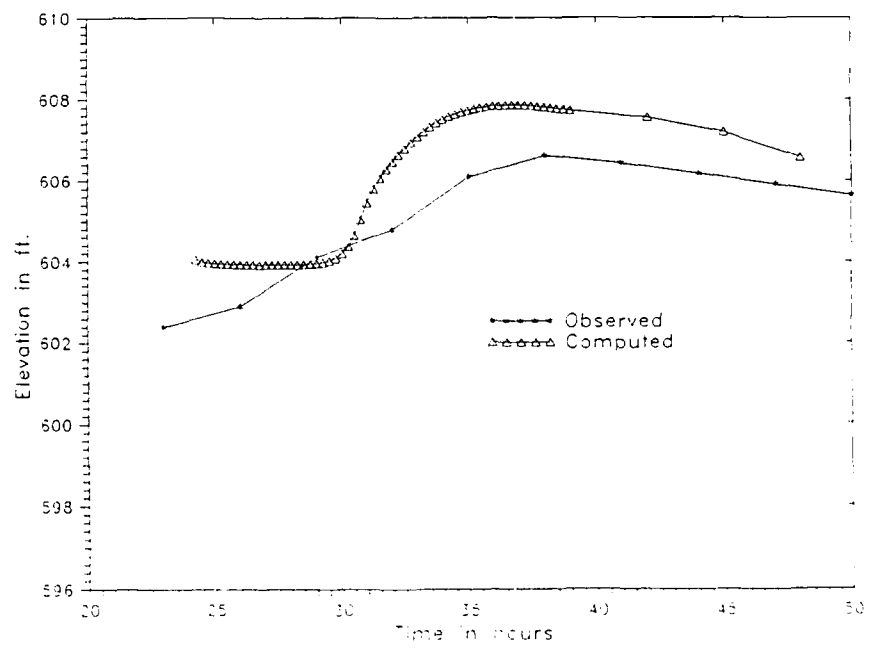
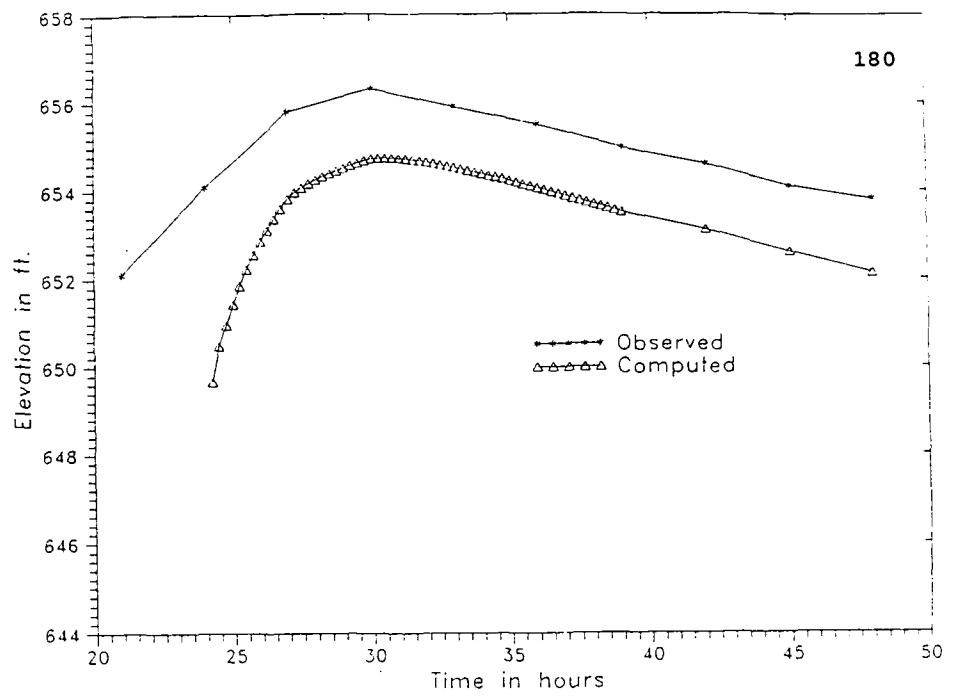


Figure 7.2

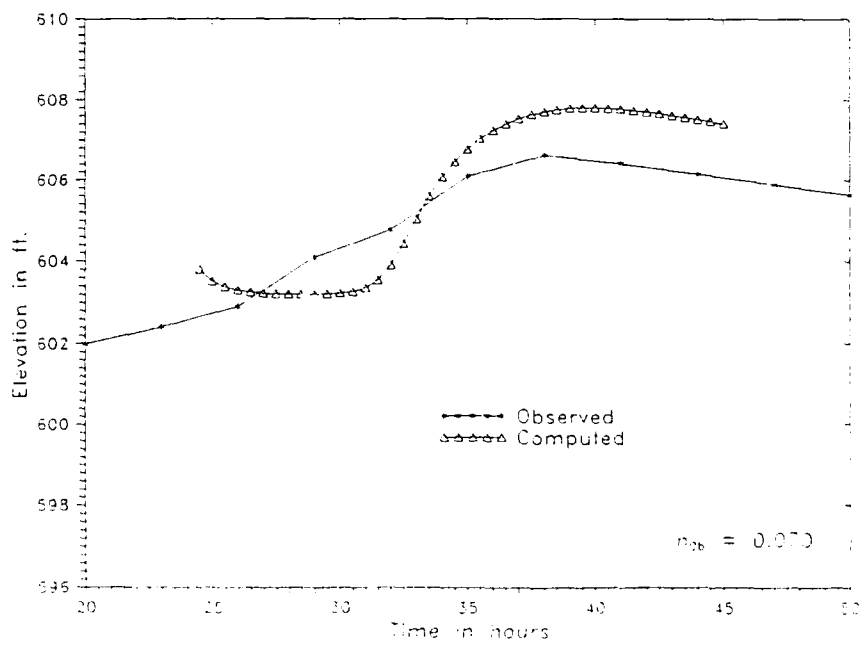
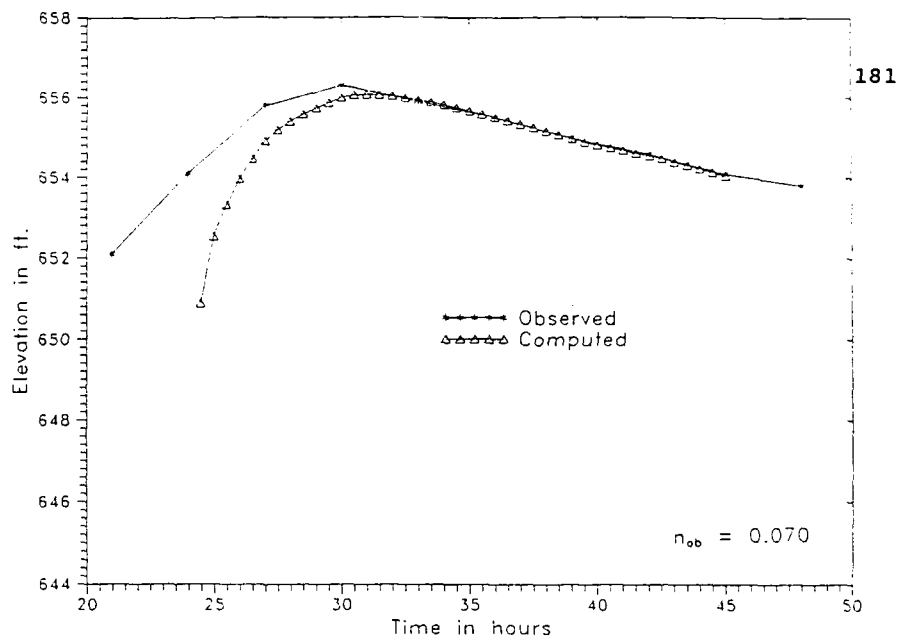


Figure 181

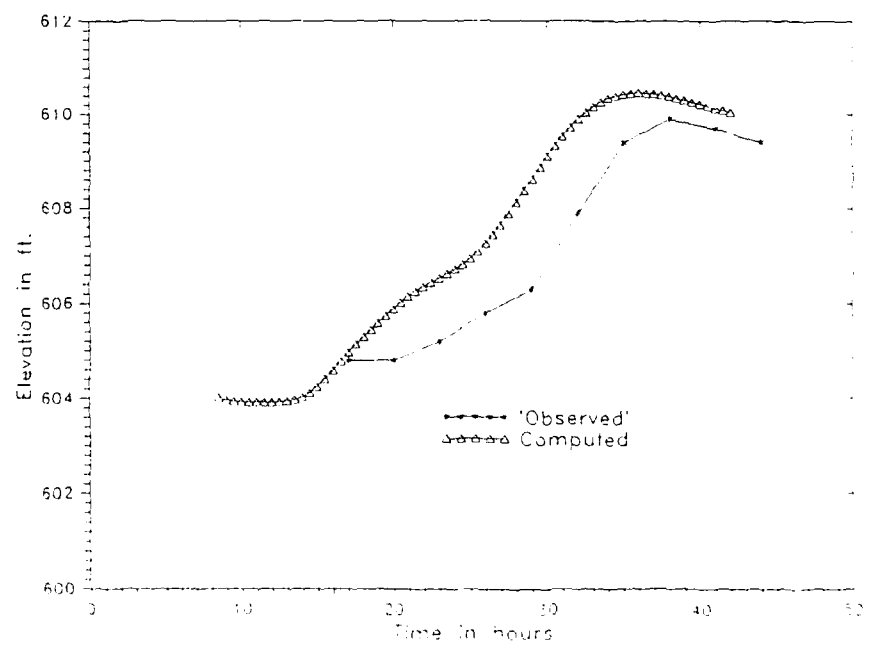
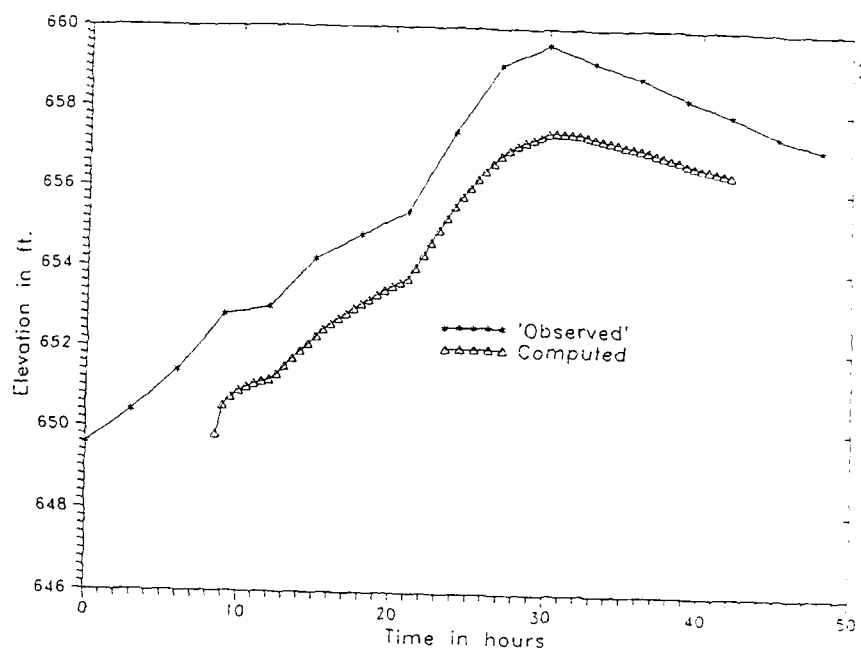


Figure 7.1

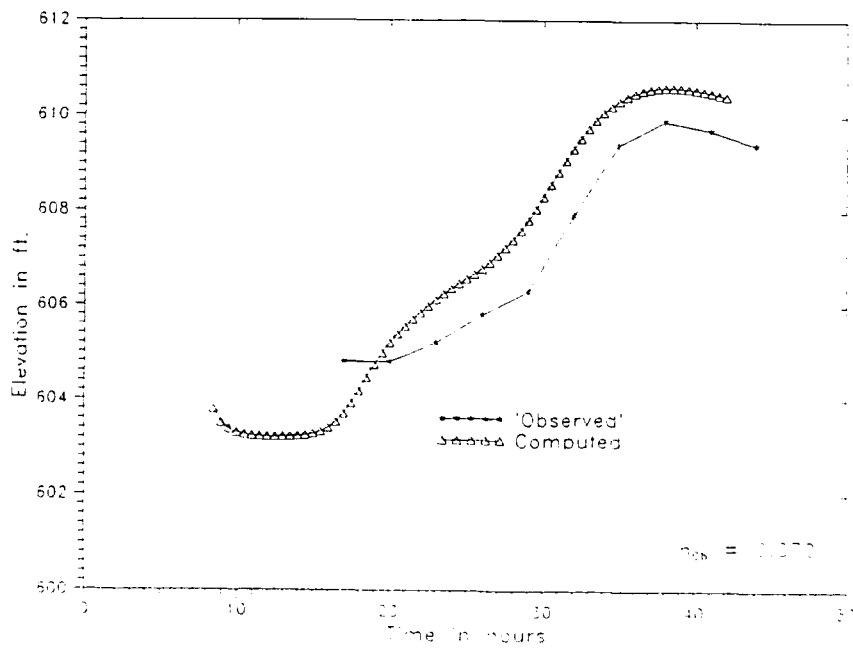
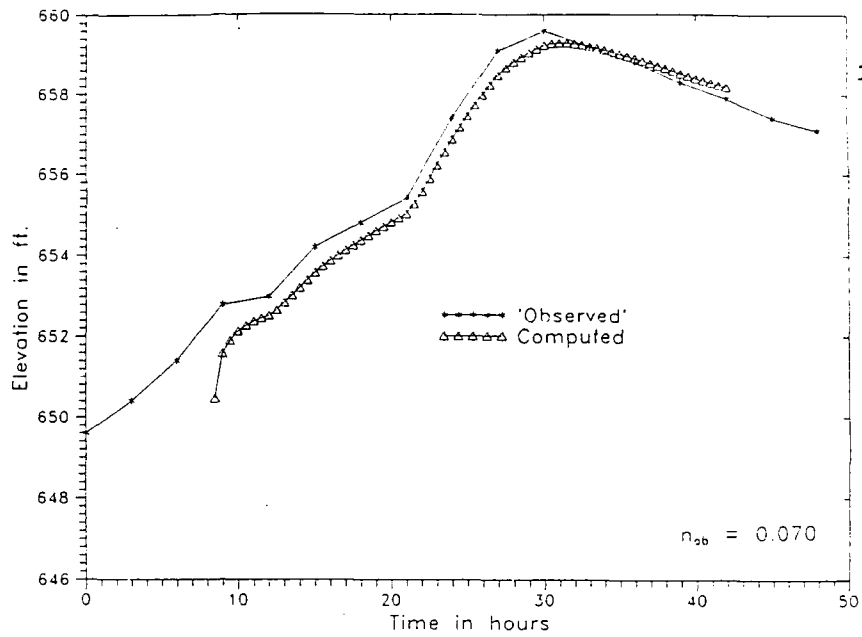
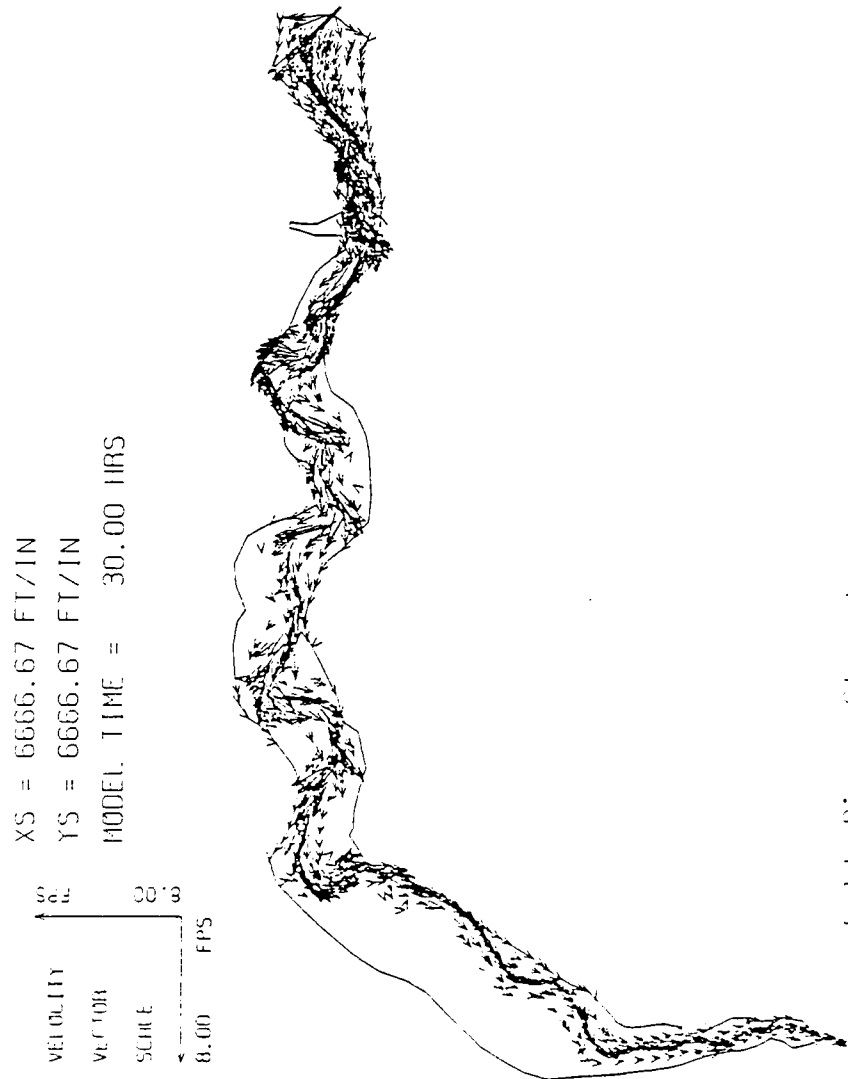


Figure 10.



Tula River, Storm 1.

Figure 7.6 : Velocity vector plot

shown in figure 4.9 (overbank n of 0.07) and the results are shown on figure 7.3.

Storm 2 was a generated flood event using the pattern of Storm 1, scaled up to a 1 in 100 year peak flow using available flood frequency data at Bad Hersfeld and Rotenburg. The results of utilizing the 0.045 and 0.035 Manning's n coefficients are shown in figure 7.4. These results show a similar trend to those depicted in figure 7.2 (Storm 1) in terms of predicted values. However, in terms of absolute stage prediction, the results for Storm 2 show a greater correspondence with the 'observed' stage. This result reinforces the observation we made above relating to floodplain roughness because in Storm 2, a significantly greater area of the floodplain is inundated. At peak stage, the over-prediction at Rotenburg is 0.6 ft. (0.2m), with the arrival of the peak being about 2 hours early (see figure 7.2b). This timing error corresponds approximately with the resolution at which it is possible to assess the stage from the gauge recordings.

Following the scheme adopted for Storm 1, a second simulation of Storm 2 was undertaken. Figure 7.5 shows the simulations corresponding to 0.07 and 0.035 roughness values for the floodplain and channel respectively for Storm 2 (see figure 4.9). Figure 7.5a indicates a particularly good correspondence with the 'observed' stage compare to figure 7.6a (floodplain roughness of 0.045). In addition, an improvement in the peak stage timing (figure 7.5b) was observed.

Intermediate stage hydrographs were also examined for locations within the study reach. These showed complete consistency with both the upstream and downstream results reinforcing the suggestion that the model may indeed be used to estimate the extent of floodplain inundation throughout an entire reach at the scale used in this study.

The two-dimensional solution obtained from RMA-2 produces velocity vectors in addition to stage at every computational node. Indeed most applications of two-dimensional flow models have focused on velocity for purposes of constituent transport or design. In the context of large

floodplain modelling velocities are important for both definition of inundated area, and definition of flood hazard. Figure 7.6 shows a typical velocity vector plot computed for the peak discharge of Storm 1 (refer to figure 7.3). For this 1 in 10 year event, the predictions shown in figure 7.6 imply substantial overbank flow throughout the entire reach. Whilst no field inundation data are available for Storms 2 or 2 for validation purposes, this prediction is consistent with the limited published field evidence relating to a 1946 flood that was larger than Storm 1. This fact, taken together with what appears to be a satisfactory reproduction of the stage hydrographs at both upstream and downstream locations for the observed Storm 1, suggests that it is reasonable to conclude from the available evidence that the predicted inundated overbank areas (figure 7.6) are realistic.

7.10 Discussion

Application of RMA-2, version 4, to the River Fulda has enabled a preliminary assessment to be made of the applicability of finite element numerical models to large scale floodplain applications. The initial results presented in this paper indicate that RMA-2 may successfully be used for estimating the depth and lateral extent of inundation at this scale. Also, the distribution of flow velocities across the floodplain is available from the simulations; there were no data, however, in this application to verify the computed velocities or the implied inundation extent. It would be desirable to consider making some future application of the model for reaches where such data are available to explore the interaction that may exist between the wetting/drying parameters used in the model and the computed overbank velocities. The model has been shown to be robust against field uncertainty in floodplain roughness estimation, evidenced by the results shown in figures 7.2-7.5. Stability of solutions for wetting and drying of large areas was greatly improved by use of the "marsh" element option in version 4 of RMA-2. Further enhancement of this capability, as well as that of channel representation and further field validation, are identified as future research needs.

8. CONCLUSIONS AND PROPOSALS FOR THE NEXT TWELVE MONTHS

8.1 Conclusions

1. The most important processes active in two-stage channels flood prediction have been identified as the turbulent exchange between the main channel and floodplain flow segments and the short-circuiting of floodplain flow downstream.
2. These two processes have been incorporated in MILHY3 whilst maintaining parsimonious data requirements and retaining the resolution of the submodels.
3. For events where at least 15% of the floodplain is apportioned to the floodplain, the application of the multiple routing and turbulent exchange routines together improves the predictive capability of MILHY.
4. For floodplain where less than 15% of the floodwave is apportioned to the floodplain, only the multiple routing routine has any impact on the hydrograph.
5. Application of RMA2 shows that the model can be reliably applied to large scale reaches and that it could provide detailed inundation predictions for ungauged catchments, utilizing MILHY3 to provide the upstream inflow hydrograph.
6. Optimization techniques provide a viable alternative method of tackling factor perturbation sensitivity analysis.

8.2 Proposals for the next twelve months

1. Continuing investigation of the feasibility of linking MILHY3 with RMA-2 for detailed two-stage channel predictions in ungauged

catchments.

2. Investigation of the use of MILHY3/RMA-2 scheme to predict the floodplain erosion and sedimentation patterns. This investigation will utilize data available from the River Culm, Devon, England.

9. REFERENCES

- Anderson, M.G. (1982). Assessment and implementation of drainage basin runoff models. US Army European Research Office. Final Technical Report DAJA37-82-C-0092, 74pp.
- Anderson, M.G. and Howes, S. (1984). Streamflow modelling. U.S. Army European Research Office. Final Technical Report DAJA37-81-C-0221, 130pp.
- Anderson, M.G. and Howes, S. (1986). Hydrological modelling in ungauged watersheds. U.S. Army European Research Office. Final Technical Report DAJA45-83-C-0029, 147pp.
- Anderson, M.G. and Singleton, L. (1987). Development of HYMO for operational forecasting. U.S. Army European Research Office. Final Technical Report DAJA45-85-C-0011, 32pp.
- Armstrong, A.C., Rycroft, D.W. and Welch, D.J. (1980). Modelling watertable responses to climatic inputs - its use in evaluating drainage designs in Britain. Journal of Agricultural Engineering Research, 25, 311-323.
- Asano, J., Hashimoto, H. and Fujita, K. (1985). Characteristics of variation of Manning's roughness coefficient in a compound cross-section. Proceedings of the 21st Congress of the International Association for Hydraulic Research, 6, 30-34.
- Beckett, P.H.T. and Webster, R. (1971). Soil variability: a review. Soil and Fertilizers, 34, 1-15.
- Bhowmik, N.G. and Demissie, M. (1982). Carrying capacity of flood plains. Journal of the Hydraulics Division, Proceedings of the American Society of Civil Engineers, 108 (HY3), 443-452.
- Brakensiek, D.L. and Rawls, W.J. (1983). Use of infiltration procedures for estimating runoff. Paper presented to United States Department of Agriculture Soil Conservation Service, National Engineering Workshop, Tempe, Az., U.S.A., 23pp.
- Cauchy, A.L. (1847). Methode generale pour la resolution des systemes d'equations simultanees. C.R. Read Sci. 25, 536-538.
- Chang, H.H. (1983). Energy expenditure in curved open channels. Journal of Hydraulic Engineering, Proceedings of the American Society of Civil Engineers, 109, 1012-22.
- Chow, V.T. (1959). Open Channel Hydraulics, McGraw-Hill Book Co., New York, N.Y.

- Croxy, P.M. and Elksawy, E.M. (1980). An experiment at investigation into the interaction between a river's deep section and its floodplain. Symposium on River Engineering and its Interaction with Hydrological and Hydraulics Research, International Association for Hydraulic Research, Belgrade, Yugoslavia, pg. 7.
- Deuller, J.W., Toebes, G.H. and Udeozo, B.C. (1967). Uniform flow in idealized channel geometrics. Proceedings of the Twelfth International Congress of the International Association for Hydraulic Research, Fort Collins, U.S.A., 1, 218-225.
- Einstein, H.A. and Shen, H.W. (1964). A study of the meandering in straight alluvial channels. Journal of Geophysical Research, 69, 5239-47.
- Ervine, D.A. and Ellis, J. (1987). Experimental and computational aspects of overbank floodplain flow. Transactions of the Royal Society of Edinburgh; Earth Sciences, 78, 315-325.
- Fread, D.L. (1976). Flood routing in meandering rivers with flood plains. Symposium on Inland Waterways for Navigation, Flood Control and Water Division, Proceedings of the American Society of Civil Engineers, Waterways, Harbors and Coastal Engineering Division, 16-35.
- Gee, D.M. and Wilcox, D.B. (1985). Use a two-dimensional flow model to quantify aquatic habitat. Proceedings of the American Society of Civil Engineers, Special Conference on Computer Applications in Water Resources, Buffalo, NY, USA.
- Ghosh, S.N. and Jena, S.B. (1971). Boundary shear distribution in open channel compound. Proceedings of the Institute of Civil Engineers, 49, 417-430.
- HEC-1. (1981). Flood Hydrograph Package Users Manual, Hydrologic Engineering Center, Water Resources Support Center, U.S. Army Corps of Engineers, Davis, California, pp.192.
- Hermann, C.F. (1967). Validation problems in games and simulations with special reference to models of behavioural politics. Behavioural Science, 12, 216-231.
- Hewlett, J.D. and Troendle, C.A. (1975). Non point and diffused water sources: a variable source area problem. Watershed Management, American Society of Civil Engineers, Logan, Utah, 21-45.
- Holden, A.P. and James, C.S. (1989). Boundary shear distribution on flood plains. Journal of Hydraulic Research, International Association for Hydraulic Research, 27, 75-89.

- Holtz, P. and Nitsche, G. (1980). Tidal wave analysis for estuaries with inter-tidal flat. Proceedings of the 3rd International Conference on Finite Elements for Water Resources, University of Mississippi, Mississippi, USA, 5113-5126.
- Hornberger, G.M. and Spear, R.C. (1981). An approach to the preliminary analysis of environmental systems. Journal of Environmental Management, 12, 7-18.
- Ibbit, R.P. and O'Donnell . (1971). Fitting methods for conceptual catchment models. Journal of Hydraulic Engineering, Proceedings of the American Society of Civil Engineers, 97(HY9), 1331-1342.
- James W.P. and Stinson, D. (1981). Student work book on streamflow forecasting: Military Hydrology Project. U.S. Army Engineer, Waterways Experiment Station, Mississippi, U.S.A., 215pp.
- Jones, D.A. (1982). Various approaches to the sensitivity analysis of SHE: a discussion. European Hydrologic System, Report 20, Institute of Hydrology, Wallingford, 10pp.
- King, I.P. and Norton, W.R. (1978). Recent applications of RMA's finite element models for two dimensional hydrodynamics and water quality. Proceedings of the 2nd International Conference on Finite Elements for Water Resources, Imperial College, London, 2, 81-99.
- Klassen, G.J. and Van der Zwaard, J.J. (1974). Roughness coefficients of vegetated flood plains. Journal of Hydraulic Research, International Association for Hydraulic Research, 12, 43-63.
- Knight, D.W. and Demetriou, J.D. (1983). Floodplain and main channel flow interaction Journal of the Hydraulics Division, Proceedings of the American Society of Civil Engineers, 109 (HY8), 1073-1092.
- Knight, D.W., Demetriou, J.D. and Hamed, M.E. (1983). Hydraulic analysis of channels with floodplains. International Conference on the Hydraulic Aspects of Floods and Flood Control, British Hydromechanics Research Association, London, England, Paper E1, 129-144.
- Knight, D.W. and Hamed, M.E. (1984). Boundary shear in symmetrical compound channels. Journal of Hydraulic Engineering, Proceedings of the American Society of Civil Engineers, 110, 1412-1430.
- Krishnappen, B.G. and Lau, Y.L. (1986). Turbulence modelling of floodplain flows. Journal of Hydraulic Engineering, Proceedings of the American Society of Civil Engineers, 112, 251-266.
- Lee, J.K. (1980). Two-dimensional finite element analysis of the hydraulic effect of highway bridge fills in a complex flood plain. Proceedings of the 3rd International Conference on Finite Elements in Water Resources, University of Mississippi, Mississippi, USA.

- Lotter, G.K. (1933). Consideration of hydraulic design of channels with different roughness of walls. Transactions of the All-Union Scientific Research, Institute for Hydraulic Engineering, Leningrad, 9, 238-241.
- MacArthur, R.C., Wakeman, T. and Norton, W.R. (1987). Numerical evaluation of environmental concerns for the Fishermans Wharf Harbor Breakwater. Proceedings of the San Francisco District Navigation Workshop, US Corps of Engineers, San Francisco District, San Francisco, California, USA.
- McAnally, W.H., Letter, J.V., Stewart, J.P., Thomas, W.A. and Brogdon, N.J. (1984). Columbia River Hybrid Modeling System. Journal of Hydraulic Engineering, Proceedings of the American Society of Civil Engineers, 110, 300-311.
- McAnally, W.H., Letter, J.V., Stewart, J.P., Thomas, W.A. and Brogdon, N.J. (1984). Application of Columbia Hybrid Modeling System. Journal of Hydraulic Engineering, Proceedings of the American Society of Civil Engineers, 110, 627-642.
- McCuen, R.H. (1973). The role of sensitivity analysis in hydrologic modelling. Journal of Hydrology, Vol. 18, 37-53.
- McCuen, R.H. (1976). The anatomy of the modelling process, in Brebbia, C.A. (ed.) Mathematical Models for Environmental Problems, Proceedings of the International Conference, edited by Brebbia, C.A., 401-412.
- Miller, D.R., Butler, G. and Bramall, L. (1976). Validation of ecological system models. Journal of Environmental Management, 4, 383-401.
- Myers, W.R.C. (1978). Momentum transfer in a compound channel. Journal of Hydraulic Research, International Association for Hydraulic Research, 16, 139-50.
- Myers, W.R.C. (1984). Frictional resistance in channels with floodplains. Proceedings of the First International Conference on Hydraulic Design in Water Resource Engineering: Channels and Channel Control Structures, Southampton, edited by Smith, K.V.H.
- Niemeyer, G. (1979). Efficient simulation of non-linear steady flow. Journal of the Hydraulic Division, Proceedings of the American Society of Civil Engineers, 105 (HY3), 185-195.
- Noutsopoulos, G. and Hadjipanios, P. (1983). Discharge computations in compound channels. Proceedings of the 20th Congress of the International Association for Hydraulic Research, Moscow, USSR. V, 173-80.

- Pasche, E. and Rouve, G. (1985). Overbank flow with vegetatively roughened floodplains. Journal of Hydraulic Engineering, Proceedings of the American Society of Civil Engineers, 111, 1262-1278.
- Patel, V.C. (1965). Calibration of the Preston tube and limitations of its use in pressure gradients. Journal of Fluid Mechanics, 23, 185-207.
- Perkins, F.E. (1970). Floodplain modelling. Water Resources Bulletin, 6, 375-383.
- Petryk, S. and Bosmajian, G. (1975). Analysis of flow through vegetation. Journal of the Hydraulic Division, Proceedings of the American Society of Civil Engineers, 101 (HY7), 871-884.
- Prinos, P., Townsend, R. and Tavoularis, S. (1985). Structure of turbulence in compound channel flows. Journal of Hydraulic Engineering, Proceedings of the American Society of Civil Engineers, 111, 1246-1261.
- Radojkovic, (1976). Mathematical modelling of rivers with floodplains, Symposium on Inland Waterways for Navigation Flood Control and Water Diversions. Proceedings of the American Society of Civil Engineers, Waterways, Harbors and Coastal Engineering Division, 56-64.
- Rajaratnam, J. and Ahmadi, R.M. (1979). Interaction between main channel and floodplain flows. Journal of the Hydraulics Division, Proceedings of the American Society of Civil Engineers, 105 (HY5), 573-588.
- Rajaratnam, N. and Ahmadi, R. (1981). Hydraulics of channels with floodplains. Journal of Hydraulic Research, International Association for Hydraulic Research, 19, 43-60.
- Samuels, P.G. (1985). Modelling of river and floodplain flow using the finite element method. Technical Report No. SR61, Hydraulics Research, Wallingford, U.K. 198pp.
- SCS (1954) (Soil Conservation Service). Handbook of Channel Design for Soil and Water Conservation, Department of Agriculture, SCS-TP-61
- Sellin, R.H.J. (1964). A laboratory investigation into the interaction between flow in the channel of a river and that over its floodplain. La Houille Blanche, 7, 793-801.
- Simonson, R.W. (1962). Soil correlation and the new classification system. Soil Science, 96, 23-30.
- Smith, V.E. (1976). The application of HYMO to study areas of southwestern Wyoming for surface runoff and soil loss estimates. Water Resources Series, 60, Water Resources Research Institute, Wyoming University, Laramie, USA, 38pp.

- Smith, C.D. (1978). Effect of channel meanders on flood stage in valley. Journal of the Hydraulics Division, Proceedings of the American Society of Civil Engineers, 104 (HY1), 49-58.
- Su, T.Y., Wang, S.Y. and Alonso, C.V. (1980). Depth-averaging models of river flows, Proceedings of the 3rd International Conference on Finite Elements in Water Resources, University of Mississippi, Mississippi, USA.
- Tingsanchali, T. and Ackermann, N.L. (1976). Effects of overbank flow in flood computations. Journal of the Hydraulics Division, Proceedings of the American Society of Civil Engineers, 12 (HY7), 1013-1025.
- Toebes, G.H. and Sooky, A.A. (1967). Hydraulics of meandering rivers with floodplains. Journal of the Waterways Harbors Division, Proceedings of the American Society of Civil Engineers, 93 (WW2), 213-236.
- Tseng, M.T. (1975). Evaluation of flood risk factors in the design of highway stream crossing. Vol. III. Finite element model for bridge backwater computation, Report No. FHWA-RD-75-53. Offices of Research and Development, Federal Highway Administration, Washington, D.C., USA.
- Williams, J.R. (1975). HYMO flood routing. Journal of Hydrology, 26, 17-27.
- Wolman, M.G. and Leopold, L.B. (1957). River floodplains: some observations on their formation. U.S. Geological Survey Professional Paper, 282pp.
- Wormleaton, P.R., Allen, J. and Hadjipanous, P. (1980). Apparent shear stresses in compound channel flow. Symposium on River Engineering and its Interaction with Hydrological and Hydraulics Research, International Association for Hydraulic Research, Belgrade, Yugoslavia.
- Wormleaton, P.R., Allen, J. and Hadjipanous, P. (1982). Discharge assessment in compound channel flows. Journal of the Hydraulic Division, Proceedings of the American Society of Civil Engineers, 108 (HY9), 975-994.
- Wright, R.R. and Carstens, H.R. (1970). Linear momentum flux to overbank sections. Journal of the Hydraulics Division, Proceedings of the American Society of Civil Engineers, 96 (HY9), 1781-1794.
- Yen, B.C. (1967). Some aspects of flow in meandering channels. Proceedings of the Twelfth Congress of the International Association of Hydraulic Research, 1, 465-471.
- Yen, B.C. and Yen, C.L. (1984). Flood flow over meandering channels, in River Meandering, Proceedings of the Conference on Rivers, American Society of Civil Engineers, edited by Elliott, C.M., 554-561.

- Yen, C.L. and Overton, D.E. (1973). Shape effects on resistance in floodplain channels. Journal of the Hydraulics Division, Proceedings of the American Society of Civil Engineers, 99 (HY1), 219-238.
- Zheleznyakov, G.V. (1965). Relative deficit of mean velocity of unstable river flow; kinematic effect in river beds with floodplains. Proceedings of the 11th Congress of the International Association for Hydraulic Research, Leningrad, USSR, Paper 3.45, 133-150.
- Zheleznyakov, G.V. (1971). Interaction of channel and floodplain streams. Proceedings of the 14th Congress of the International Association for Hydraulic Research, Paris, France, 5, 144-148.
- Zielke, W. and Urban, W. (1981). Two-dimensional modelling of rivers with floodplains. Proceedings of the Conference on Numerical Modelling of River Channel and Overland Flow for Water Resources and Environmental Applications, International Association for Hydraulic Research, Bratislava, Delft, Netherlands.